UNIVERSIDADE DA BEIRA INTERIOR
Ciências da Saúde

Desenvolvimento de novos micro- e nano-sistemas responsivos para entrega de drogas anti-tumorais

André Ferreira Moreira

Dissertação para obtenção do Grau de Mestre em
Ciências Biomédicas
(2º ciclo de estudos)

Orientador: Prof. Doutor Ilídio Joaquim Sobreira Correia
Coorientador: Mestre Vítor Manuel Abreu Gaspar

Covilhã, junho de 2014

"YOU, ME OR NOBODY IS GOING TO HIT AS HARD AS LIFE. BUT IT AIN'T ABOUT HOW HARD YOU'RE HIT, IT IS ABOUT HOW HARD YOU CAN GET HIT AND KEEP MOVING FORWARD, HOW MUCH CAN YOU TAKE AND KEEP MOVING FORWARD. THAT'S HOW WINNING IS DONE!"

Rocky Balboa (2006)

Acknowledgements

Firstly, I would like to thank to my supervisor the Professor Ilídio Correia for the opportunity to develop my master thesis in his group, and for all the efforts and time spent to help me to improve myself.

I thank to Vítor Gaspar, my co-supervisor for always making me go further and also for his friendship, guidance and endless support. Our constant work discussions contributed to develop my focus and technical skills as a researcher and also, improved my ability to interpret and criticize results. His continuous orientation was very important in the development of my work and in my growth as a person.

Also, I would like to thank to Elisabete Costa and to Duarte Diogo, for their fellowship, trust and endless support. They accompanied me throughout this year helping me to surpass all the barriers and frustrations. One word also for the other elements of this research group, thank our joyful conviviality it was very easy to work and become integrated.

I thank all my family, especially to my father, mother and brother for their support, patience, love and affection.

Lastly, and foremost, a very special thanks to my girlfriend, Ana Catarina, for all her love, comprehension, patience and support. Also for her continuous encouragement to me in order to continue to move forward during this difficult year.

Abstract

Cancer is a major health care problem with growing incidence, not only at a national level but also worldwide. Due to this urgency in reducing cancer prevalence, the scientific community has put forward a great attention in the search for novel anti-cancer treatments, particularly, in the development of nanocarriers capable to control and promote drug delivery to target cells. These drug delivery systems are capable to overcome the limitations presented by the conventional chemotherapeutic treatments. Among the various types of nanocarriers developed so far, mesoporous silica nanoparticles (MSNs) possess unique structural properties that make them highly suitable to encapsulate and deliver drugs to cancer cells. However, for these specialized nanocarriers to be applied in cancer therapies it is still of critical importance to control the time frame of drug release at the tumor microenvironment or inside cancer cells, in order to maximize the therapeutic effect and reduce unspecific cytotoxicity. One alternative to control drug release is to endow the nanocarriers with a pH responsive drug release that takes advantage of the naturally acidic tumor microenvironment and also of the acidic pH of lysosomes.

In this thesis the development of dual drug loaded pH-responsive mesoporous silica nanoparticles (MSNs) with a calcium carbonate-based coating is presented as an effective alternative to deliver drugs to prostate cancer cells. This approach allowed the simultaneous co-encapsulation of a non-steroidal anti-inflammatory drug (Ibuprofen) and Doxorubicin (an anti-tumoral drug), with high efficiency. Furthermore, the idealized calcium carbonate coating successfully promoted a pH sensitive drug release from the MSNs matrix. The delivery systems proved to be capable of maintaining the drugs inside their mesoporous structure under physiological pH, and to prompt its release in acidic environments. The resulting dual loaded MSNs coated with calcium carbonate have spherical morphology and a mean size of 167 nm, presenting therefore, good characteristics to be applied as nanocarriers. Such, is supported by the cytotoxicity studies where the idealized MSNs produced a 93% higher anti-proliferative effect than the non-coated silica nanoparticles, being even more effective than the dual free drug administration, as well. Overall, the carbonate coating of MSNs showed to be a simple and cost-effective approach for cancer therapy, in particular for a pH-triggered drug delivery. Moreover, the versatile nature of these nanocarriers allows surface modifications that can improve the selectivity to target cells, allow imaging or even a combination of them both.

Keywords

Calcium carbonate, cancer therapy, co-delivery of drugs, mesoporous silica nanoparticles, pH responsive release.

Resumo Alargado

O cancro é atualmente um dos maiores problemas que afeta a saúde pública, tanto ao nível nacional como mundial. Apesar de grande parte das terapias convencionais possuírem a potencialidade de eliminar a maioria das células cancerígenas, estas apresentam vários problemas associados. Um dos que mais se destaca é a falta de especificidade, o que se traduz frequentemente em danos de células e tecidos saudáveis, que constituem efeitos secundários nefastos. Aliado a este facto, normalmente, também se verifica uma baixa biodisponibilidade e, por isso, são muitas vezes utilizadas concentrações mais elevadas dos agentes terapêuticos na tentativa produzir algum efeito benéfico para o paciente. Estes aumentos nas concentrações administradas acarretam consigo um acréscimo dos efeitos nocivos. Como tal, esta doença tem atraído a atenção da comunidade científica para o desenvolvimento de novas terapias. Uma boa abordagem para ultrapassar estas desvantagens é a entrega combinada de diferentes agentes terapêuticos. Esta múltipla administração utiliza os compostos em quantidades inferiores à da sua aplicação isolada, tentando assim tirar partido de um possível efeito terapêutico sinérgico resultante da combinação do ataque a diferentes caraterísticas chave das células cancerígenas. Contudo, mesmo esta abordagem não tem conseguido ultrapassar os efeitos secundários produzidos nas células saudáveis.

Nos últimos anos, uma estratégia que tem sobressaído é a utilização da Nanotecnologia para a administração destes agentes terapêuticos. A utilização de nanotransportadores concede a oportunidade de ultrapassar algumas das limitações apresentadas anteriormente. De fato, no geral os nanoveículos são capazes de aumentar a solubilidade dos agentes terapêuticos, protegê-los e transportá-los na circulação sanguínea. Simultaneamente, também podem controlar a libertação destes compostos bioativos, aumentando a seletividade e penetração/absorção dos mesmos no tecido alvo. Dentro dos diferentes tipos de nanopartículas que têm vindo a ser estudados as nanopartículas mesoporosas de sílica (MSNs) apresentam características estruturais que as tornam muito adequadas para esta aplicação. Estas partículas possuem uma estrutura porosa singular, com um grande número de poros que nunca se interconectam, aliada à capacidade de armazenarem uma grande quantidade de agentes terapêuticos. Além disso, as MSNs apresentam uma estrutura rígida muito resistente à temperatura, pH e stress mecânico o que lhes garante uma elevada estabilidade. Contudo, apesar das boas propriedades que as MSNs apresentam, é ainda necessário conferir-lhes a capacidade de libertarem a sua carga na presença de um determinado estímulo para que os agentes terapêuticos sejam apenas libertados quando cheguem a um ambiente que possua esses estímulos. O estímulo pode ter como origem alterações no pH, luz, enzimas, temperatura entre outros. A sensibilidade ao pH é um dos estímulos que melhor se adequa para ser utilizado na terapia do cancro, pois as diferenças de pH observadas no microambiente tumoral e também nas vias endocíticas no interior das células cancerígenas podem ser aproveitadas para

desencadear a libertação dos agentes terapêuticos. Nas MSNs esta sensibilidade a estímulos é geralmente conseguida através da ligação de polímeros na sua superfície. Porém, esta estratégia apresenta algumas desvantagens como a necessidade de utilização de processos de purificação complexos, custos elevados e um potencial de aplicação clínica limitado.

Assim sendo, o trabalho de investigação desenvolvido nesta tese descreve não só o desenvolvimento de nanopartículas de sílica mesoporosas carregadas com dois agentes terapêuticos, Doxorrubicina e Ibuprofeno mas, também a nova aplicação do carbonato de cálcio para tornar as MSNs sensíveis ao pH. O carbonato de cálcio forma-se preferencialmente nos poros das MSNs impedindo assim a libertação da sua carga, e quando em meio ácido este sofre uma rápida degradação desimpedindo os poros e permitindo a libertação da Doxorrubicina e do Ibuprofeno. Este sistema foi desenvolvido e testado para a entrega de agentes terapêuticos a células do cancro da próstata. As nanopartículas produzidas apresentaram um tamanho na ordem dos 160 nm e uma morfologia esférica uniforme. Além disto, os estudos efetuados demostraram que as partículas são capazes de armazenar grandes quantidades de Doxorrubicina e Ibuprofeno na sua matriz porosa. Por outro lado, apenas perdas residuais destes agentes terapêuticos foram detetadas nos passos subsequentes ao seu armazenamento nas MSNs. Os resultados obtidos demostraram também que o revestimento de carbonato de cálcio é sensível ao pH, visto que a um pH acídico (5,6) os agentes terapêuticos apresentaram uma rápida libertação e a um pH fisiológico (7,4) a libertação foi retardada. Os estudos realizados *in vitro* com células do cancro da próstata (PC-3) mostraram que estas partículas eram capazes de penetrar nas células e entregar os agentes terapêuticos no seu local de ação. Em particular, foi comprovado que uma quantidade substancial de Doxorrubicina se localizava no núcleo das células tumorais após administração. Estes resultados são essenciais para verificar a eficácia desta estratégia uma vez que este agente anti-tumoral atua no núcleo ao nível do ADN. Adicionalmente, as partículas de sílica revestidas com carbonato de cálcio contendo os fármacos apresentaram uma maior atividade citotóxica do que os agentes terapêuticos na forma livre e mesmo do que as nanopartículas não revestidas.

Em geral, o revestimento de carbonato de cálcio mostrou-se capaz de imprimir um comportamento sensível ao pH por parte das nanopartículas de sílica, e futuramente permitir a sua utilização na terapia do cancro. Além disto, a versatilidade que este sistema apresenta, permite modificações futuras que podem melhorar a sua seletividade para as células de interesse ou mesmo adicionar funções permitindo por exemplo o diagnóstico e a terapia em simultâneo.

Palavras-chave

Carbonato de cálcio, co-entrega, nanopartículas de sílica mesoporosas, responsividade ao pH, terapia do cancro.

List of Publications

Articles in peer reviewed international journals:

André F. Moreira , Vítor M. Gaspar, Elisabete C. Costa, Duarte de Melo-Diogo, Paulo Machado, Catarina M. Paquete and Ilídio J. Correia, "Preparation of end-capped pH-sensitive mesoporous silica nanocarriers for on-demand drug delivery", European Journal of Pharmaceutics and Biopharmaceutics (3.826), submitted.

Duarte de Melo-Diogo, Vítor M. Gaspar, Elisabete C. Costa, André F. Moreira , David Markl, Eugénia Gallardo and Ilídio J. Correia, "Combinatorial delivery of Sildenafil-Crizotinib-Palbociclib by TPGS-PLA micelles for improved cytotoxic effect in lung cancer", European Journal of Pharmaceutics and Biopharmaceutics (3.826), submitted.

Posters communications:

André F. Moreira, Vítor M. Gaspar, Elisabete C. Costa, Duarte de Melo-Diogo, Paulo Machado, Catarina M. Paquete and Ilídio J. Correia, Synthesis and characterization of MCM-41 type sílica nanoparticles by a Stöber modified method, Encontro Bienal das Divisões Técnicas da Sociedade Portuguesa de Materiais (SMP), 4th of May, Covilhã, Portugal.

Elisabete C. Costa, Vítor M. Gaspar, Duarte de Melo-Diogo, André F. Moreira, João F.G. Marques, Paula Coutinho and Ilídio J. Correia, Evaluation of nanoparticles uptake in breast cancer co-cultures, Encontro Bienal das Divisões Técnicas da Sociedade Portuguesa de Materiais (SMP), 4th of May, Covilhã, Portugal.

Awards:

INESPO II project (2014) - 3000 Euros Grant winner for prototypes development, and enrollment in CEBT Ibérico - Competências Empreendedoras De Base Tecnológica.

Index

Figure Index

…

Table Index

List of abbreviations

ATP	Adenosine Triphosphate
Bcl-2	B-cell lymphoma 2
BET	Brunauer–Emmett–Teller
BJH	Barrett-Joyner-Halenda
$CaCl_2$	Calcium Chloride
$CaCO_3$	Calcium Carbonate
CO_2	Carbon Dioxide
COX-1	Cyclooxygenase 1
COX-2	Cyclooxygenase 2
CTAB	Hexadecyltrimethylammonium Bromide
DGS	Direção Geral de Saúde
DLS	Dynamic Light Scattering
DMEM-F12	Dulbecco's Modified Eagle Medium: Nutrient Mixture F-12
DNA	Deoxyribonucleic Acid
Dox	Doxorubicin
Dox-Ibu-MSNs	Doxorubicin and Ibuprofen loaded Mesoporous Silica Nanoparticles
Dox-Ibu-MSNs-$CaCO_3$	Doxorubicin and Ibuprofen loaded Mesoporous Silica Nanoparticles coated with Calcium Carbonate
Dox-MSNs	Doxorubicin loaded Mesoporous Silica Nanoparticles
EDX	Energy Dispersive X-Ray
EMA	European Medicines Agency
EPR	Enhanced Permeability and Retention
FBS	Fetal Bovine Serum
FDA	Food and Drugs Administration
FGF	Fibroblast Growth Factor
FibH	Primary Normal Human Dermal Fibroblasts
FITC	Fluorescein Isothiocyanate
FTIR	Fourier Transform Infrared Spectroscopy
HCl	Hydrochloric Acid
HSA	Human Serum Albumin
Ibu	Ibuprofen
Ibu-MSNs	Ibuprofen loaded Mesoporous Silica Nanoparticles
MCM-41	Mobil Crystalline Materials
MFI	Mean Fluorescence Intensity
MSNs	Mesoporous Silica Nanoparticles
MSNs+CTAB	Non-Purified Mesoporous Silica Nanoparticles
MSNs-$CaCO_3$	Calcium Carbonate coated Mesoporous Silica Nanoparticles
MTS	3-(4,5-Dimethylthiazol-2-Yl)-5-(3-Carboxymethoxyphenyl)-2-(4-Sulfophenyl)-2H-Tetrazolium
Na_2CO_3	Sodium Carbonate
NAD(P)H	Nicotinamide Adenine Dinucleotide Phosphate-Oxidase
$NaHCO_3$	Sodium Bicarbonate
NaOH	Sodium hydroxide
NSAID	Non-Steroidal Anti-Inflammatory Drug
PAA	Poly(Acrylic Acid)

PBS	Phosphate Buffered Saline
PC-3	Human Prostate Cancer Cells
PCA3	Prostate Cancer Antigen 3
PDFG	Platelet Derived Growth Factor
PDI	Polydispersity index
PEG	Polyethylene Glycol
PGE	E series prostaglandins
PMS	Phenazine Methosulfate
PSA	Prostate Specific Antigen
PSCA	Prostate Stem Cell Antigen
PSMA	Prostate Specific Membrane Antigen
PTEN	Phosphatase and Tensin Homolog
RES	Reticuloendothelial System
RPMI-1640	Roswell Park Memorial Institute 1640
SEM	Scanning Electron Microscopy
SLN	Solid Lipid Nanoparticles
TEM	Transmission Electron Microscopy
TEOS	Tetraethyl Orthosilicate
TMOS	Tetramethyl Orthosilicate
USA	United States of America
UV-vis	Ultraviolet–visible
VEGF	Vascular Endothelial Growth Factor
WGA	Wheat Germ Agglutinin
XRD	X-Ray Powder Diffraction

Chapter 1
Introduction

1. Cancer

1.1. Cancer development and main hallmarks

Cancer is a major health care problem with growing incidence around the globe (Lozano *et al.*, 2012). It is estimated that cancer is responsible for 25% of total deaths in the United States of America (USA). Furthermore, a total of 1,665,540 new cases are expected to be diagnosed in 2014, which is equivalent to more than 4,500 newly diagnosed cancers each day (Siegel *et al.*, 2014). Moreover, in Europe, in 2012, there were an estimated 3,450,000 new cancer cases and around 1,750,000 deaths (Ferlay *et al.*, 2013). These numbers helps to understand the efforts put in the development of new cancer treatments that are more effective than those currently available.

Cancer is a disease that is originated from normal cells that by accumulating multiple transformations can become malignant. When this transformed phenotype is acquired these abnormal cells can affect the function of any organ of the body. Cancer cells generally present features like loss of differentiation and uncontrolled proliferation (Floor *et al.*, 2012). Also, these cells are often capable of invasion of surrounding tissues or even the extravasation to other sites in the body, by a process termed metastasis (Floor *et al.*, 2012). However, this minimalistic concept of cancer has been evolving (Figure 1), instead of a single mass of cancer cells in proliferation, cancer is now considered as much more complex tissue surrounded by the tumor microenvironment (Hanahan and Weinberg, 2000).

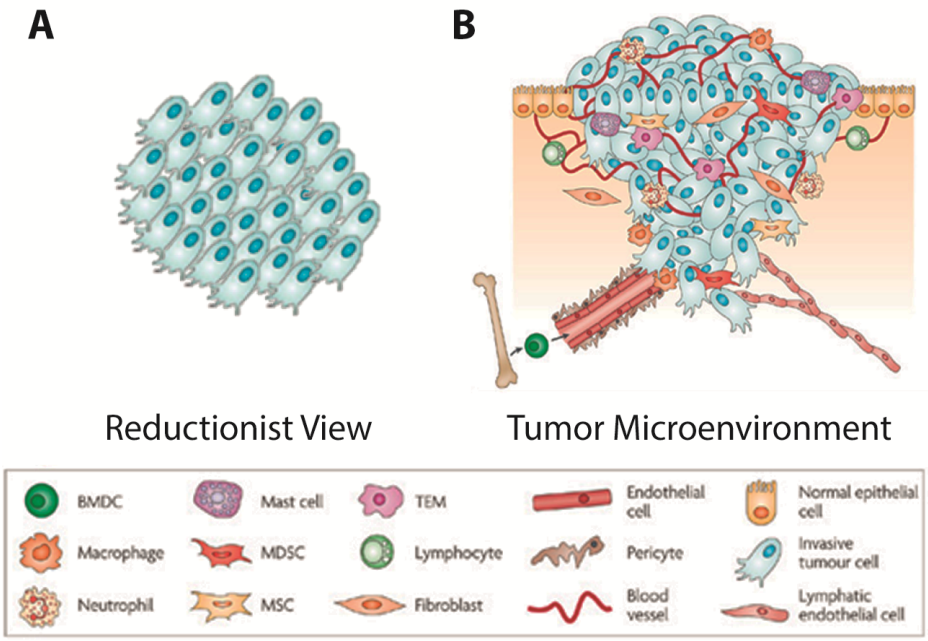

Figure 1 - Evolution of cancer concept. From reductionist a view (A) to tumor microenvironment (B) (Adapted from Joyce and Pollard, 2009).

This complex rich tumor microenvironment is established by resident tumor associated fibroblasts, macrophages, endothelial cells, pericytes, leukocytes, and extra-cellular matrix (Pietras and Ostman, 2010). The individual functions of the various microenvironment elements are summarized in Figure 2 (Hanahan and Coussens, 2012). In general, the cross-talk between tumor cells and their microenvironment elements triggers pro-survival, proliferation and invasion pathways in cancer cells (Liotta and Kohn, 2001, Quail and Joyce, 2013).

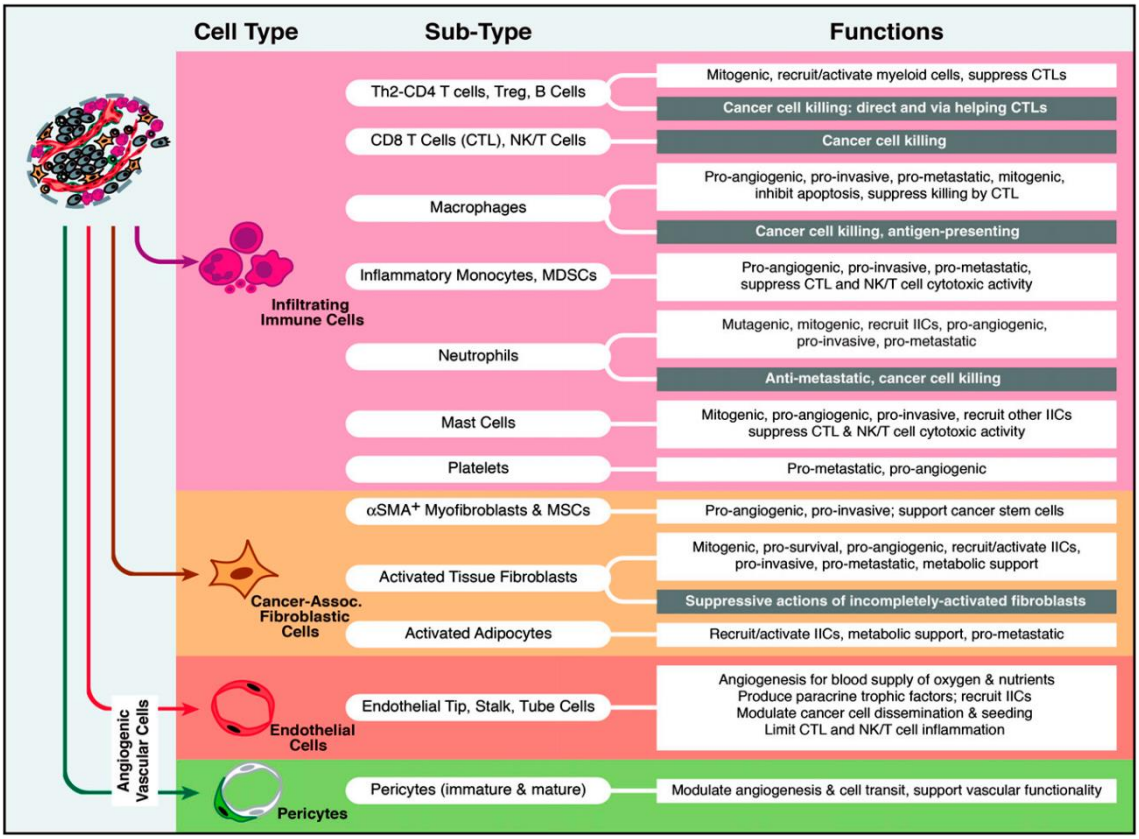

Figure 2 – Major components of the tumor microenvironment. Major cell subtypes and their key functions for tumor development (Adapted from Hanahan and Coussens, 2012).

This combined interaction between the microenvironment elements and cancer cells helps them to maintain certain key characteristics that were described by Hanahan *et al.* as "hallmarks of cancer" (Figure 3) (Hanahan and Weinberg, 2011). One of the first proposed hallmarks and one of the most important, is cancer cells capacity to sustain proliferative signaling, a unique characteristic achieved by the capacity to deregulate growth-promoting pathways (Hanahan and Weinberg, 2000, Daroqui *et al.*, 2012, Quail and Joyce, 2013, Cheng *et al.*, 2008a). However, in order to achieve this sustained proliferation, cancer cells also have to be capable of resisting anti-proliferation signals like those mediated by retinoblastoma protein and its two relatives, p107 and p130 (Hanahan and Weinberg, 2000, Costa *et al.*, 2013, Di Fiore *et al.*, 2013). Another strategy that allows continuous cancer proliferation is the cells ability to avoid programmed cell death, i.e., apoptosis (Hanahan and Weinberg, 2000, Evan and Vousden, 2001). This exceptional capacity arises from the ability to bypass pro-apoptotic signals

commonly present in healthy cells. This gain of function is generally obtained by the loss of *p53* function derived from gene mutation (Wade *et al.*, 2013, Muller and Vousden, 2013), or by overexpression of anti-apoptotic proteins like those of the B-cell lymphoma 2 (Bcl-2) family (Kelly and Strasser, 2011). Other important characteristic is cancer cells limitless replicative potential (Hanahan and Weinberg, 2000). In fact, cancer cells can acquire the capacity to surpass senescence, by up-regulating telomerase expression (Shay and Wright, 2011). Telomerase is a deoxyribonucleic acid (DNA) polymerase that adds repeat segments to telomeric DNA ends, its expression is almost absent in non-immortalized cells (i.e., the majority of cells that compose our organs), but with significant levels of expression in cancer cells (Mocellin *et al.*, 2013). Telomerase overexpression prevents DNA damage and cell death associated to end-to-end fusion of chromosomes (Saharinen *et al.*, 2011). Adding to this, like other tissues, cancer cells require the continuous supply of nutrients, oxygen and means to dispose of all the metabolic waste and carbon dioxide produced during their life (Chung *et al.*, 2010). This nutrient supply/waste exchange mechanism is primarily supported by the tumor surrounding vasculature (Chung *et al.*, 2010). In order to achieve a sustained angiogenesis, cancer cells activate the angiogenic cascade through changes in the balance of angiogenesis inducers and inhibitors (Hanahan and Weinberg, 2000). Tumors appear to have an increased vascular endothelial growth factor (VEGF) expression and other secreted pro-angiogenic factors like fibroblast growth factor (FGF), platelet-derived growth factors (PDGF) and angiopoietins (Weis and Cheresh, 2011). This overexpression results in heterogeneously distributed blood vessels, enlarged, tortuous, with excessive ramifications, large fenestrations (400-600 nm), leakiness, erratic blood flow and abnormal levels of endothelial cell apoptosis (Serres *et al.*, 2014, Fukumura and Jain, 2008). Moreover, at certain point, cancer cells acquire the capacity to invade, survive and proliferate in other tissues and generate metastasis, a characteristic responsible for around 90% of cancer associated mortality (Hanahan and Weinberg, 2011, Chaffer and Weinberg, 2011). A well-known alteration in invasive cancer cells is the down-regulated expression of the protein E-cadherin, which plays an important role in cell-to-cell adhesion (Canel *et al.*, 2013). Other characteristics that influence cancer cell invasion are the modifications in cellular morphology, the expression of matrix-degrading enzymes (matrix metalloproteinases) and an increased cell motility (Yilmaz and Christofori, 2009, Sahai, 2005). Finally, recently, two additional characteristics were proposed as cancer hallmarks, the cells ability to reprogram their metabolism and the ability to avoid immune system mediated destruction (Hanahan and Weinberg, 2011).

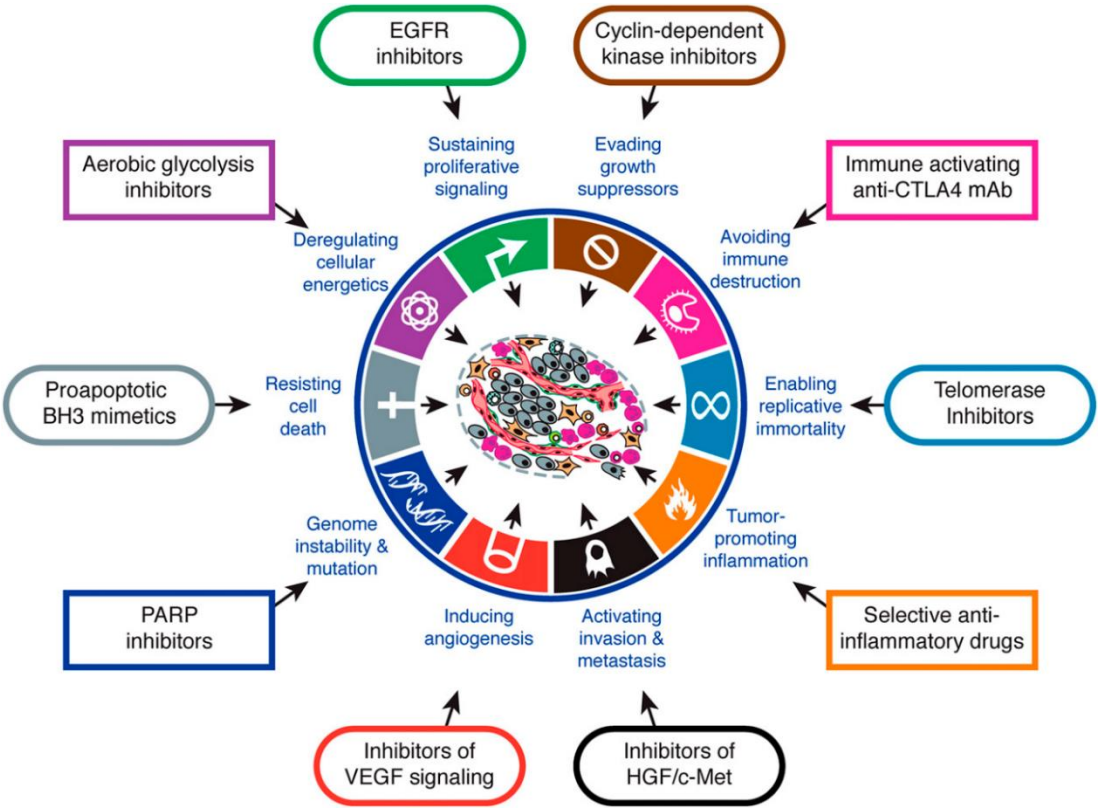

Figure 3 – Cancer hallmarks and therapeutic targets of each key characteristic in cancer cells (adapted from Hanahan and Weinberg, 2011).

1.2. Prostate cancer prevalence and development

Prostate cancer is the most incident cancer in men (Figure 4), with 233,000 expected new cases in USA in 2014 (Siegel *et al.*, 2014). Furthermore, prostate cancer will be responsible for around 30,000 deaths, being the second deadliest cancer for men in USA (Siegel *et al.*, 2014). In Portugal, according to official data from *Direção Geral de Saúde* (DGS), in 2007, prostate cancer presented an incidence of 114 cases per 100,000 and resulted in 1,654 deaths, a mortality rate of around 37%.

Prostate cancer is predominantly diagnosed at an old age, being rare before 50 years of age. More than 75% of men over the age 75 presently have been diagnosed with this type of malignancy (Arcangeli *et al.*, 2012, Siegel *et al.*, 2014). Thus the leading risk factor for prostate cancer is advanced age, followed by race (Grönberg, 2003). The African-American men presents the highest rate (137 cases per 100,000), followed by North American and Scandinavian individual. On the opposite side, the prevalence of prostate cancer in Chinese people is relatively low in comparison to other countries (1.9 cases per 100,000) (Center *et al.*, 2012). Despite these relevant differences, a common risk factor to prostate cancer is family history, i.e. genetic predisposition to prostate cancer. Since, the probability to be diagnosed with prostate cancer increases two-fold for men who have or had a first degree relative that suffered from it (Loeb and Schaeffer, 2009).

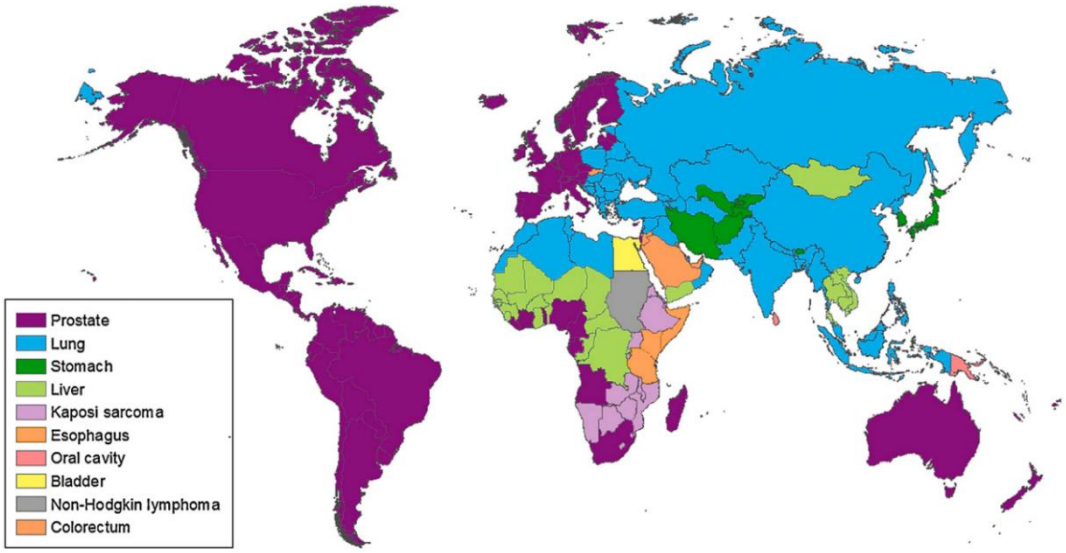

Figure 4 –Most commonly diagnosed types of cancers worldwide in men, in 2008 (adapted from Center *et al.*, 2012).

The prostate is a glandular and muscular organ that works as a reproduction accessory gland. It is located in the lower pelvis around the beginning of the urethra (Lee *et al.*, 2011a). The prostate has 5 anatomic zones (Figure 5) the peripheral, central, transition, fibromuscular, and periurethral gland region and its primary function is to secrete a fluid, which aids in motility and nourishment of the sperm (McNeal, 1981).

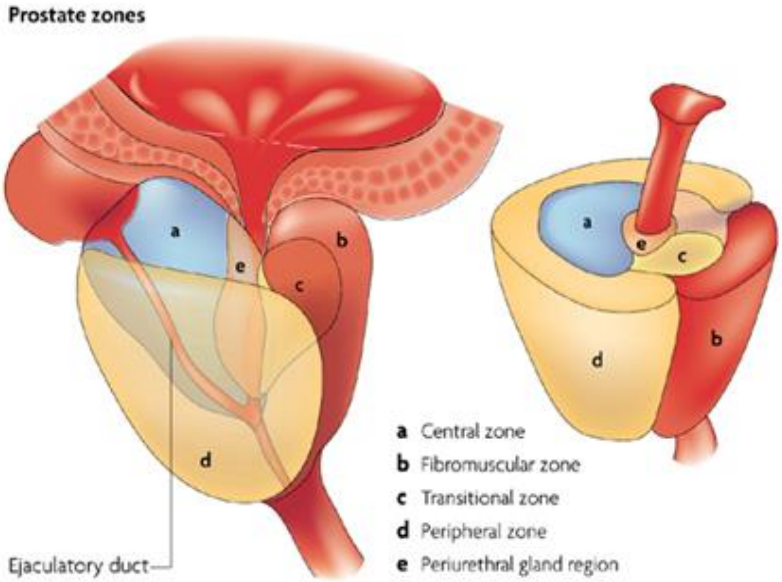

Figure 5 – Representation of Prostate anatomic zones (Adapted from De Marzo *et al.*, 2007).

Prostate cancer development is generally characterized by a phenotype transition (So *et al.*, 2003). In an initial phase of development, prostate cancer is mainly composed by a mass of androgen dependent cells, where growth and survival signaling are closely regulated by the androgen receptors (Taplin, 2007, Jenster, 1999). During cancer progression a phenotype transition to androgen independent cells is observed, and is strongly correlated with genetic modifications like Bcl-2 overexpression, oncogenes activation and inactivation of tumor suppressor genes (Feldman and Feldman, 2001). This phenotype modification, normally originates a much more aggressive type of prostate cancer with great metastatic capacity (Feldman and Feldman, 2001). Furthermore, in prostate cancer several molecules responsible for cell cycle control, cell growth and proliferation have their expression diminished (De Marzo *et al.*, 2007). Some examples are the p27 (an inhibitor of cell cycle progression), the NKx3.1 gene (a prostate cell growth suppressor gene) and the PTEN (a tumor suppressor) (De Marzo *et al.*, 2007, Shen and Abate-Shen, 2003). On the other side, various molecules produced either by the original tumor or in response to the malignant cells presence can be used as biomarkers for this disease (Romero Otero *et al.*, 2014). Some examples for prostate cancer are PCA3 (prostate cancer antigen 3) and PSA (prostate-specific antigen), being the latter extensively used for prostate cancer screening (Romero Otero *et al.*, 2014).

The most common prostate cancer and representing more than 95% of prostate cancers arises from the prostate gland epithelial cells (Goldstein *et al.*, 2010). Nonetheless, there are other types of prostate cancers like the transitional cell cancer, the squamous cell prostate cancer, the carcinoid of the prostate and the small cell prostate cancer (Goldstein *et al.*, 2010). Normally, prostate cancer is asymptomatic, particularly in the early development stages making difficult its early detection (Shen and Abate-Shen, 2003). Moreover, prostate cancers retain many of the healthy prostate properties, including their ability to form the secretory proteins and, ejaculate major components (Shen and Abate-Shen, 2003).

1.3. Anti-tumoral drugs used in prostate cancer

Currently there are several strategies that can be applied for prostate cancer treatment, these include: radiation, proton beam therapy, chemotherapy, hormonal therapy, cryosurgery, and high intensity focused ultrasound (Porche, 2011).

Chemotherapy arises as a first-line therapy for prostate cancers in advanced stages, it has shown some improvements in pain reduction and increase the life quality of prostate cancer patients (Picard *et al.*, 2012). Some of the most commonly used chemotherapeutic drugs for prostate cancer treatment include Docetaxel, Doxorubicin, Mitoxantrone, Paclitaxel, Vinblastine, and others (Saad and Miller, 2014). In the USA, Europe, and Canada the standard chemotherapeutic treatment is Docetaxel, which is administered every 3 weeks in combination with corticosteroids (Prednisone) (Saad and Hotte, 2010). Docetaxel is a member of taxane family, which promotes tubulin assembly in microtubules and inhibits their depolymerization

(Lavelle *et al.*, 1995). The administration of Docetaxel has shown to improve patient survival average in 2 months, at the cost of significant toxicity like some cardiac dysfunctions, fatigue, and sensory neuropathy (Tannock *et al.*, 2004). Other alternative drug commonly used is Mitoxantrone, a DNA intercalator that causes crosslinks and strand breaks (Fox, 2004). It is less toxic, but not so effective in cancer treatment, presenting only palliative benefits (Tannock *et al.*, 2004). The additionally used drugs presented above namely, Doxorubicin, Paclitaxel and Vinblastine can also be effectively in the treatment of prostate cancer (Saad and Miller, 2014). However, the side effects (e.g. cardiotoxicity and hepatoxicity) resulting from their administration restrains their widespread use in clinical practice (Monsuez *et al.*, 2010).

In fact, it is generally recognized that free drug administration (e.g., administration of bioactive compounds without any pharmaceutical excipient) shows some disadvantages that reduce its effectiveness and discourage long-term application (Evans and McLeod, 2003). Some of the conventional problems of free drug formulations are: i.) low specificity (side effects), ii.) poor solubility and iii.) tissue partitioning that consequently lowers drug bioavailability (Allen and Cullis, 2004). These sub-optimal physicochemical characteristics often lead to the necessity to administer higher doses in order to produce a therapeutic effect, which in turn increases the probability of severe side effects. A potential solution that might contribute for the use of lower drug concentration is their combined administration, in order to achieve a synergistic therapeutic effect, when the drug combination produces an effect greater than the sum of their individual components (Nabholtz and Riva, 2001). Since the combination of two or more anti-tumoral pharmaceutics unlocks the possibility to simultaneously target different intracellular pathways, or even different cancer hallmarks such as those that support cell survival (Ferlini *et al.*, 1997).

Examples of this co-delivery concept for application in prostate cancer treatment is the mainstream treatment of Docetaxel/Prednisone. Moreover, ongoing phase III clinical trials involving their combination with other therapeutic agents are also trying to discover novel drug synergies (Saad and Miller, 2014). Quinn and coworkers, 2013, tested the combination of Docetaxel/Prednisone with Atrasetan (endothelin A receptor antagonist). Their results showed that no additional benefits for patient survival were obtained with this combination, moreover, similar toxicity to Docetaxel/Prednisone alone was verified (Quinn *et al.*, 2013). Other combinatorial formulation tested was Dasatinib conjugated with Docetaxel/Prednisone (Saad and Miller, 2014). This ongoing phase III clinical trial is estimated to have 1,500 patients, and is supported for its promising data in phase I/II trial (Araujo *et al.*, 2012). This combination showed higher tumor response than the studies with Docetaxel alone, followed by reduction of some tumor biomarkers (Araujo *et al.*, 2012). However, in these studies no significant improvements in Docetaxel/Prednisone derived toxicity was observed (Allen and Cullis, 2004).

Other chemotherapeutic drugs like Doxorubicin and Ibuprofen can also be used for the treatment of prostate cancer. Doxorubicin is a first line cancer therapy that is routinely used

in the treatment of breast, lung, and gastric cancers (Thorn *et al.*, 2011). Doxorubicin (Figure 6) belongs to a class of compounds called anthracyclines and has a planar structure that intercalates between neighboring DNA pairs anchored to one side through a covalent bond to one or more sugar units, and establishes formaldehyde and hydrogen bonds with a guanine on the opposing strand (Yang *et al.*, 2014). The Doxorubicin intercalation in DNA promotes an increase in torsional stress, which can affect the nucleosomes structure and dynamics (Yang *et al.*, 2014). Two major doxorubicin associated mechanisms of action (Figure 6) are generally described: i.) the disruption of topoisomerase-II repair and ii.) the generation of free radicals (Thorn *et al.*, 2011, Yang *et al.*, 2014).

Topoisomerases are enzymes responsible for regulate the DNA topology to facilitate DNA replication, transcription, and other nuclear processes (Nitiss, 2009). Particularly, topoisomerase II activity involves DNA entangling, and the cleavage of one strand of DNA duplex and the subsequent passage to a second duplex, through a transient cleavage (Swift *et al.*, 2006). The anti-tumoral drug Doxorubicin impairs this cleavable complex, inhibiting the reconnection of the cleaved strands (Yang *et al.*, 2014), which in turn triggers programmed cell death, i.e., apoptosis.

Other mechanism by which Doxorubicin can led to cell death is through the generation of free radicals (Keizer *et al.*, 1990). The quinone structure can be oxidized by a number of nicotinamide adenine dinucleotide phosphate (NAD(P)H) oxidoreductases, the resulting semiquinones react quickly with oxygen and generate superoxide and hydrogen peroxide (Yang *et al.*, 2014, Keizer *et al.*, 1990). Doxorubicin easily binds to iron, and the formed complex catalyzes the hydrogen peroxide conversion into hydroxyl radicals (Thorn *et al.*, 2011). The formed radicals can damage cell membranes, DNA, and proteins that can promote cell death.

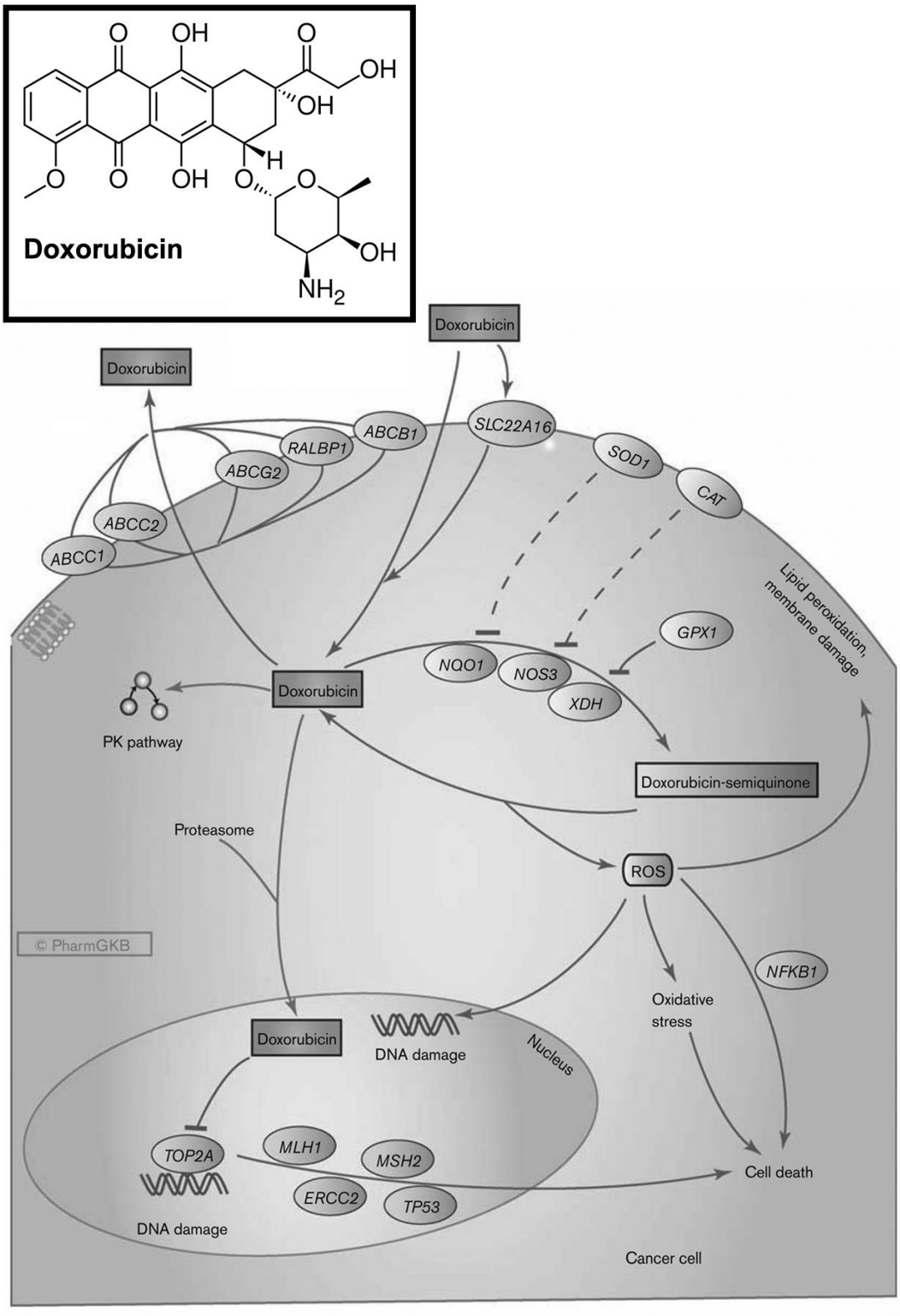

Figure 6 – Doxorubicin molecular structure and the representation of its mechanisms of action (Adapted from Thorn *et al.*, 2011).

Ibuprofen (Figure 7) is a non-steroidal anti-inflammatory drug (NSAID) that inhibits the cyclooxygenases 1 and 2 (COX-1 and COX-2). It has been applied in the treatment of several pathologies. Moreover, NSAIDs have been associated with cancer prevention, and NSAIDs such

as Aspirin and Ibuprofen promoted a significant anti—cancer activity (Marques *et al.*, 2014, Baek *et al.*, 2002). COX-2 expression activates the body inflammatory response, in the presence of stimulus such as traumas, foreign bodies, toxins, and bacteria, and their expression quickly results in the production of E-series prostaglandins (PGE) particularly PGE-2 (Harris *et al.*, 2012). This inflammatory response, as all processes in human body is tightly controlled, but the continuous overexpression of COX-2 could initiate and promote carcinogenesis by several pathways (Figure 7) (Dannenberg *et al.*, 2001). One option is the increase production of PGE-2 and other factors that promote cell proliferation. Also, the overexpression of COX-2 could increase the production of malondialdehyde and other oxygen reactive species (Nie *et al.*, 2001). Moreover, it can stimulate the production of VEGF and PDGF promoting angiogenesis and metalloproteinases production, thus enhancing the invasive potential of cancer cells (Harris *et al.*, 2012). Moreover, COX-2 can stimulate malignant cell proliferation through Bcl-2 stimulation, and also at the same time, contribute to inhibit the proliferation of B and T lymphocytes, reducing their antineoplastic activity (Nie *et al.*, 2001, Harris *et al.*, 2012).

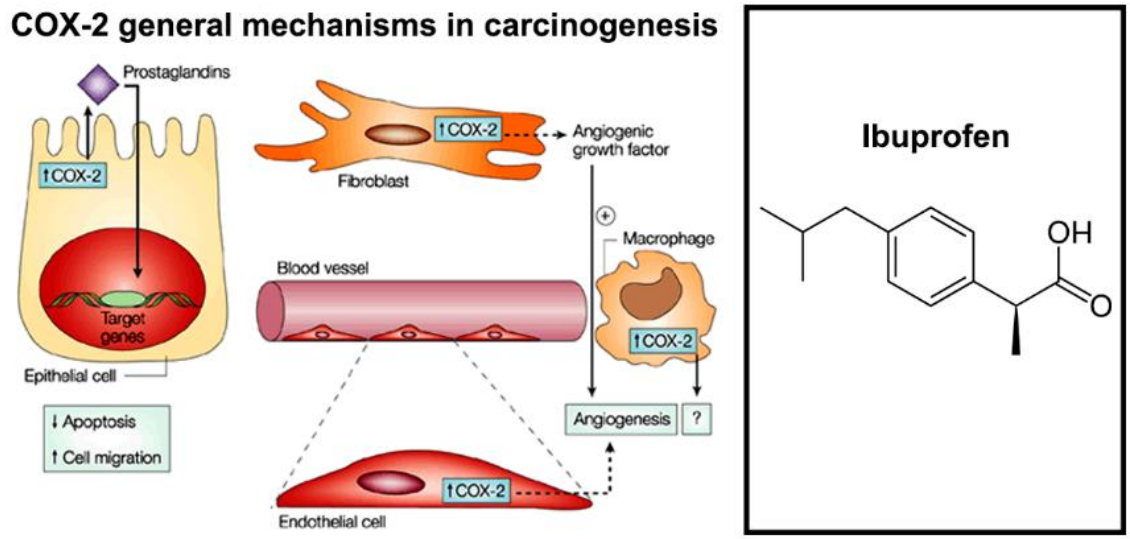

Figure 7 – Ibuprofen molecular structure and COX-2 role in tumor development, cell-directed and microenvironment general effect (Adapted from Gupta and Dubois, 2001).

2. Nanotechnology and drug delivery systems

However, even using these combined therapies the side effects associated to drug administration are still prevalent. Moreover, the expected augmented therapeutic effect is not always obtained, due to problems that include rapid metabolism, poor solubility and inconsistent bioavailability (Greco and Vicent, 2009). These facts demonstrate the necessity to develop alternatives to conventional drug administration, in order to enhance their *in vivo* efficacy.

2.1. Nanosized delivery systems for delivery of bioactive molecules

The application of Nanotechnology in healthcare is becoming a very common strategy. Moreover, it arises as one of the most compelling solutions to the problems faced by biotechnological and pharmaceutical industries in the development efficient and non-toxic cancer therapeutics (Akhter *et al.*, 2013). The development of the so-termed nanomedicines offers the opportunity to overcome the several limitations associated to conventional drug delivery (Cho *et al.*, 2008). These nanocarriers, i.e. delivery vehicles with nanoscale size can be easily tailored to possess unique compositions and functionalities that will improve the transported cargo therapeutic effect (Wang and Wang, 2014). Therefore, the nanocarriers can offer many advantages over free drug administration. They have the capacity to increase the solubility and at the same time protect bioactive molecules from premature degradation and interaction with blood components such as serum albumin (Davis *et al.*, 2008). Furthermore, nanocarriers can improve the tissue penetration and accumulation, intracellular penetration and drug absorption in a selected tissue, improving their bioavailability (Alonso, 2004). Finally, the nanocarriers have the capacity to transport a large drug payload and control its release (Ganta *et al.*, 2008). These advantages decrease the toxic side effects and promote an enhanced therapeutic outcome. Nevertheless, in order to be applied as delivery systems the nanocarriers need to possess an array of key properties that must be taken into account during nanodevices production process (Davis *et al.*, 2008). One of the most important characteristics is particle size, that should be in the range of 10-200nm (Ernsting *et al.*, 2013). The lower bound is the estimated size threshold where the particles are readily eliminated by kidneys, being excreted in urine (Ernsting *et al.*, 2013). On the other side, the upper limit it is not so well defined but it is influenced by the tumor permeability and splenic filtration (Davis *et al.*, 2008). Other important feature is morphology, in fact it has been described that nanocarriers geometry and surface orientation influence their cellular uptake (Herd *et al.*, 2013). The surface properties are also a very important characteristic (Davis *et al.*, 2008). Due to the high surface-volume ratios presented by nanocarriers, their surface properties play an important role in the interactions with the complex biological environment. Characteristics like

hydrophobicity and surface charge will influence the nanocarrier biological processing and fate (Ernsting *et al.*, 2013). Changes in these parameters will modify their interaction with cells, proteins and even influence particle-particle agglomeration. Gessner *et al.*, studied nanoparticles with decreasing surface hydrophobicity and their influence on plasma protein adsorption (Gessner *et al.*, 2000). In this study the authors verified that a reduction in surface hydrophobicity led to decrease in protein adsorption (Gessner *et al.*, 2000). The surface charge effect in nanocarrier interaction with cells is dependent of the cell type, probably because the differences verified in the molecules present in cell surface that will influence the cell-nanoparticle interaction (He *et al.*, 2010a). But, in general, the particles with surface charge within ±10 mV showed optimal properties, exhibiting lower reticuloendothelial system interaction and extended circulation time (Ernsting *et al.*, 2013).

2.2. Classes of nanocarriers

Due to the unique characteristics presented by nanosized systems, in the last years, several different types of nanocarriers have been developed to be applied in different therapies.

The major classes of nanocarriers comprise (Figure 8): i.) liposomes, ii.) solid lipid nanoparticles, iii.) dendrimers, iv.) micelles, v.) polymeric nanoparticles and vi.) inorganic nanoparticles (including iron, gold, carbon and silica).

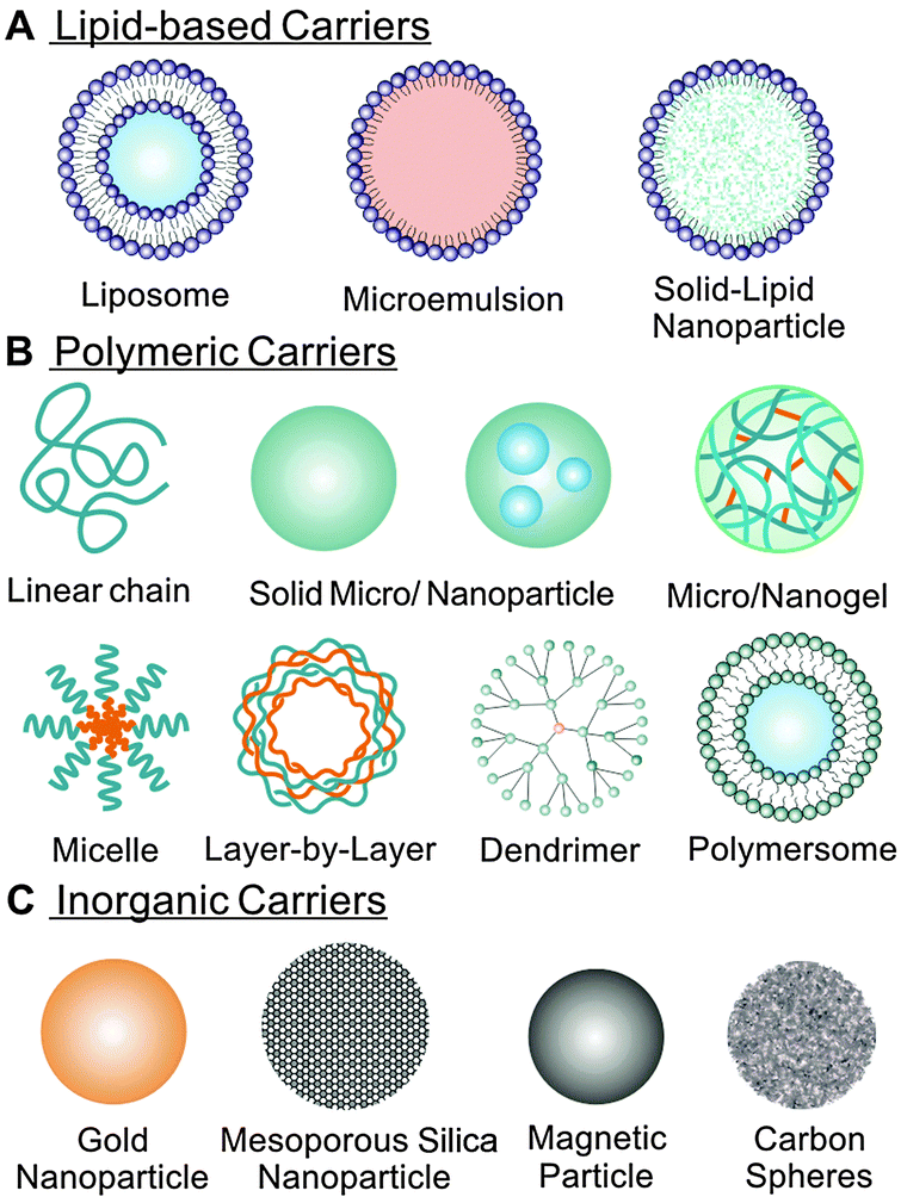

Figure 8 – General nanocarrier-based strategies employed for drug delivery, and their structure representation (Adapted from Mo *et al.*, 2014). (A) Lipid-based nanocarriers; (B) Polymeric nanocarriers; and (C) Inorganic nanocarriers.

Liposomes were the first nanocarriers used to deliver drugs to cancer cells that were approved by European Medicines Agency (EMA) and Food and Drugs Administration (FDA) for cancer treatment (Wang and Thanou, 2010). Examples of these systems are Doxil® (Doxorubicin encapsulated in a PEGylated liposome), DepoCyt (Cytarabine loaded liposome), Myocet (Doxorubicin loaded liposome) and Daunoxome (Daunorubicin loaded liposome) systems that have been used to treat cancer and other diseases (Zhang *et al.*, 2011). They present a huge diversity of structure and compositions, but in general they are closed spherical vesicles constituted by a membranous lipid bilayer that surrounds an aqueous core compartment (Figure 8 A) (Al-Jamal and Kostarelos, 2011). It is worth to notice that the vesicles can be organized in single or multiple concentric bilayers (Allen and Cullis, 2013). Furthermore, the lipid bilayer

can be made from natural or synthetic phospholipids and cholesterol. These various combinations will in turn affect the liposome physicochemical properties, including their permeability, charge density and steric hindrance (Zhang *et al.*, 2011). Other important characteristic is the liposomes capacity to load hydrophilic or hydrophobic bioactive molecules (Yang *et al.*, 2011). Although, it is important to notice that liposomes present some limitations in their *in vivo* application. Some of the observed problems are correlated with short blood circulation time, *in vivo* instability, low solubility, opsonization and content leakage (Akbarzadeh *et al.*, 2013).

Solid lipid nanoparticles (SLNs) are made from solid lipids stabilized by surfactants (Mehnert and Mader, 2001). SLNs are solid at room temperature and body temperature, can be comprised highly purified triglycerides (tricaprin, trilaurin, tripalmitin and others), complex glyceride mixtures (glyceryl palmitostearatea and glyceryl monostearate) or even waxes (cetyl palmitate) (Wissing *et al.*, 2004). SLNs generally form structures that have a solid hydrophobic core having a layer of phospholipid coating (Figure 8 A) (Mehnert and Mader, 2001). Being the cargo dissolved or dispersed in the solid matrix, they possess the ability to carry lipophilic or hydrophilic bioactive compounds (Kaur *et al.*, 2008). The solid nanoparticle properties are mainly influenced by their lipid composition, production method and surfactant type (Mehnert and Mader, 2001). But they present some advantages like their composition (physiological compounds), biocompatibility, and potential for large scale production (Mehnert and Mader, 2001). Furthermore, their content release can be modulated depending on the drug loading process (Almeida and Souto, 2007). On the other hand, these nanocarriers present some disadvantages namely their low drug loading capacity and presence of alternative colloidal structures, beyond nanoparticles micelles, liposomes and drug nanocrystals can also be formed (Mehnert and Mader, 2001). Moreover, the lipids can suffer transformations after the production process, also the sample dilution or water removal can change the particle stability and these modifications can originate premature drug release (Wissing *et al.*, 2004).

Dendrimers are globular nanosized macromolecules with a characteristic branched structure that can be divided in three domains (Wijagkanalan *et al.*, 2011). A core consisting in an atom or molecule, the interior shell formed by branches deriving from the core, and the terminal functional groups (Figure 8 B) (Frechet, 1994). These three domains can be tailored to serve various purposes, such as drug and gene delivery (Somani *et al.*, 2014, Kesharwani *et al.*, 2014). The high level of control over the dendrimer architecture, branching length and density, makes it easy to tailor their size, shape, and surface functionality (Svenson and Tomalia, 2005). However, they present immunogenicity, and also cationic dendrimers are highly cytotoxic hindering their application in the clinic (Lee *et al.*, 2005).

Micelles are formed by blocks of copolymers consisting in hydrophilic and hydrophobic monomer units (Yih and Al-Fandi, 2006). Their hydrophobic core functions as a reservoir for poorly water-soluble drugs and the hydrophilic shell protects and controls the release of entrapped bioactive

molecules (Figure 8 B) (Zhang *et al.*, 2011). Polymeric micelles have been reported as physiologically stable, biodegradable, with a surface suitable to be functionalized with cell targeting ligands, and with a long half-life in the body (Cho *et al.*, 2008). Despite these valuable properties, micelles still show poor penetration into solid tumors, and also a burst drug release is verified in some micellar formulations (Miller *et al.*, 2013).

Polymeric nanoparticles can be formed by synthetic or natural polymers. Moreover, the drugs can be immobilized on their surface or encapsulated in the polymeric structure, which gives the possibility to transport a wide range of therapeutics including drugs, proteins and nucleic acids (Faraji and Wipf, 2009). Most polymeric nanoparticles are biodegradable and biocompatible, present a surface suitable to be functionalized with various moieties and tunable drug release (Parveen *et al.*, 2012).

Inorganic nanoparticles (Figure 8 C) comprise carbon nanotubes, gold nanoparticles, magnetic nanoparticles, mesoporous silica nanoparticles (MSNs), and quantum dots (Ladj *et al.*, 2013). These different types of inorganic nanocarriers possess unique features to be used as delivery carriers, like a robust and stable structure, high loading capacity and a surface easily modified with different components to give them multifunctional capabilities (Jia *et al.*, 2013). Furthermore, inorganic nanoparticles can exhibit imaging capacities through their magnetic properties and photothermal capabilities (Liong *et al.*, 2008). However, the inorganic nanocarriers present some drawbacks, since they have a low biocompatibility and some aggregation issues (Ladj *et al.*, 2013).

2.2.1. Mesoporous silica nanoparticles

Among the different carriers types presented above, ceramic particles have also been presented as a very interesting carriers. They have been highlighted due to their mechanical strength, chemical stability, porosity, relative biocompatibility and their resistance to microorganisms (Rosenholm *et al.*, 2010). Moreover, the ceramic matrix does not suffer swelling or porosity changes, and also it is capable to protect the guest molecules from the action of enzymes and degradation resulting from pH or temperature (Rosenholm *et al.*, 2010).

Inside the different ceramic particles, mesoporous silica nanoparticles have attracted a significant research attention for their potential application in Nanomedicine (Figure 9). A particular type of MSNs, mobil crystalline materials (MCM-41), contain a characteristic honeycomb-like porous structure with a large number of empty channels (mesopores) running from one end of the structure to the other without interconnectivity. They also possess unique properties like tunable particle size, stable and rigid framework (compared to polymer based nanocarriers, MSNs are more resistant to pH, heat and mechanical stress), a high surface area (>700m^2/g), large pore volume (>0.6cm^3/g), uniform and tunable pore size (2-10nm) and good chemical and thermal stability (Li *et al.*, 2012, Tang *et al.*, 2012). Moreover, their large surface area, pore volume and the possibility to use the optimal solvent with no negative consequences

for the particle allows high loadings of therapeutic biomolecules with great efficacy (Slowing *et al.*, 2008).

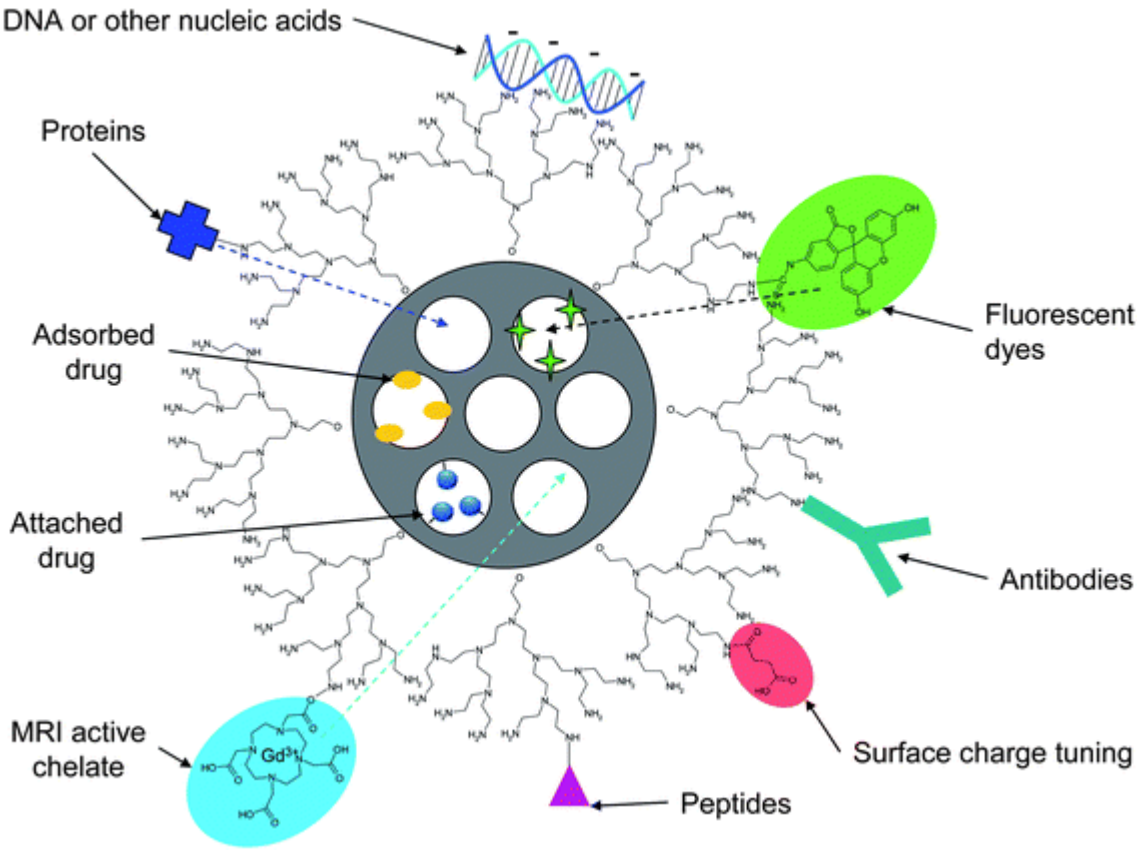

Figure 9 – Mesoporous silica nanoparticles general structure, and their cargo loading and possibilities of surface functionalization (Adapted from Rosenholm *et al.*, 2010). Silica nanoparticles are capable to encapsulate several different biomolecules and are easily to functionalize with polymers and other components that will confer specific properties.

2.2.1.1. Chemical production of MSNs – The Stöber modified method

In 1968, Stöber and collaborators applied an effective method for the controlled growth of uniform silica particles, which involves the hydrolysis of tetra alkyl silicates in a mixture of alcohol and water using ammonia as a catalyst (Stöber *et al.*, 1968). Actually, most of the reported synthesis processes for mesoporous silica nanoparticles are based in the Stöber method. Generally they involve the use of an organosilane precursor (e.g. tetramethyl orthosilicate (TMOS) and tetraethyl orthosilicate (TEOS)), a cationic surfactant hexadecyltrimethylammonium bromide (CTAB), that will work as a structure guiding agent, water as solvent, and sodium hydroxide as morphological catalyst (Slowing *et al.*, 2008). Afterwards, the template surfactant (CTAB) is removed by solvent extraction (hydrochloric acid (HCl) in alcohol solution) or calcination to originate nanopores. The particle formation in this process occur by base-catalyzed sol–gel condensation around the hexagonally packed micelle structures.

2.2.1.2. Surface functionalization of MSNs

Beyond the above presented characteristics, MSNs also present a modifiable surface, which is easy to functionalize with various types of biomolecules, including fluorescent dyes, antibodies, peptides, proteins, surface charge tuning molecules and others (Figure 9) (Wu *et al.*, 2014). Moreover, it can be considered that MSNs have two surfaces that can be functionalized, an internal surface (cylindrical surface pores) and external surface (exterior particle surface) (Slowing *et al.*, 2008). This interestingly feature allows a selective particle functionalization, where the surface to functionalize can be chosen accordingly to a particular application and also allows the use of multiple moieties in external and internal surfaces (Slowing *et al.*, 2008). Regarding surface functionalization two different methods are generally used, condensation and chemical grafting (Slowing *et al.*, 2008). In the condensation method, organic alkoxysilanes are added to the synthesis reaction and bonded to the particle during its assembly (Radu *et al.*, 2005). In the grafting method, the functionalization occurs post synthesis, and the chosen moiety binds to the particle surface silanol groups (He *et al.*, 2010c). In order to use the grafting method, it is important to not use calcination as the purification process, since it promotes the condensation of MSNs silanol groups reducing the number of groups available for functionalization (Slowing *et al.*, 2008).

2.2.1.3. Mesoporous silica nanoparticles uptake and biocompatibility

The nanocarrier cellular uptake is a very important process in the delivery of anti-tumoral drugs via the action of nanocarriers. Unmodified MSNs present affinity for some of the head-groups of cell membrane phospholipids, particularly for the positive charged ones like 1,2-dioleoyl-3-trimethylammonium-propane. This affinity to the cell surfaces greatly facilitates the uptake process (Mornet *et al.*, 2005). Moreover, further studies demonstrated that MSNs uptake is dependent on size, shape and surface functionalization, but it mainly occurs through the clathrin-coated endocytosis pathway and trough pinocytosis (Figure 10) (Huang *et al.*, 2010).

Other uptake routes for MSNs can be also verified, like caveolin-dependent and receptor mediated (Li *et al.*, 2012). The surface shape can also affect MSNs uptake, Trewyn *et al.* found that spherical and rod shape MSNs needed 180 min and 360 min, respectively, to be completely internalized by cells (Trewyn *et al.*, 2008).

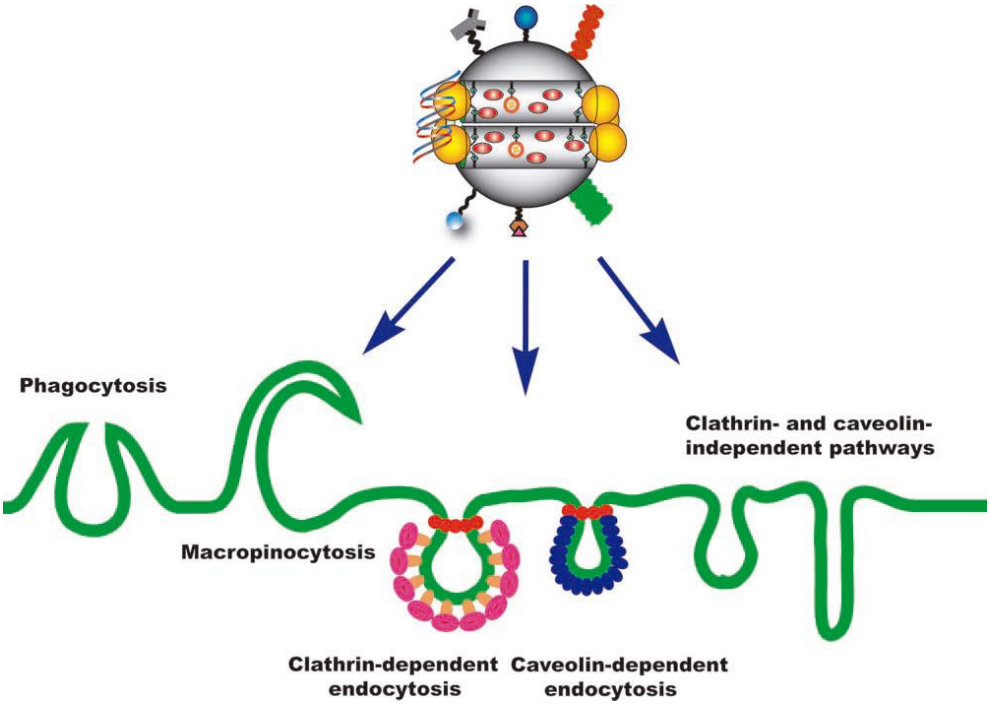

Figure 10 – Pathways used by mesoporous silica nanoparticles for cellular internalization (Adapted from Vivero-Escoto *et al.*, 2010). The uptake pathway will be depend from the physicochemical properties possessed by the MSNs.

Other important parameter for assessing the applicability of MSNs is their biocompatibility. MSNs surface charge and size largely influence their toxicity. Concerning particle size it was demonstrated by Napierska and coworkers that particles with size lower than 50 nm induced cell death and even necrosis in human endothelial cells, whereas particles above 100 nm presented minor toxicity (Napierska *et al.*, 2009). It is worth to notice that larger particles and even particles with rod morphology have higher cytotoxicity, since these particles cause a great disorder in F-actin formation and therefore disturbance in the organization of the cytoskeleton and cell membrane (Huang *et al.*, 2010). This fact can lead to cell membrane disruption and cell death (Huang *et al.*, 2010). Nanoparticle surface charge can also affect MSNs biocompatibility, Shahbazi *et al.* showed that negatively charged MSNs (-31 mV) produced less adenosine triphosphate (ATP) depletion and genotoxicity than those positively charged (32 mV) (Shahbazi *et al.*, 2013).

In general, MSNs are reported to be safe in concentrations lower than 100 µg/mL, which is superior to the particle concentrations needed in most therapeutic treatments (Rosenholm *et al.*, 2010). Furthermore, in this concentration range the morphology of healthy cells and

membrane integrity is conserved (Slowing *et al.*, 2008). Also the growth rates remain unchanged indicating that no damage to the cells replication machinery occurs (Slowing *et al.*, 2008).

2.3. Administration routes and barriers

Nanocarriers can be administered by several different administrations routes such as nasal, ocular, oral, intradermic and intramuscular or intravenous (Rabanel *et al.*, 2012). Moreover, depending on the chosen route of administration the nanocarriers will have to surpass several barriers in order to reach the desired site (Ferrari, 2010). Therefore, as above mentioned, their size and surface properties assume a critical role in their ability to overcome these major obstacles upon delivery in human body (Figure 11).

One route of administration of MSNs is the intravenous injection. Which is the quickest and simplest method for delivering therapeutics to systemic circulation, and it is a relatively invasive approach that reduces the losses associated to other approaches like nasal, ocular and oral (Cheng *et al.*, 2008b). However, this route has a variety of barriers associated with, that difficult an effective nanoparticles delivery.

The reticuloendothelial system (RES) is a global system comprised by phagocytic cells in the liver, spleen, and bone marrow, whose primary function is to eliminate foreign objects, such as microbes and also nanocarriers (Ernsting *et al.*, 2013). The RES does not have the capacity to recognize these foreign bodies, first they have to be coated by a protein layer in a process called opsonization (Steichen *et al.*, 2012). These proteins called opsonins adhere to the foreign particles by ionic, the electrostatic and hydrophobic forces and can be immunoglobulins, components from complement system (C3,C4 and C), fibronectin, and others (Steichen *et al.*, 2012). The macrophages will recognize the opsonin coated particles and will attack them leading to their clearance from circulation (Elsabahy and Wooley, 2012).

Other important barrier is the first pass renal filtering, where the kidneys filter the blood through the glomerular wall, and normally particles with size smaller than 8 nm are rapidly eliminated from circulation (Ernsting *et al.*, 2013). The particle excretion is also observed in the liver and spleen, where particles with size higher than 200 nm are cleared into bile, and then into feces (Elsabahy and Wooley, 2012). On the other hand it is also crucial that particles extravasation to the tumor site occur. This process is largely influenced by the heterogeneous blood flow and high tumor interstitial pressure (Ernsting *et al.*, 2013). The heterogeneous blood flow arises as result of the characteristic aberrant an unorganized tumor vasculature, that will difficult the uniform particle dispersion in the tumor (Serres *et al.*, 2014). The high tumor interstitial pressure is promoted by the high vascular permeability and lack of lymphatic drainage, and as the pressure increases in the tumor center it inhibits the drug accumulation and dispersion in the diseased tissues (Ernsting *et al.*, 2013).

One last barrier that the particles have to surpass is intracellular trafficking to the site of action, where the particles must be internalized, transpose the cell membrane through the complex cell cytoplasm (Chithrani and Chan, 2007, Ruenraroengsak *et al.*, 2010). Subsequently, the particles have to be capable of escaping from lysosomes and protect their cargo from the action of intracellular enzymes in order to assure its therapeutic efficacy.

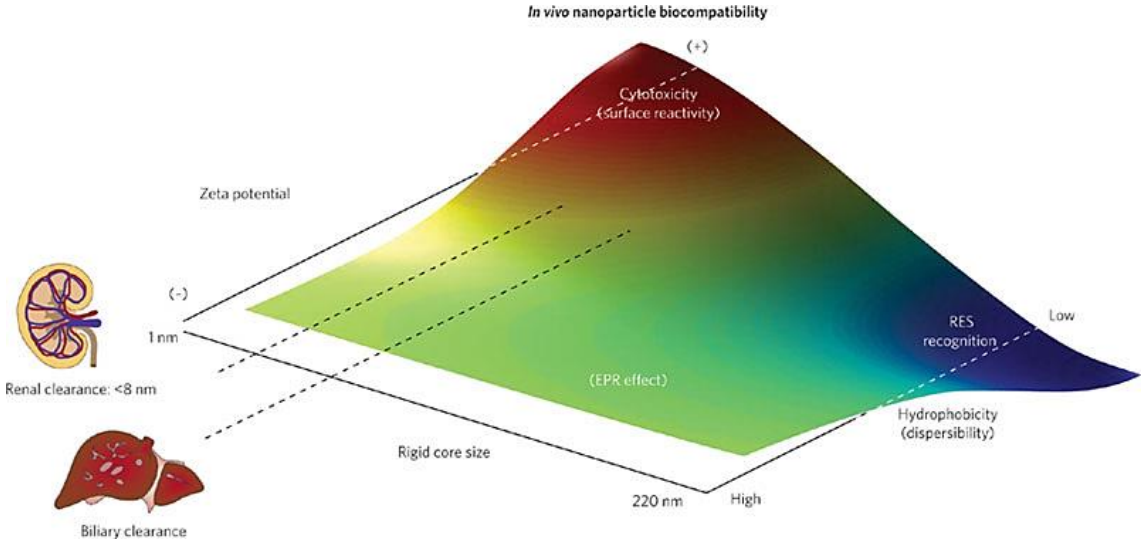

Figure 11 – Physical characteristic of nanoparticles that determine their biocompatibility and capacity to surpass certain barriers (Adapted from Nel *et al.*, 2009). Red representing likely toxicity, blue likely safety and blue–green–yellow intermediate levels of safety.

2.4. Nanocarriers targeting to tumor tissues

2.4.1. Passive Targeting

As described above the rapid vascularization in tumors results in leaky, and defective vasculatures and impaired lymphatic drainage (Nie *et al.*, 2007). Therefore the combination between the large gap sizes in vessels (100 nm to 2 μm) with poor lymphatic drainage allows high retention times for particles that gain interstitial access to tumors, an effect known as Enhanced Permeability and Retention (EPR) effect (Figure 12 A) (Byrne *et al.*, 2008). Nanoparticles smaller than the defective fenestrations (400-600 nm) can escape from the vasculature and accumulate in the tumor. Actually, the EPR effect is present in almost all the tumors with exception for the hypovascular ones, such as prostate or pancreatic tumors (Danhier *et al.*, 2010).

In order to really benefit from the EPR effect and increase the possibilities to accumulate in the tumor, the nanocarriers need to remain in circulation as much time as possible (Ernsting *et al.*, 2013). The most commonly chosen method is the nanocarrier PEGylation (Owens and Peppas, 2006). The nanocarrier PEGylation refers to the particle decoration by covalently grafting, entrapping or adsorbing polyethylene glycol (PEG) molecules (Owens and Peppas, 2006). PEG is FDA approved polymer described as a nontoxic, non-immunogenic, non-antigenic,

and a highly soluble in water (Veronese and Pasut, 2005). The PEG chains create a barrier layer that blocks opsonins adhesion, making the particles remain “camouflaged” or “invisible” to phagocytic cells (Greenwald *et al.*, 2003). Furthermore, it will promote a prolonged residence in body and a decreased degradation by metabolic enzymes (Veronese and Pasut, 2005). He *et al*. studied the effect of MSNs PEGylation on nonspecific binding of serum proteins and cellular responses, applying PEGs with different sizes (He *et al.*, 2010c). In their results they verified that all the tested molecular weights influenced the nonspecific binding to human serum protein (HSA), and also red blood cells hemolysis.

Another alternative to passively target MSN to tumors is the localized delivery (Parveen *et al.*, 2012). In accessible tumors like breast, colon, prostate and neck can be realized a direct intra-tumoral delivery of nanocarriers or therapeutic agents (Parveen *et al.*, 2012), avoiding systemic circulation and the majority of biological barriers.

2.4.2. Active Targeting

Active targeting is usually achieved by nanocarrier conjugation with a targeting component, which will promote a preferential accumulation in the tumor itself, in the tumor-bearing organ or in individual cancer cells (Figure 12 B) (Nie *et al.*, 2007). This approach takes advantage of ligand-receptor, antigen–antibody and other forms of molecular recognition to privilege one specific site in the target cells (Steichen *et al.*, 2012). The targeting component is chosen to bind to a unique molecule overexpressed by the tumor and at the same time it is not expressed or presents a limited expression in normal cells (Danhier *et al.*, 2010). This active targeting strategy has the potentiality to enhance the therapeutic effectiveness, and at the same time decreases the delivery of chemotherapeutic molecules to healthy cells (Steichen *et al.*, 2012). Consequently, minimizing the potential side effects.

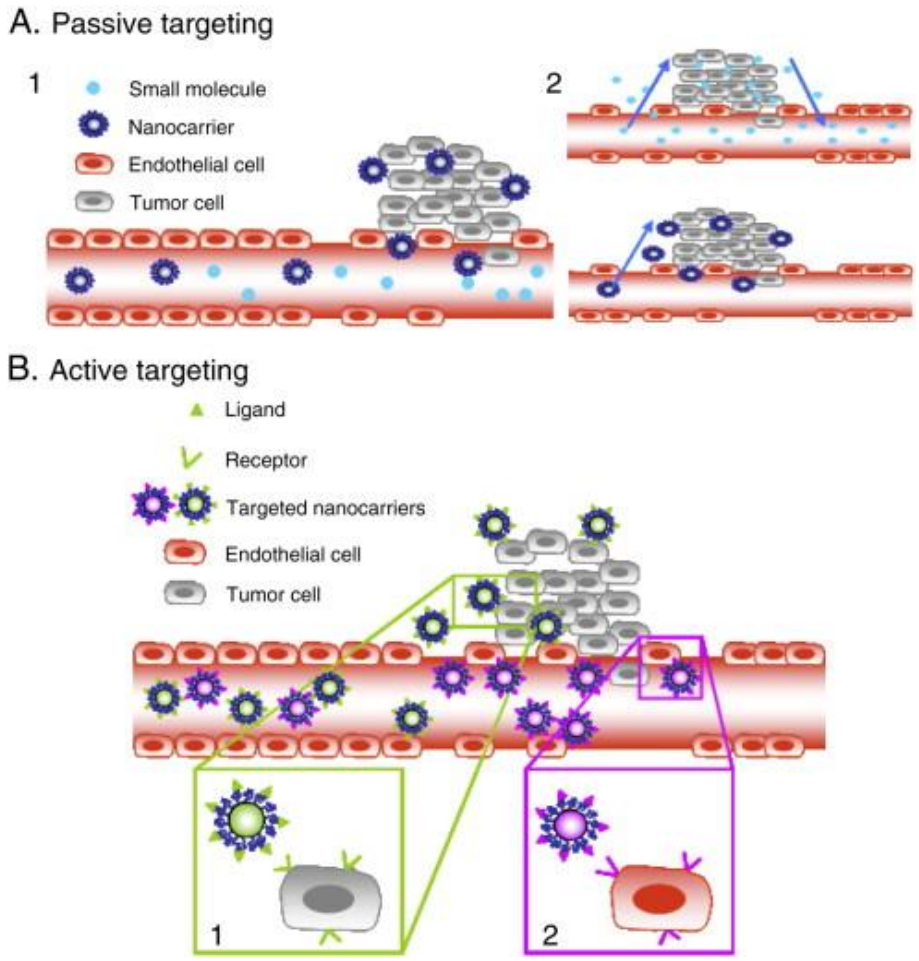

Figure 12 – Nanocarriers targeting, passive vs active targeting strategies (Adapted from Danhier *et al.*, 2010a). In (A) passive targeting, nanocarriers advantages over the free drug administration. In (B) possibility to target different cells associated to tumor development.

Focusing on prostate cancer, there are different molecules that can be used for nanoparticle targeting as shown in Figure 13. One of the major molecules associated to prostate cancer is the prostate-specific membrane antigen (PSMA) (Romero Otero *et al.*, 2014). PSMA is a transmembrane protein produced nearly exclusively by prostate epithelial cells, and it is overexpressed in prostate cancer and other nonmalignant prostate conditions (Romero Otero *et al.*, 2014). Other possible target is the prostate stem cell antigen (PSCA), this molecule is highly upregulated in prostate cancer and can be targeted by antibodies (Guo *et al.*, 2013).

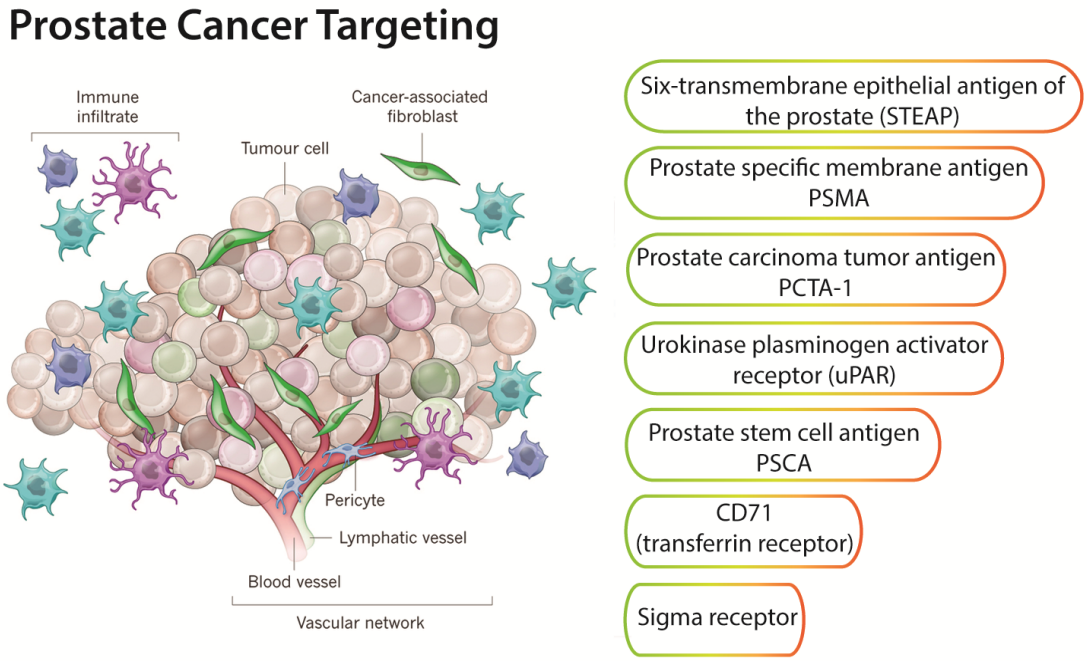

Figure 13 – Summary of some overexpressed biomolecules on prostate cancer (adapted from Junttila and de Sauvage, 2013).

When biomolecules are used for targeting specific sites is of great importance to guarantee the correct ligand-receptor or antigen-antibody interaction (Mahon *et al.*, 2012). In order to achieve a correct nanoparticle-cell interaction in the nano-bio interface it is necessary to assure that the active site in the targeting ligand is presented in the correct special conformation (i.e., 3-dimensional arrangement), optimal density and spacing must be considered (Mahon *et al.*, 2012). Stimuli-responsive nanocarriers

2.5. Stimuli-responsive nanocarriers

Despite the major improvements in nanoparticles mediated drug delivery, it is still of critical importance to control the time frame of drug release at the tumor microenvironment or inside cancer cells (Lehner *et al.*, 2012). Since this controlled release would maximize the therapeutic effect through the rapid increase in drug concentration inside the cancer cell, and at the same time decrease the toxic side-effects by minimizing drug distribution in healthy tissues (MacEwan *et al.*, 2010). This tight control can be promoted by taking advantage of external stimulus that can either trigger a modification of the nanocarrier or of the drug-carrier interaction, as recently reported by Lehner et al., 2012 (Lehner *et al.*, 2012). Several types of stimulus can be used to modulate the drug release profile of nanocarriers including: i.) extracellular/intracellular pH changes (Gaspar *et al.*, 2013), ii.) redox potentials (Wang *et al.*, 2013), iii.) light-triggered modifications (Ji *et al.*, 2013), and also v.) temperature changes (Wadajkar *et al.*, 2013).

The pH responsiveness is one of the most frequently used stimulus, it takes advantage from the pH differences in the tumor microenvironment and in the endocytic pathways inside cancer cells to trigger the release of bioactive molecules from the nanocarriers. The unique tumor microenvironment presents a more acidic pH than normal tissues, 6.5-7.2 in tumor to 7.4 in normal tissues (Tian and Bae, 2012). This more acidic pH is explained by the cancer cells high metabolic rates, and plasma membrane proton-pump activity (Du *et al.*, 2013). The cancer cells instead of normally using the mitochondrial oxidative phosphorylation pathways to generate adenosine triphosphate, they rely on aerobic glycolysis a much less efficient process (Vander Heiden *et al.*, 2009). Moreover, this altered metabolism leads to a persistent lactate production by tumors in the presence of oxygen, a phenomenon named as the Warburg effect. This effect is characterized by the exocytosis of the excessively produced lactate (Vander Heiden *et al.*, 2009). Lactate production in conjugation to the characteristic tumor inadequate blood supply and poor lymphatic drainage, originates the tumor microenvironment acidity (Du *et al.*, 2013). The other pH gradient that can be used to trigger the cargo release from nanocarrier is the even lower pH verified in lysosomes. Where a pH ranging 4.5-6 can be found for the degradation of undesired internalized molecules (Lehner *et al.*, 2012). The nanocarrier modification with switches responsive to pH changes that the nanocarrier will encounter allows the cargo tight spatiotemporal release control enhance the tumor accumulation.

2.5.1. pH-responsive nanocarriers

Several pH responsive nanocarriers have been developed to achieve a controlled release of chemotherapeutic biomolecules. In order to acquire this pH-responsiveness several different strategies can be employed (Figure 14) (Wang *et al.*, 2014). Different materials whose structural conformation or hydrophobicity is sensitive to pH changes can be used. Some of these materials are biocompatible polymers containing ionizable groups such as amines and carboxylic acids, like polysulfonamides, poly(acrylic acid) and various acrylic acid derivatives like polymethyl methacrylate (Fleige *et al.*, 2012). Other type of materials that can be used are calcium phosphate and calcium carbonate, these materials undergo a fast dissociation in acidic environments and remain relatively stable at physiological pH (Min *et al.*, 2012, Parakhonskiy *et al.*, 2012).

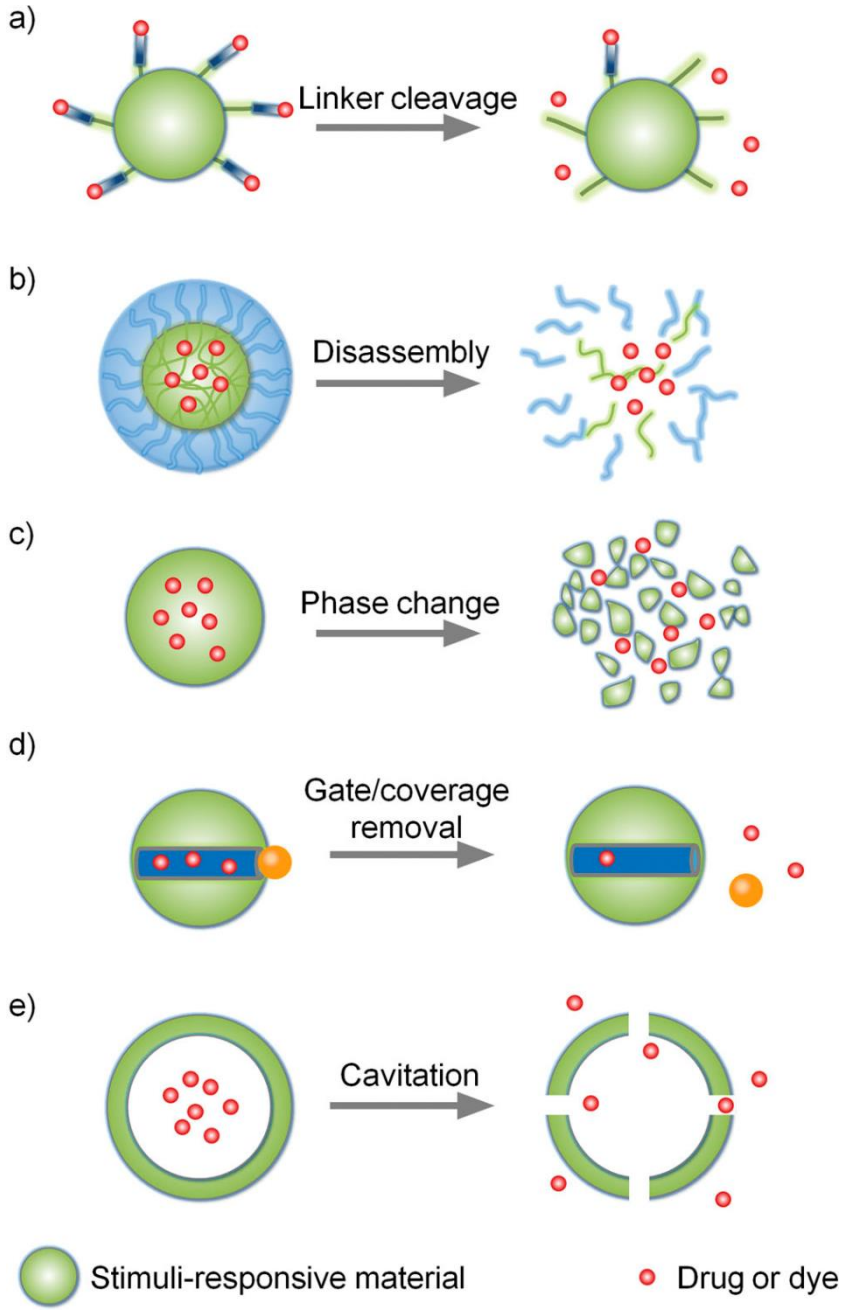

Figure 14 – Major strategies employed in the development of pH responsive nanocarriers (adapted from Wang *et al.*, 2014). (a) direct conjugation bioactive cargo-nanocarrier through a labile linker, (b) nanocarrier disassembly by degradation of the linkages between their molecular structures, (c) nanocarrier phase change in response to a stimulus, (d) bioactive cargo entrapped inside the nanocarrier by utilization of a stimuli-responsive capping that stops the cargo release, (e) use of bubble generating molecules to create pores in nanocarrier walls under the presence of a particular stimulus.

Relatively to MSNs, a controlled release is also a highly desired property, hence, several systems are being developed based on the approaches presented above. Popat *et al.* developed a pH responsive system based on the use of chitosan coated MSNs (Popat *et al.*, 2012). In this report chitosan was covalently bond to MSNs, forming a coating layer in MSNs. This layer responds to pH variations through the protonation changes in chitosan, in basic pH the chitosan

deprotonation forms an insoluble gel like structure blocking the pores and the cargo release (Popat *et al.*, 2012). Such, leads to chitosan swelling due to amine protonation in acidic pH, thus facilitating drug diffusion. With this coating the authors were capable to promote a controlled release at pH 7.4, with 25 % of cargo released. In contrast in acidic pH 5 a rapid release was verified, with almost 90% of the cargo being released. A similar strategy was used by Yuan *et al.*, where poly (acrylic acid) (PAA) was grafted to MSNs (Yuan *et al.*, 2011). The PAA will have a behavior similar to chitosan, when the pH decreases the PAA will become more protonated and will swell. After 24h at pH 5.6, 6.8 and 7.4 a release of 70%, 42% and 13% was verified, respectively, showing a clearly pH dependent content release (Abu Lila *et al.*, 2012). Chen *et al.* reported a different alternative to achieve a pH controlled release, in their work they reported the use of gold nanoparticles to end-cap MSNs mesoporous structure. The use of L-cysteine modified gold nanoparticles linked to MSNs through a copper bridging ion promoted a pH-responsive release. The pH-dependent behavior is the result of charge interactions between the L-cysteine, copper and amino modified MSN surface. In pH above 5, L-cysteine is negatively charged and attracted to MSN positive surface, with the pH decrease the L-cysteine will become positively charged creating a repulsion between the gold nanoparticles and MSN surface prompting cargo release (Chen *et al.*, 2014).

Aims

The overall objective of this thesis was to develop a new carbonate end-capped mesoporous silica nanoparticle for a pH responsive dual drug delivery to prostate cancer cells. More specifically the aims of this research include:

- Synthesis and characterization of mesoporous silica nanoparticles;
- Efficacy evaluation of previously synthetized dual drug loaded nanoparticles;
- End-cap the silica mesoporous with calcium carbonate;
- Evaluate calcium carbonate coating pH-responsiveness;
- Assessment of nanoparticle uptake by prostate cancer cells;
- Evaluate the drug delivery system anti-tumoral efficacy.

Chapter 2

Materials and Methods

2. Materials and Methods

2.1. Materials

Primary normal human dermal fibroblasts (FibH) cells were obtained from Promocell (Heidelberg, Germany) and human prostate cancer cells (PC-3) from ATCC (Middlesex, UK). Fetal bovine serum (FBS) was acquired from Biochrom AG (Berlin, Germany). Cell imaging plates were acquired from Ibidi GmbH (Ibidi, Munich, Germany). Cell culture T-flasks were obtained from Orange Scientific (Braine-l'Alleud, Belgium). TEOS was purchased from Acros Organics (Geel, Belgium). Doxorubicin hydrochloride was obtained from Tocris Bioscience (Bristol, UK). Hexadecyltrimethylammonium Bromide (CTAB) and Ibuprofen were obtained from Tokyo Chemical Industry (Tokyo, Japan). 3-(4,5-dimethylthiazol-2-yl)-5-(3-carboxymethoxyphenyl)-2-(4-sulfophenyl)-2H-tetrazolium (MTS) and phenazine methosulfate (PMS) were purchased from Promega (Madison, WI, USA). Hoechst 33342® and Wheat Germ Agglutinin (WGA), Alexa Fluor® 594 conjugate were provided by Invitrogen (Carlsbad, CA, USA). Calcium Chloride ($CaCl_2$), Dulbecco's Modified Eagle Medium: Nutrient Mixture F-12 (DMEM-F12), Fluorescein isothiocyanate (FITC), resazurin, Roswell park memorial institute medium 1640 (RPMI-1640), sodium carbonate (Na_2CO_3) and trypsin were purchased from Sigma–Aldrich (Sintra, Portugal). All reagents were used as received.

2.2. Methods

2.2.1. Mesoporous silica nanoparticles synthesis

MSNs were synthesized by adapting the method developed by He and co-workers, 2010 (He *et al.*, 2010c). In this synthesis TEOS was used as a silica source, a cationic surfactant, CTAB, was used as structure directing agent, water was used as solvent and sodium hydroxide as a morphological catalyst (Rosenholm *et al.*, 2010). The particle formation occurs by the condensation of negatively-charged silicates around the cationic template (CTAB) by electrostatic interactions (Slowing *et al.*, 2008).

Briefly, silica nanoparticles were synthesized by adding TEOS, into a solution containing ultrapure water, NaOH (2M), and a predetermined amount of CTAB in a round bottom flask (He *et al.*, 2010c). The reaction was performed at 80 ºC for 2 h. The produced particles were recovered by centrifugation. To remove the CTAB residues, ethanol and HCl were added to powder nanoparticles. The purification stage proceeded for 24 h. Finally, the solution was centrifuged and washed several times with ultrapure water and ethanol to completely remove all CTAB traces as above mentioned.

2.2.2. Drug loading

Drug loading was accomplished by using the solvent evaporation method with slight modifications (Charnay *et al.*, 2004). For Doxorubicin loading, MSNs were dispersed several times in a methanolic Doxorubicin solution. The solvent was then evaporated between each round of loading in order to achieve maximum efficiency. After the last evaporation, MSNs were washed with ultrapure water and recovered by centrifugation. For Ibuprofen loading, empty or Doxorubicin loaded MSNs were suspended in an Ibuprofen solution. The drug-nanoparticle mixture was then stirred at 25 ºC for 1 h, and the previous procedure of encapsulation and solvent evaporation was repeated. Afterwards, drug loaded MSNs were centrifuged and the remaining solvent was removed from MSNs by freeze drying. Thereafter, drug loaded MSNs, Dox-MSNs, Ibu-MSNs and Dox-Ibu-MSNs were prepared. The drug loading quantification can be assessed by subtracting the amount of drug present in supernatant in the washing step from the total amount of drug added. Ibuprofen and Doxorubicin concentrations were determined by analysing the absorbance at λ= 263nm and λ= 585nm, respectively, by using an UV-vis spectrophotometer Shimadzu – 1700 (Shimadzu Inc., Japan). The encapsulation efficiency was calculated by (Yuan *et al.*, 2011):

$$\text{Encapsulation Efficiency} = \frac{\text{Drug weight in MSNs}}{\text{Initial drug weight}} \times 100 \quad (1)$$

2.2.3. Mesoporous silica nanoparticles coating

For MSNs coating with $CaCO_3$, empty or loaded MSNs were dispersed in a calcium chloride solution. After stirring for 5 min, sodium carbonate was added and the mixture stirred 1 h, at room temperature. The dispersion was then centrifuged to collect the coated MSNs and remove traces of the carbonate coating. The prepared particles were identified as MSNs-$CaCO_3$ and Dox-Ibu-MSNs-$CaCO_3$.

2.2.4. Mesoporous silica nanoparticles morphological characterization

Morphological properties of synthetized particles were visualized by Scanning Electron Microscopy (SEM) and Transmission Electron Microscopy (TEM). The MSNs samples were dispersed in a cover glass and dried overnight. Afterwards, the samples were mounted on aluminum stubs and sputter coated with gold by using an Emitech K550 sputter coater (Emitech Ltd, UK). The MSNs samples where then observed, and all the images were obtained in a Hitachi S-2700 (Tokyo, Japan) electron microscope at an accelerating voltage of 20 kV with different magnifications and acquisition modes.

2.2.5. Mesoporous silica nanoparticles size and zeta potential characterization

The size and zeta potential of MSNs samples was determined by dynamic light scattering (DLS) by using a Zetasizer Nano ZS (Malvern Instruments, Worcestershire, UK). Previous to all the analysis, the samples were resuspended in ultrapure water. All data was collected at 25 ºC in a disposable capillary cell at a detection angle of 173°. Particle size was determined by Cumulants analysis and by the Stokes-Einstein equation for colloidal dispersions:

$$D = \frac{K_B T}{6\pi\eta r} \quad (2)$$

Where D the translational diffusion coefficient, K_B the Boltzmann's constant, T the thermodynamic temperature, η the dynamic viscosity and r is the hydrodynamic diameter.

Zeta potential of MSNs was calculated by using the Smoluchowski model (f(ka)=1.50) included in the Zetasizer software (v 7.03).

$$U_E = \frac{2\epsilon\zeta f(ka)}{3\eta} \quad (3)$$

Where ζ is the zeta potential, U_E the electrophoretic mobility, ε the dielectric constant, f(Ka) the Henry's equation and η the dynamic viscosity.

2.2.6. Mesoporous silica nanoparticles porosity analysis

MSNs porosity analysis and surface characterization was performed with nitrogen sorption isotherms at -196.15 ºC by using a Nova 2200e surface area and pore size analyzer (Quantachrome Instruments Corporate, Florida, USA). Prior to analysis the samples were degassed under a flow of dry, inert gas. The Adsorption Isotherm is obtained by measuring the amount of gas adsorbed across a wide range of relative pressures at a constant temperature. On the other side, desorption Isotherms are delineated by measuring the removed gas as pressure is reduced. The surface areas were calculated by the Brunauer-Emmett-Teller (BET) method using experimental points at a relative pressure of P/P_0 = 0.05-0.25.

$$\frac{1}{W((p_0/P)-1)} = \frac{1}{W_m C} + \frac{C-1}{W_m C}\left(\frac{P}{p_0}\right) \quad (4)$$

$$S_t = \frac{W_m N A_{cs}}{M} \quad (5)$$

Where W is the weight of gas adsorbed, P/P_0 the relative pressure, W_m the weight of adsorbate monolayer, C the BET constant, S_t the total surface area, N the Avogadro's number, M the molecular weight of adsorbate and A_{cs} the adsorbate cross sectional area.

Porosity was determined by the Barrett-Joyner-Halenda (BJH) method and the pore volume was estimated from the amount of adsorbed nitrogen at the relative pressure of 0.99.

$$r_k(°A) = \frac{4.15}{\log\left(\frac{P_0}{P}\right)} \quad (6)$$

$$r_p = r_k + t \quad (7)$$

Where $r_k(°A)$ is the Kelvin radius of the pore, r_p the actual radius of the pore and t the thickness of the adsorbed film.

2.2.7. X-ray powder diffraction of mesoporous silica nanoparticles

The characteristic crystallinity of MSNs samples was assessed by X-ray powder diffraction (XRD) analysis. To perform the analysis, freeze-dried MSNs samples were mounted in silica supports using a double side adhesive tape. The samples XRD spectra were acquired on a Rigaku Geiger Flex D-max III/c diffractometer (Rigaku Americas Corporation, Texas, USA) operated at a voltage of 30 kV, 20 mA current and a 2θ scanning range from 5° to 90° at a rate of 1° per minute.

2.2.8. Energy dispersive X-ray spectroscopy of mesoporous silica nanoparticles

The chemical characterization of MSNs samples was performed by energy-dispersive X-ray spectroscopy (EDX). The samples were then mounted on aluminum stubs and the analysis was performed in a Rontec EDS system (Rontec, Watford, UK) by scanning random areas during 100 s. Data analysis and peak assignment were performed in Rontec EDWIN software.

2.2.9. Fourier transform infrared spectroscopy analysis

The MSNs were also analyzed by Fourier transform infrared (FTIR) spectroscopy. This analysis gives information about the chemical linkages present in the tested sample, being important to confirm the CTAB removal efficacy. The interferograms were recorded in a Nicolet iS10 spectrometer (Thermo Scientific Inc., Massachusetts, USA) by acquiring 256 scans with a spectral width ranging from 4000 cm^{-1} to 600 cm^{-1}, at a spectral resolution of 4 cm^{-1}. A baseline correction and atmospheric suppression was performed in all acquired data in order to avoid possible interferences in the FTIR spectra. Data analysis was executed in the OMNIC spectra software (Thermo Scientific).

2.2.10. Drug release analysis

After MSNs loading and successful $CaCO_3$ pore closure, the release studies were performed through the dialysis method, using a dialysis bag with a molecular cutoff of 1500 Da. Dialysis was performed at 37 ºC with magnetic stirring in phosphate buffer saline (PBS) solution 1%, with different pH (5.6 and 7.4). At different time intervals, samples were removed and the same volume of PBS was refilled. The Ibuprofen and Doxorubicin concentrations were determined by analysing the sample absorbance as described before for encapsulation analysis.

2.2.11. Cytotoxicity assays

The cytotoxicity of the synthesized MSNs was evaluated by using the resazurin assay. This method uses a non-toxic reagent (resazurin), which when inside the cells becomes reduced from a non-fluorescent blue resazurin compound, to the fluorescent pink-reddish resorufin (O'Brien *et al.*, 2000). This transformation occurs by action of mitochondrial enzymes such as flavin mononucleotide dehydrogenase and nicotinamide adenine dehydrogenase (O'Brien *et al.*, 2000).

To evaluate MSNs cytotoxicity FibH cells were cultured in DMEM-F12 medium, supplemented with 10 % fetal bovine serum and 1 % antibiotics/antimycotics (streptomycin and gentamycin), at 37 °C in a humid atmosphere containing 5 % CO_2. PC-3 cells were cultured in RPMI-1640 medium, in the same conditions as described before for FibH.

Later, the PC-3 and FibH cells were seeded into a 96-well flat bottom culture plates at a density of 10 x 10^3 cells/well, with the respective culture medium. Cells were cultured for 24 h, at 37 ºC in an incubator with humid atmosphere containing 5 % CO_2. After the culture medium was exchanged, the cells were incubated with different concentrations of MSNs, ranging from 10 to 120 µg/mL. After 24, 48 and 72 h of exposure, the medium was replaced and cells were incubated with 10% (v/v) of resazurin (1 mg/mL), at 37 ºC and 5 % CO_2, during 4 h. The produced resorufin present in culture medium was then quantified by spectrofluorimetry (Spectramax Gemini XS, Molecular Devices LLC, USA) at an excitation/emission wavelength of λ_{ex}=560 nm and λ_{em}=590 nm. Cells incubated with absolute ethanol were used as positive control (K^+) and cells without being exposed to MSNs samples were used as negative controls (K^-).

2.2.12. Nanoparticles cellular uptake

The MSN uptake by PC-3 malignant cells was studied by confocal laser scanning microscopy (CLSM). For the visualization of MSNs uptake, 20 x 10^3 PC-3 cells were seeded in µ-Slide 8 well Ibidi imaging plates (Ibidi GmbH, Germany) and incubated at 37 ºC and 5 % CO_2. After 24 h, cells were exposed to different formulations of MSNs during 4 h. After incubation, the cells were washed with PBS, fixed with paraformaldehyde 4 %, for 15 min at room temperature and rinsed with PBS 1%. Subsequently, the cells were treated with WGA, Alexa Fluor® 594 conjugate for 30 min at room temperature and washed several times with PBS 1%, for cell cytoplasm

staining. The cell nucleus was labeled with Hoechst 33342® and the cells were washed several times with PBS 1%. Imaging experiments were performed in a Zeiss LSM 710 confocal microscope (Carl Zeiss SMT Inc., USA), equipped with a Plan Apochromat 63x/1.4 Oil Differential Interference Contrast (DIC) objective. To obtain the images consecutive z-stacks were acquired and the 3D reconstruction and image analysis was performed in Zeiss Zen 2010 software.

2.2.13. IC50 determination

To evaluate the IC50 of PC-3 cells relatively to Doxorubicin or Ibuprofen, PC-3 cells were seeded at a density of 10 x 10^3 cells/well into 96-well flat bottom culture plates, containing RPMI-1640 medium supplemented with 10 % of FBS. After 24 h of incubation, at 37 ºC in an humid atmosphere with 5 % CO_2, the culture medium was replaced and cells were incubated with different concentrations of Doxorubicin (0.1 µM to 300 µM) or Ibuprofen (0.1 mM to 50 mM). After 48 h of exposure, the medium was replaced and cells were incubated with 10% (v/v) of resazurin (1 mg/mL), at 37 ºC and 5 % CO_2, during 4 h. The produced resorufin present in culture medium was then transferred to a black clear bottom 96-well plates for analysis. The fluorescence of the samples was quantified by spectrofluorimetry (Spectramax Gemini XS, Molecular Devices LLC, USA) at an excitation/emission wavelength of λ_{ex}=560 nm and λ_{em}=590 nm. Cells incubated with absolute ethanol were used as positive control (K^+) and cells without being exposed to drugs were used as negative controls (K^-).

2.2.14. Cytotoxic activity of drug loaded mesoporous silica nanoparticles

The cytotoxic activity of dual or single loaded MSNs was determined by using an MTS assay, following the manufacturer instructions. In brief, PC-3 cells were seeded in 96-well culture plates at a density of 10 x 10^3 cells/well and incubated at 37 ºC and 5 % CO_2. One day later, PC-3 cells were incubated with Doxorubicin and Ibuprofen (DD), Dox-Ibu-MSN and Dox-Ibu-MSN-$CaCO_3$. At predetermined time points, the medium was exchanged and 20 µL of a mixture of MTS/PMS was added to each well (Gaspar *et al.*, 2011). This allowed the assessment of viable cells mitochondrial redox activity, by the MTS reduction into the water-soluble brown formazan product. After 4 h of incubation, the absorbance measurements of the produced formazan were performed in a microplate reader (Anthos 2020, Biochrom UK) at λ=492 nm. Cells incubated with absolute ethanol were used as positive control (K^+) and cells in the absence of drugs or materials were used as negative controls (K^-).

2.2.15. Statistical analysis

Each experiment was carried at least in triplicate and data is presented as mean ± standard deviation (s.d.). One-way analysis of variance (ANOVA) with the Student–Newman–Keuls test was used to compare different groups used in the various assays. A value of p inferior to 0.05 was considered statistically significant. Statistical analysis was performed using GraphPad Prism v.5.0 software (Trial version, GraphPadSoftware, CA, USA).

Chapter 3

Results and Discussion

3. Results and Discussion

3.1. Synthesis of mesoporous silica nanoparticles

Silica nanoparticles, especially those with mesopores, offer a particularly valuable platform for cell-specific delivery and their unique characteristics currently attract the attention of several researchers involved in the study of drug delivery applications (Li *et al.*, 2012). These nanocarriers possess a tunable particle size and shape which can be modified to facilitate the endocytosis by living cells. Also, the rigid and stable framework provided by MSNs is more resistant to pH, heat, mechanical stress and other degradation cues than their polymer based counterparts (Vivero-Escoto *et al.*, 2010). Furthermore, MSNs possess a unique, uniform and tunable porous structure that allows loading of hydrophilic and hydrophobic drugs. Moreover, there is no interconnectivity between the porous channels, a fact that assumes a great importance in case of incomplete capping of the nanoparticle pores. Since the individual pores work as independent reservoirs for drug encapsulation and release, an incomplete pore capping will promote only drug leakage from the non-covered pores and not from the entire particle (Slowing *et al.*, 2008).

The synthesis of MSNs (Figure 15) is based on the formation of surfactant micelles that serve as template for silica condensation on their surface. In a commonly used synthesis process, CTAB is used as surfactant at a concentration above the critical micellar concentration to assure CTAB self-aggregation in micelles (Tang *et al.*, 2012). The silica precursor, TEOS, undergoes a base-catalyzed hydrolysis since the OH^- groups present in solution attack the TEOS molecule by a nucleophilic reaction mechanism (Harris *et al.*, 1990). This nucleophilic attack will promote the alkoxy group removal ($O\text{-}CH_2\text{-}CH_3$) and TEOS hydrolysis, in the final a silicic acid is formed (Harris *et al.*, 1990). At the same time, the hydrolysis intermediates start to condensate via siloxane bonds (Si-O-Si) in the surface of surfactant micelles, this occurs by electrostatic interaction between the cationic template (CTAB) and the negative charged silica species (Wu *et al.*, 2013). The condensation around surfactant micelles forms a silica wall and the combination of several of these structures will result in the formation of silica nanoparticles with the pores occluded by CTAB micelles.

The purification step is of great importance in the MSNs properties, as the CTAB is very cytotoxic and an incomplete purification will impair the MSNs applicability as drug reservoirs. Furthermore, the pore accessibility is influenced by the purification effectiveness, and depending on the purification method the surface silanol groups can be lost. This MSNs purification is normally carried out by calcination or by solvent extraction methods (Slowing *et al.*, 2008). The calcination method typically at 400-550 ºC promotes the condensation of the surface silanol groups decreasing their surface density (Rosenholm *et al.*, 2010). The extraction

processes minimizes silanol losses, in this case the use of acid/alcohol mixture promotes the CTAB removal by electrostatic repulsion (Rosenholm *et al.*, 2010). Since in the acidic solution the MSNs possess a positive surface charge repelling the cationic surfactant CTAB.

Being the pores accessible, loading of drugs in the MSNs matrix can be performed. The MSNs are well suitable for drug loading, their structure integrity is kept intact even in organic solvents, and therefore the optimal solvent can be chosen to fine-tune the drug loading conditions. In order to promote a more effective pore filling a solvent evaporation method can be used. The successive MSNs impregnations in drug solutions results in an improvement in drug loading, since at each impregnation/evaporation the drug molecules diffuse deeper into the pores by capillarity, increasing the loading efficiency.

In order to prevent the drug leakage from MSNs, several strategies can be applied. One alternative is the pore blockage by a stimuli-responsive material like $CaCO_3$. The $CaCO_3$ end-capping was formed as referred in Section 2.2.3 (Page 28) from an aqueous solution containing $CaCl_2$ and Na_2CO_3 by precipitation under the presence of MSNs. Choi and Kuroda (Choi and Kuroda, 2012) described that silica mesoporous surface increases the stability of initially formed calcium carbonate crystals and it can also work as a medium for the "confinement effect" that can stabilize the formed calcium carbonate (Choi and Kuroda, 2012). Therefore the $CaCO_3$ crystals preferential formation in silica mesopores, will obstruct them and prevent drug release. Furthermore, the $CaCO_3$ crystals are responsive to acidic environments (pH 5-6) in such a way that the $CaCO_3$ progressively dissociates into Ca^{2+} and CO_3^{-2} ions, promoting the pore opening (Min *et al.*, 2012). Interestingly, $CaCO_3$ crystals are also relatively stable at physiological pH (7.4), contributing for maintaining the drugs inside MSNs during systemic circulation (Parakhonskiy *et al.*, 2012).

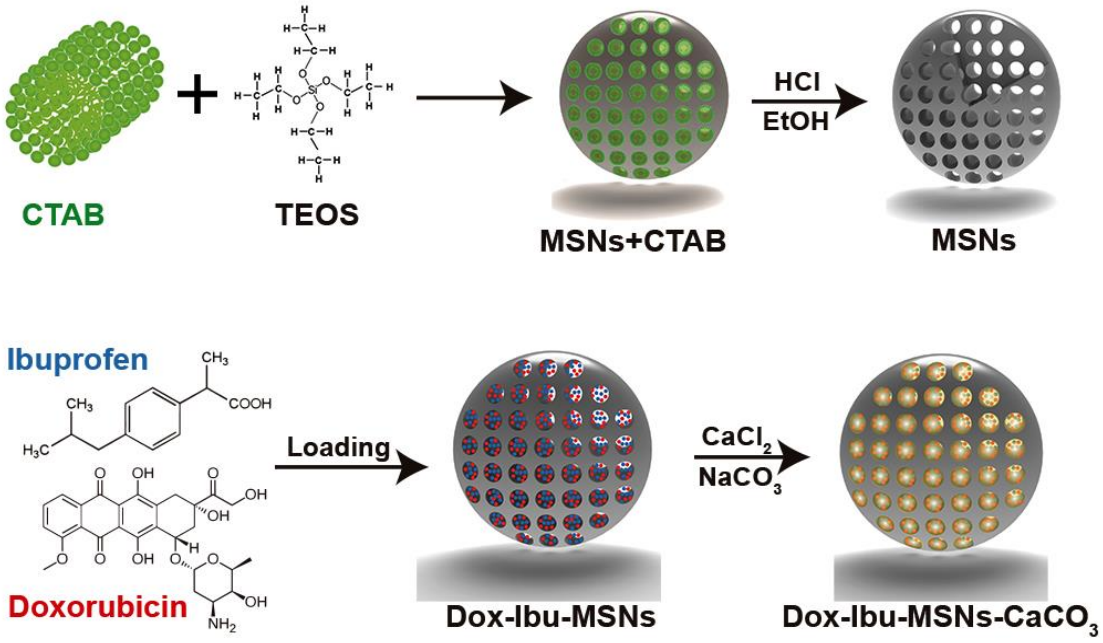

Figure 15 – Schematic representation of MSNs and Dox-Ibu-MSN-$CaCO_3$ synthesis.

3.2. Morphological characterization mesoporous silica nanoparticles

The produced MSN and MSN-$CaCO_3$ particles were characterized by SEM (Figure 16). The observed particles were homogeneous and presented spherical morphology regardless of being non-coated or coated with calcium carbonate. These results are supported by different studies in the literature that applied a similar synthesis method to produce spherical mesoporous silica nanoparticles (Lee *et al.*, 2011b, He *et al.*, 2010b). The nanoparticles morphology has a great importance in nanoparticle cytotoxicity, uptake and circulation capacity. Huang *et al.* demonstrated that MSNs shape influences the cellular uptake and viability (Huang *et al.*, 2010). Sphere like nanoparticles showed lower cytotoxicity when compared to those with rod form, this is probably due to the higher cell cytoskeleton disruption and disorganization caused by the particles with rod shape. Moreover, the spherical MSNs are completely internalized by cells in 180 min whereas those with rod shape take 360 min (Trewyn *et al.*, 2008).

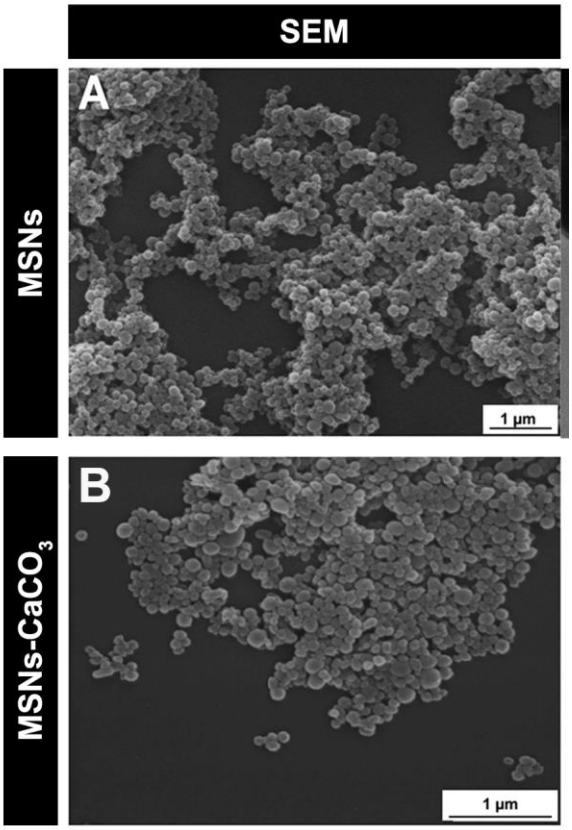

Figure 16 – Morphology analysis. SEM images of MSNs (A) and MSNs-$CaCO_3$ (B).

3.3. Size and zeta potential characterization of mesoporous silica nanoparticles

The MSNs size and surface charge are parameters with great importance in the particle capacity to have prolonged blood circulation and accumulate in tumor tissues through the EPR effect. The size characterization by DLS analysis (Figure 17 A) showed that MSNs had an average diameter of 157 nm and a zeta potential of -38.5 mV, which is consistent with the data reported in literature for this type of synthesis (Coti *et al.*, 2009). Furthermore, the formation of $CaCO_3$ coating on MSNs (Figure 17 B) resulted in a slight size increase to 167 nm, and in contrast a slight increase of zeta potential to -32.8 mV. This zeta potential difference is attributed to $CaCO_3$ crystals (-15 mV) that promotes an overall increase in particle zeta potential, according to a study of El Sheikh and collaborators (El-Sheikh *et al.*, 2013). Moreover, the presence of $CaCO_3$ coating also slightly increases MSNs mean size. Finally, the observed polydispersity index (PDI) values indicates that the samples are monodispersed. However, as expected, the $CaCO_3$ coating added some variability in MSNs sizes, resulting in higher PDI values.

The presented MSNs-$CaCO_3$ small size is suitable for promoting their extravasation from the blood vasculature into the tumor microenvironment via the EPR effect, promoting therefore a preferential nanoparticle accumulation in tumor after systemic administration (Dreher *et al.*,

2006, Matsumura and Maeda, 1986). Furthermore, the negative zeta potential observed in MSNs diminish their non-specific interactions with blood components and serum protein aggregation (Ernsting *et al.*, 2013).

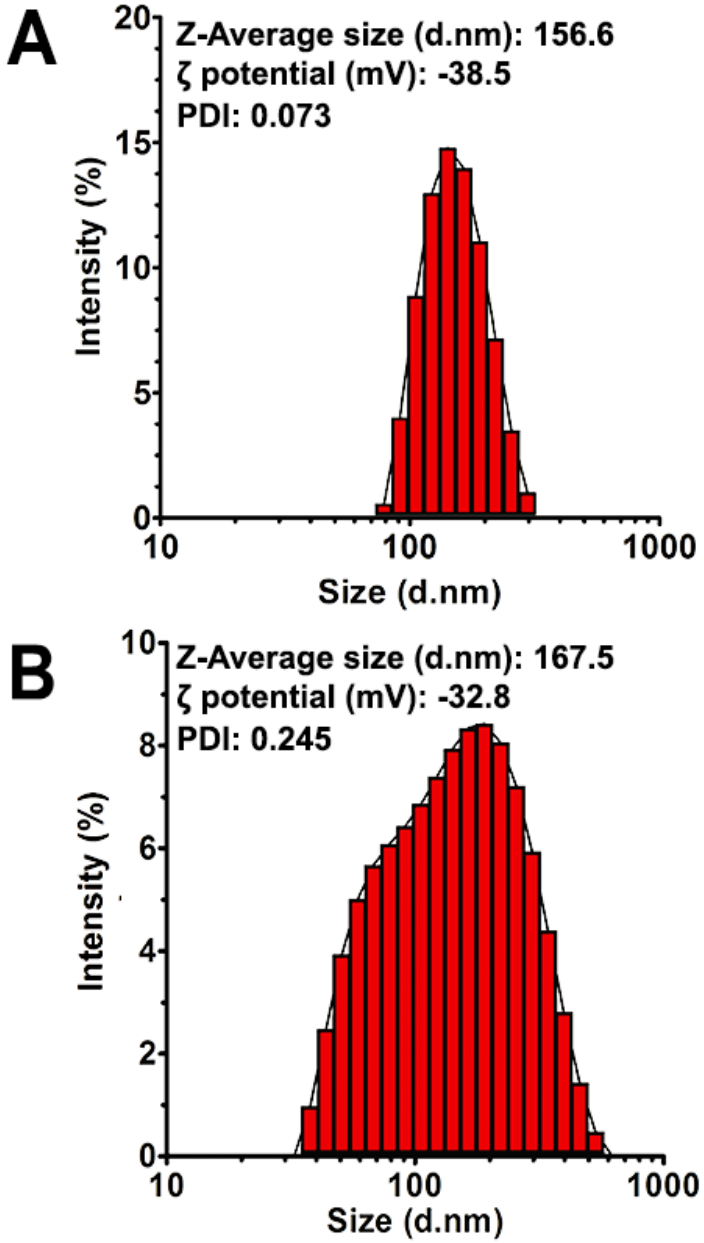

Figure 17 – Size and zeta potential characterization of MSNs particles. (A) MSNs particles and (B) MSNs-$CaCO_3$ particles.

3.4. Porosity analysis of mesoporous silica nanoparticles

The total surface area and the average pore diameter of the coated and uncoated MSNs was evaluated by nitrogen adsorption/desorption isotherm analysis. As shown in Table 1, the MSNs before the CTAB removal presents a low pore volume and surface area (0.339 cm^3/g and 32.346

m^2/g, respectively) and also a short particle surface area 196.319 m^2/g. These results prove that before the CTAB removal the pores are inaccessible and the loading cannot be achieved.

After the CTAB removal the values for pore volume, pore surface area and particle surface area have increased to 0.415 cm^3/g, 75.235 m^2/g and 857.586 m^2/g, respectively. These values are in agreement with those reported in literature for MCM-41 MSNs, a high surface area (>700m^2/g), large pore volume, uniform and tunable mesopores (Li *et al.*, 2012, Tang *et al.*, 2012). Moreover, these results indicate that the CTAB removal is effective, making the pores accessible and allowing the loading of a considerable drug payload.

After coating with $CaCO_3$, a decrease in surface area, pore volume and pore surface area was verified, up to values similar to those of MSNs before the CTAB removal. Indicating that the pores were closed by $CaCO_3$, and that the end-capping procedure was successful in creating a barrier to drug release from nanoparticles. Furthermore, the values obtained in this pore closure are similar to the polymer coated MSNs reports (Parala *et al.*, 2000, Yuan *et al.*, 2011).

Relatively to the pore diameter, it remains relatively constant (~3.20 nm). The small variations that were observed between each sample can be probably attributed to some error associated to the measurement technique or even some oscillations that are intrinsic to the synthesis process. It is worth to notice that the pore diameter allows the encapsulation of several different biopharmaceutical molecules.

Table 1 Porosity analysis of non-purified MSNs (MSNs+CTAB), MSNs after purification step (MSNs), and MSNs after calcium carbonate coating (MSNs-$CaCO_3$).

Samples	Surface Area (m^2/g)	Pore Diameter (nm)	Pore Surface Area (m^2/g)	Pore Volume (cm^3/g)
MSNs+CTAB	196.319	3.206	32.346	0.339
MSNs	857.586	3.1816	75.235	0.415
MSNs-CaCO3	161.436	3.2124	49.818	0.288

3.5. X-ray powder diffraction of mesoporous silica nanoparticles

The inclusion of the carbonate coating (MSN-$CaCO_3$) and its influence on the crystallinity of the particles was further evaluated by XRD. By analyzing the X-ray spectra a broad peak at $2\theta = 20^\circ$ is observed and it can be concluded, that the MSNs have an amorphous nature (Figure 18). Similarly, after $CaCO_3$ coating the amorphous structure is maintained. Furthermore, a small peak assigned to $CaCO_3$ was visualized at 32º (Figure 18 A, square) (El-Sheikh *et al.*, 2013), the small peak intensity is explained by the low amount of $CaCO_3$ in MSNs when compared to silica. Therefore this peak indicates the presence of $CaCO_3$ in the sample, which probably is due to the $CaCO_3$ coating formation observed in porosity analysis.

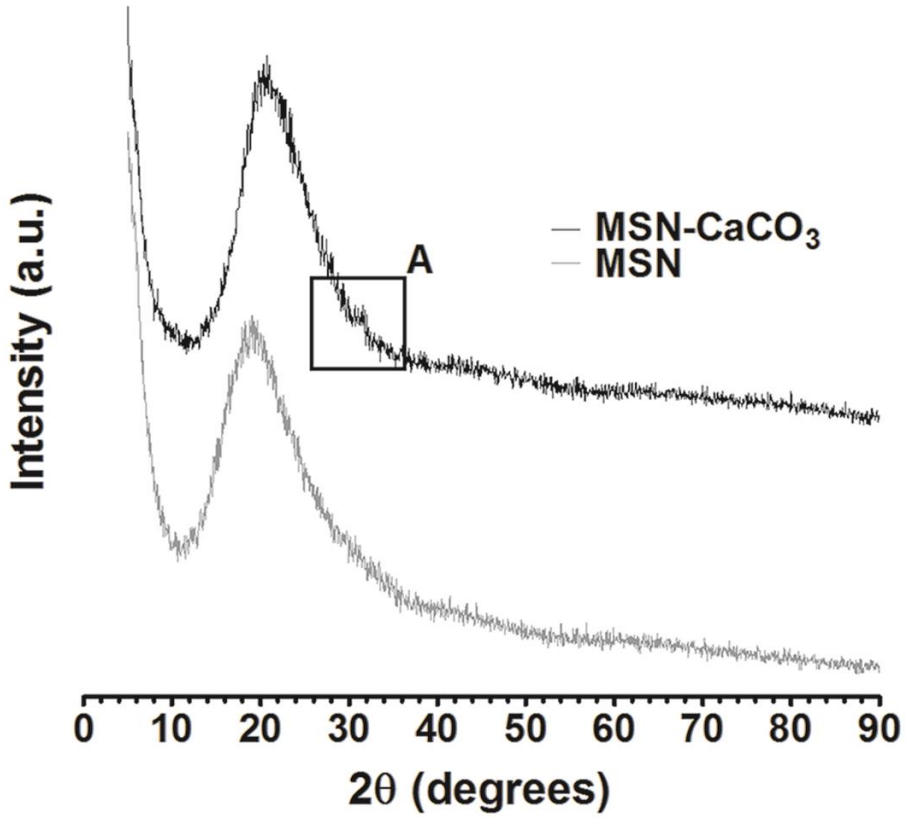

Figure 18 - X-ray diffraction spectra of MSN and MSN-$CaCO_3$. The square region (A) delimits the peak corresponding to $CaCO_3$.

3.6. Energy dispersive X-ray spectroscopy of mesoporous silica nanoparticles

To confirm the presence of $CaCO_3$ in MSNs and their sensibility to acidic pH, MSNs, and MSNs-$CaCO_3$ exposed to acidic environment an elemental analysis was performed by EDX.

As can be observed in Figure 19, the MSNs presented a high content of Silica (Si) and Oxygen (O) elements, which are the structural constituents of MSNs. After the $CaCO_3$ coating, apart from the Si and O elements the presence of Calcium (Ca) was also observed. The Ca presence in this sample corroborates the successful formation of a $CaCO_3$ coating in MSNs. In the EDX spectra of MSN-$CaCO_3$ exposed to acidic environment for 5 h only the structural Si and O elements of MSNs were observed (Figure 19). A fact that indicates the dissociation of $CaCO_3$ crystals when in acidic environments, confirming the possibility that this $CaCO_3$ coating grants a pH sensitive release of MSNs content.

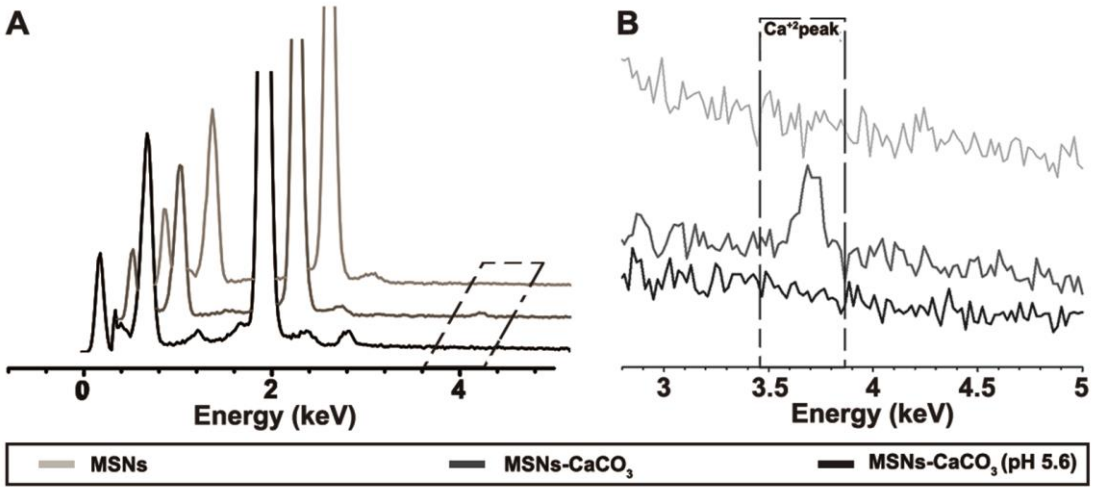

C

	C	O	Si	Ca
MSNs	11.01±9.2	56.19±8.3	32.80±5.5	-----
MSNs-$CaCO_3$	11.23 ± 9.0	53.55 ± 8.2	34.82 ± 5.1	0.40 ± 25.8
MSNs-$CaCO_3$ (pH 5.6)	12.55 ± 8.9	55.68 ± 8.2	31.76 ± 4.9	-----

Figure 19 - Energy-dispersive X-ray spectroscopy (EDX) analysis of MSNs. (A) full spectra and (B) zoom of full spectra (dashed region). (C) elemental analysis table, data presented in atomic mass percentage. Elemental analysis of MSNs, MSNs after the $CaCO_3$ coating, and MSNs-$CaCO_3$ after 5 h incubation in acidic medium.

3.7. Fourier transform infrared spectroscopy analysis

The FTIR analysis was performed to evaluate the CTAB removal efficacy in MSNs and also observe the presence of drug molecules in Dox-Ibu-MSNs (Figure 20). As can be seen in FTIR spectra of MSNs prior CTAB removal (MSNs+CTAB) the characteristic peaks of silica nanoparticle are observed at ~1050 cm^{-1}, ~955 cm^{-1} and ~800 cm^{-1} assigned to the siloxane bonding (Si-O-Si), the silanol surface groups (Si-OH) and the Si-O bond, respectively. Also in this sample it is possible to observe the C-H stretching vibrations at 2942 cm^{-1} and 2871 cm^{-1} and CH_3 deformation around 1478 cm^{-1}, these bands are assigned to CTAB present in these particles. Following CTAB removal the previous C-H peaks assigned to CTAB completely disappeared, indicating that the purification process was effective. Furthermore, the peak corresponding to surface silanol groups (Si-OH, at 955 cm^{-1}) became more defined, indicating a great quantity of these groups in free state.

The FTIR spectra of the dual loaded-MSNs showed several peaks assigned to the two chemotherapeutic drugs (Figure 20). Particularly, Ibuprofen characteristic high intensity bands

from C-H stretching vibrations at 3103 cm^{-1}, 3062 cm^{-1} and 2999 cm^{-1} and C=O stretching at 1851 cm^{-1}, were obtained (Marques *et al.*, 2014). Also, the characteristic peaks from Doxorubicin can be identified at 848 cm^{-1} and 820 cm^{-1} an N-H wagging and a C-C stretching at 1470 cm^{-1} (Jayakumar *et al.*, 2012). These results further indicate that the sequential loading process was effective, and the drugs were successfully entrapped inside the MSNs.

Additionally in all the three samples a broad adsorption peak in the range of 3700-2700 cm^{-1} can also be observed and is assigned to the adsorbed water in particles.

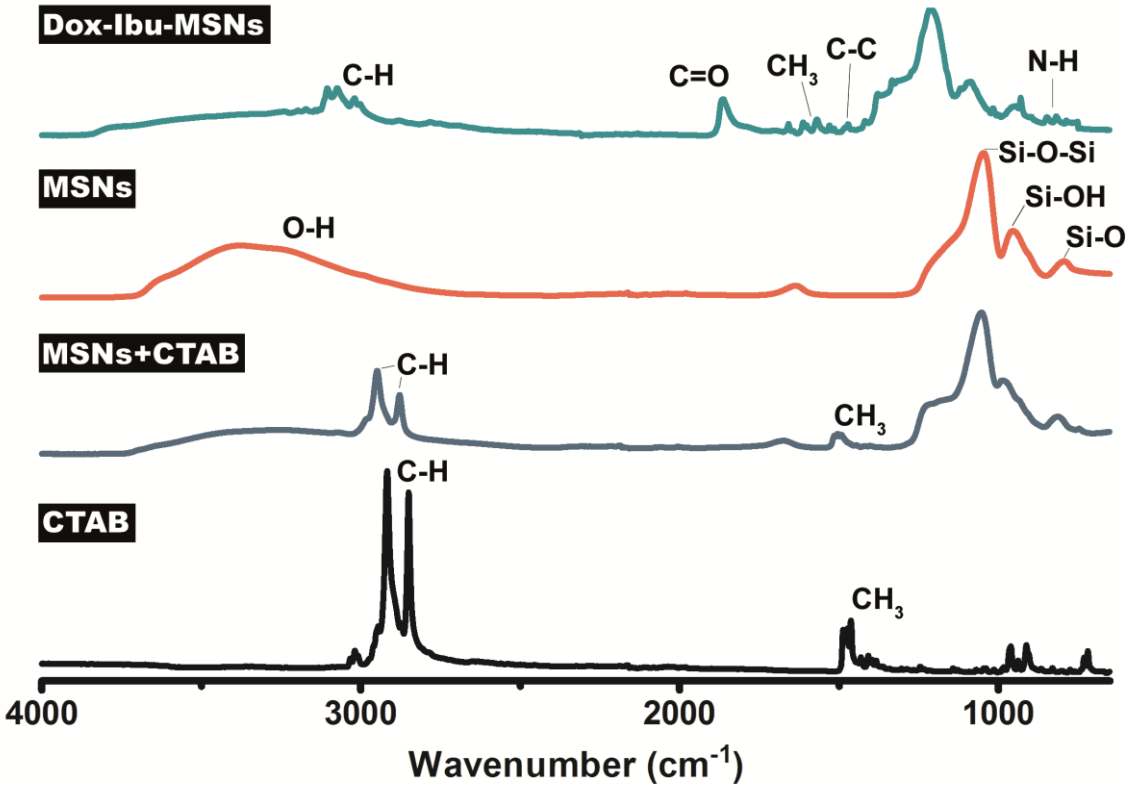

Figure 20 - FTIR spectra of CTAB, MSNs+CTAB, MSNs and Dox-Ibu-MSNs.

3.8. Analysis of drug loading and release

Two different anti-tumoral drugs (Doxorubicin and Ibuprofen) were selected to be delivered to cancer cells. Doxorubicin is broadly used as a first-line chemotherapy. Its main mechanism of action is based on DNA intercalation and disruption of topoisomerase-II-mediated DNA repair (Thorn *et al.*, 2011). Ibuprofen is a non-steroidal anti-inflammatory drug that has shown to have relevant anti-cancer activity by its non-selective inhibition of COX-1 and -2 (Andrews *et al.*, 2002). Since COX-2 overexpression is one key element on carcinogenesis linked to mutagenesis, mitogenesis, angiogenesis, dysfunctional apoptosis, immune suppression and metastasis (Harris *et al.*, 2012). This drug combination is expected to present a synergistic effect further increasing the anti-tumoral effect and avoiding the establishment of a drug resistant phenotype by cancer cells. For the dual drug loading a straightforward approach based on a sequential

loading procedure was adapted from the literature (Charnay *et al.*, 2004). The step-wise resuspension of MSNs in Doxorubicin and then in Ibuprofen solutions promoted their effective encapsulation in a short time, since at each impregnation/evaporation step the drug molecules diffuse more deeper into the pores by capillarity, increasing the loading efficiency. The amount of Doxorubicin and Ibuprofen encapsulated in MSNs was quantified by UV-vis spectrophotometry (Zhang *et al.*, 2013). The obtained results (Figure 21) showed a high encapsulation efficiency, ~90 % for Ibuprofen and ~77 % for Doxorubicin in single drug loading. These values correspond to ~45 mg of Ibuprofen and ~770 µg of Doxorubicin per 50 mg of MSNs. More importantly, during sequential loading of both drugs no significant differences in the encapsulation efficiency were observed and the same tendency was also verified during the coating procedure. This data indicates that drug loss is negligible in the subsequent loading steps, and calcium carbonate coating formation, does not impact the amount of drug in MSNs pores.

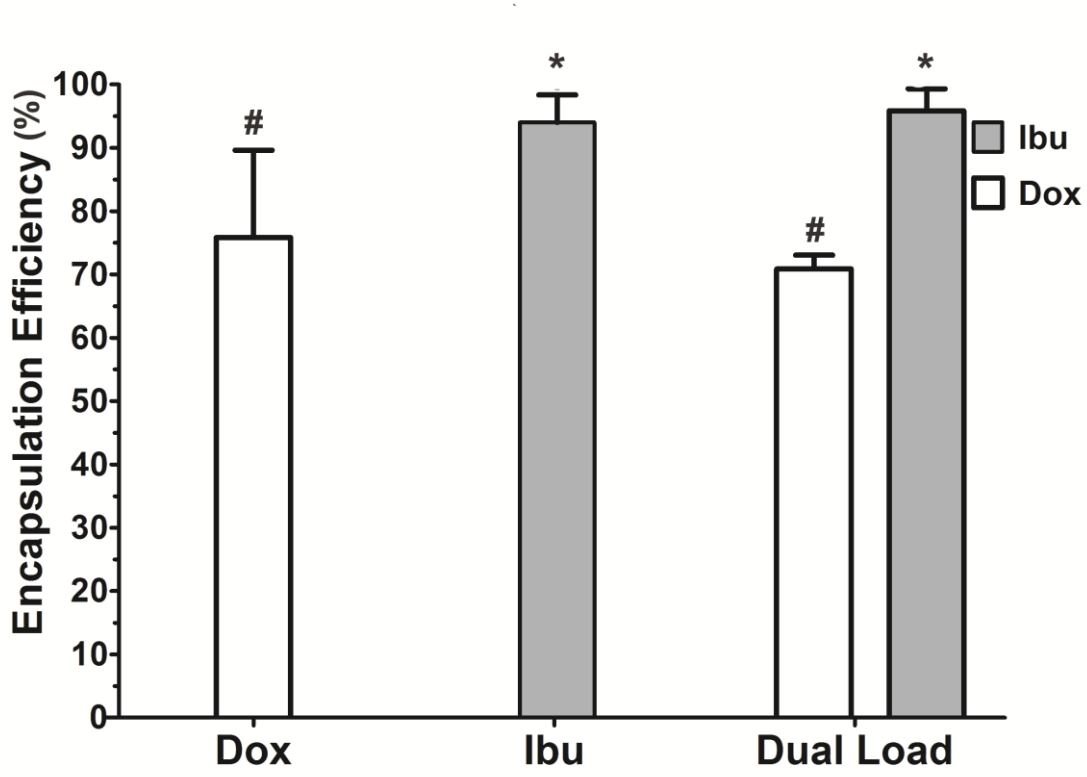

Figure 21 - Drug encapsulation efficiency analysis calculated from Eq.(1). Single loading of Doxorubicin (Dox), single loading of Ibuprofen (Ibu), and dual loading of Doxorubicin and Ibuprofen (Dual Load). Data is presented as mean ± s.d., *$p<0.05$, n=3, # and * difference not significant.

After completing MSNs loading, the particles were coated with $CaCO_3$ and the drug release profile of Dox-Ibu-MSNs-$CaCO_3$ at two pH values, 5.6 (to simulate the tumor microenvironment and lysosomal compartments) and 7.4 (to simulate physiological conditions) was evaluated. It is very important to retain the drug in the pores interior during long periods of time to provide a controlled release in the local of interest and not during blood circulation. Other important

characteristic is to maintain the drug concentration in the therapeutic window during prolonged periods for enhancing the therapeutic effect and reduce the number of administrations. This can be achieved by a tight control over the release and circulation time of nanoparticles, in such a way that a preferential particle accumulation in tumor cells is promoted and that drug release only occurs in the target site.

As shown in Figure 22 the carbonate coated nanoparticles present a pH sensitive release since their incubation in acidic media prompted an evident increase in the amount of released drug in comparison with the particles incubated at physiological pH (Figure 22 A and B). This rapid increase in the release of both Doxorubicin and Ibuprofen is a consequence of the disassembly of the calcium carbonate coating, which in turn lead to pore opening in silica nanoparticles. This data is in agreement with the results obtained in EDX analysis (Figure 19). It is also interesting to denote that the release at physiological pH presents slower kinetics (Figure 22). Due to the gradual $CaCO_3$ dissolution at physiological pH, a drug release is observed leading to a slight increase in the quantity of drug released. It is also worth to notice that the obtained results are similar to those reported in literature for complicated, costly and laborious polymer coatings (Liu *et al.*, 2011).

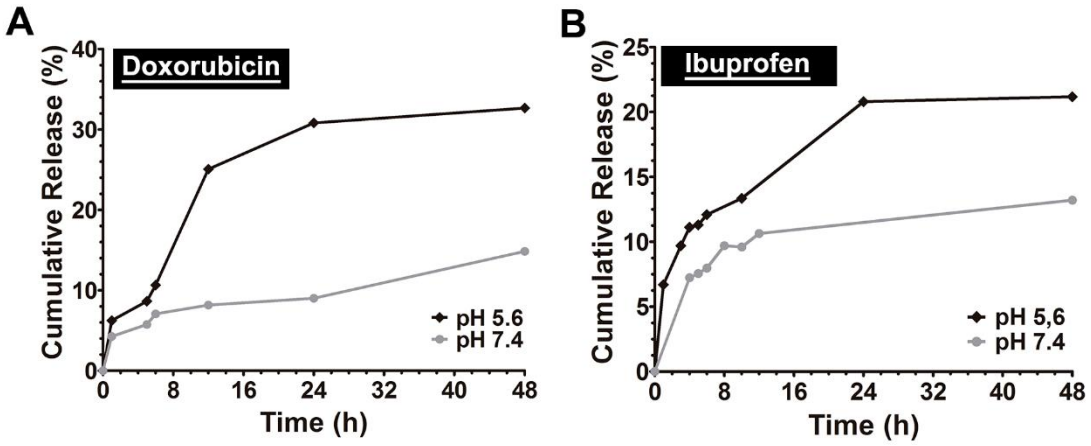

Figure 22 - pH-sensitive release kinetics of (A) Doxorubicin and (B) Ibuprofen from Dox-Ibu-MSNs-$CaCO_3$. The particles were incubated in PBS at two different pH in order to simulate the physiological pH (7.4) and the tumor microenvironment pH (5.6). Samples were collected at different time points and the drug concentration was assessed by UV–vis spectrophotometry.

3.9. Cytotoxicity assays

The biocompatibility of MSNs was investigated using FibH and also PC-3 cells. Although the MSNs cytotoxicity can depend on the type of cell, particle size and charge, in general, the MSNs are reported to be safe in concentrations below 100 μg/mL, which is a concentration of particles higher than that needed in most therapeutic treatments (Rosenholm *et al.*, 2010).

As shown in Figure 23, the MSNs did not presented any cytotoxic effect for FibH and PC-3 cells at concentrations ranging from 10 to 100 µg/mL after incubation for 24, 48 and 72 h. For 120 µg/mL a slight decrease in cell viability, (~90%), was observed on PC-3 cancer cell line (Figure 23 B). These results demonstrated that MSNs are highly biocompatible at concentrations lower than 120 µg/mL, which is in agreement with the results previously reported in the literature for the MCM-41 silica nanoparticles (Hudson *et al.*, 2008). Furthermore, optical microscopy images do not show any changes in cell morphology (Figure 23 C_1, C_2 and C_3) after incubation with MSNs. Moreover, the cells were able to adhere and proliferate in a similar way to the negative control. These findings allowed to assess whether the MSNs could negatively influence PC-3 cell viability masking Doxorubicin and Ibuprofen anti-tumoral activity and demonstrated that this is not expected.

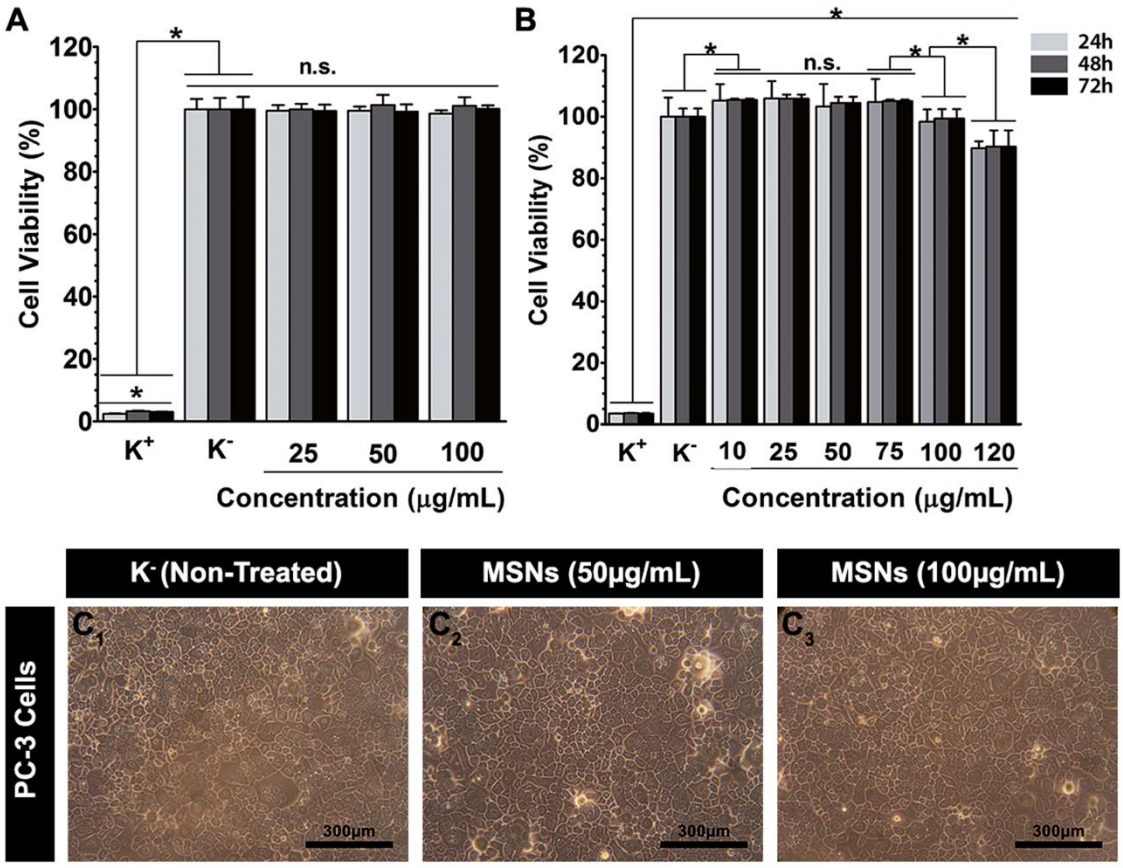

Figure 23 - Evaluation of the cytotoxic profile of MSNs (A) in FibH, and (B) in PC-3 cell lines at 24, 48 and 72 h. (C) Representative optical microscopy images from PC-3 cells incubated with MSNs at 72 h, (C1) negative control, (C2) and (C3) incubation with MSNs at concentrations of 50 and 100 µg/mL, respectively. Data is presented as mean ± s.d. *$p<0.05$, n=5; n.s.: not significant.

3.10. Mesoporous silica nanoparticles cellular uptake

Following the analysis of multi-drug-loading and of the release profile for MSNs, the cell internalization capacity of these nanocarriers in PC-3 cancer cells was evaluated. The cellular uptake capacity and the MSNs ability to deliver the loaded drugs in their local of action assumes great importance in the final treatment efficacy.

The cellular uptake capacity of blank MSNs, Ibu-MSNs, Dox-MSNs and Dox-Ibu-MSNs-$CaCO_3$ was visualized through CLSM using FITC to label blank MSNs and Ibu-MSNs and by using Doxorubicin fluorescence to visualize Dox-MSNs and Dox-Ibu-MSNs-$CaCO_3$ uptake (Figure 24). After an incubation of 4 h, it was observed that MSNs are present in the cytoplasm of PC-3 cells (Figure 24; white arrows). The intracellular localization is evident for all MSNs formulations, despite the lower fluorescence observed for MSNs, Ibu-MSNs and Dox-MSNs conditions. Which could be related to the FITC and Dox release from the non-coated particles, and therefore a small signal is observed.

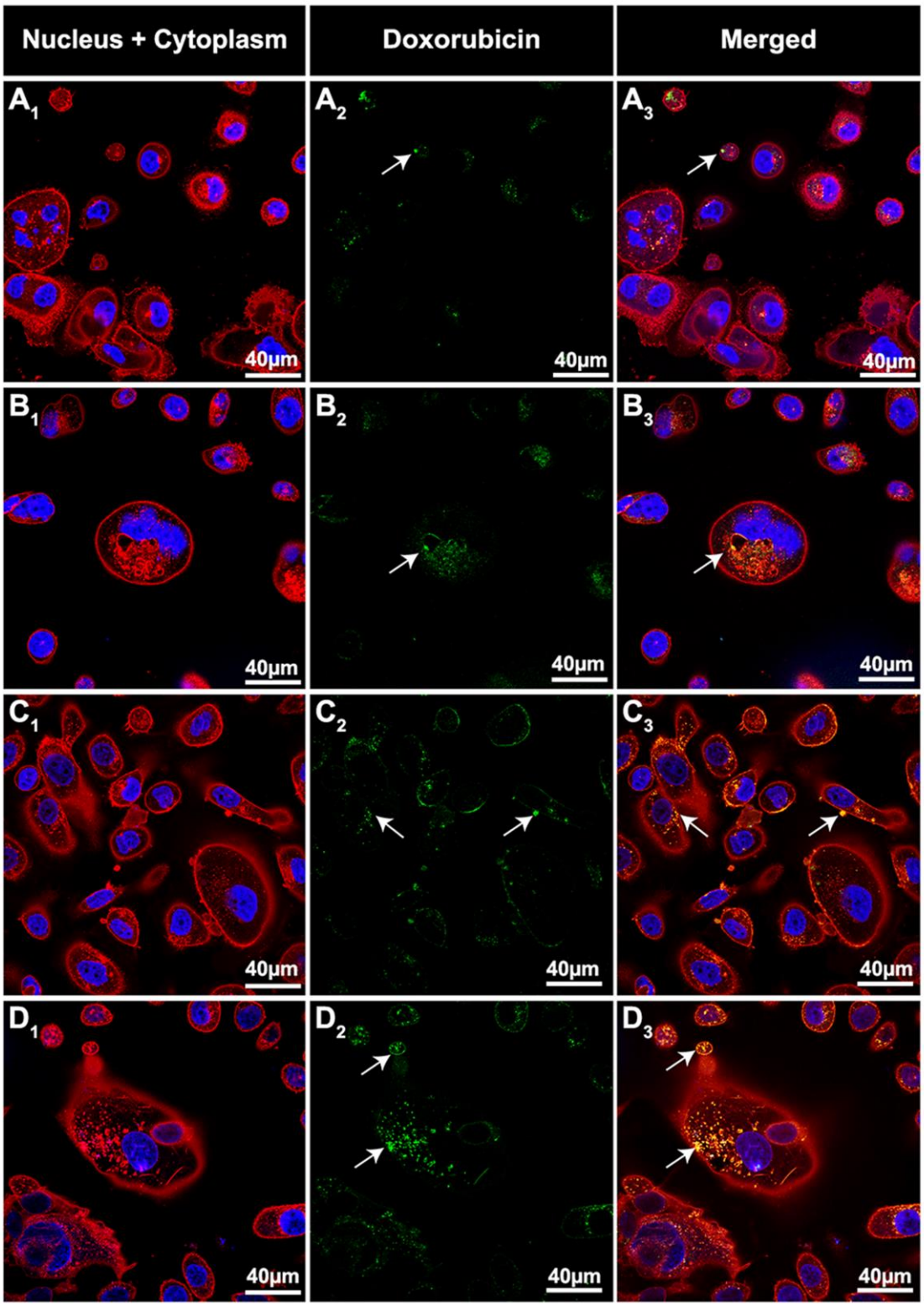

Figure 24 - Confocal microscopy images of MSNs uptake in PC-3 cancer cells. (A) MSNs, (B) Ibu-MSNs, (C) Dox-MSNs and (D) Dox-Ibu-MSNs-$CaCO_3$. The white arrows are pointing to internalized nanoparticles. Blue channel: Hoechst 33342® stained nucleus; Red channel: Alexa Fluor® 594 Conjugate for cell cytoplasm staining, green channel: (A) and (B) FITC loaded particles, (C) and (D) Doxorubicin fluorescence.

The intracellular localization of MSNs formulations is achieved after the nanocarriers transpose the extracellular membrane. Silica nanoparticles present a high affinity to the polar groups of various phospholipids, which facilitates their adsorption on cell surfaces leading to endocytosis (Xing *et al.*, 2005). In the case of silica nanoparticles the most common uptake pathways are clathrin-coated endocytosis, and pinocytosis (Slowing *et al.*, 2008). The successful internalization by these pathways will expose the MSNs to acidic environments of lysosomes. From this standpoint a fast dissociation of $CaCO_3$ coating would be promoted and this would consequently lead to the release of Doxorubicin and Ibuprofen entrapped inside the coated MSNs. Moreover, since this release takes place inside the cells the drugs are slowly released into the perynuclear region, as previously described, thus lowering the potential drug efflux to the extracellular medium (Ke *et al.*, 2013).

In fact, one important characteristic in drug delivery systems is the capacity to deliver the loading content to its intracellular targets. As can be seen in Figure 25, an increase in Doxorubicin fluorescence inside cells can be observed along time, more precisely an initial release in the cell cytoplasm, with a posterior accumulation in the cell nucleus (Figure 25 B_3, C_3 and D_3). This was confirmed by comparing the mean fluorescence intensity at 6 h, between the nucleus and cell cytoplasm in Zeiss Zen 2010 software (Figure 26). This analysis revealed that a higher intensity of Doxorubicin fluorescence in the nucleus was obtained in comparison to that of cytoplasm. Furthermore, taking into account the release data (Figure 22) we propose that Ibuprofen, when delivered by MSNs, is simultaneously released to the cell cytoplasm.

This data assumes great importance since it demonstrates that the drugs, specifically in this case Doxorubicin, can escape from lysosomal compartments and favors the drug accumulation inside the cancer cells. Furthermore, it is also possible to observe that MSNs facilitate the interaction between drugs and their intracellular targets, since the drugs and in particular Doxorubicin, can successfully reach its main local of action (nucleus) to exert the therapeutic effect. Also, it is clear that a bolus drug release inside the cells is achieved. This fact is due to the fast $CaCO_3$ dissolution in acidic lysosomal compartments.

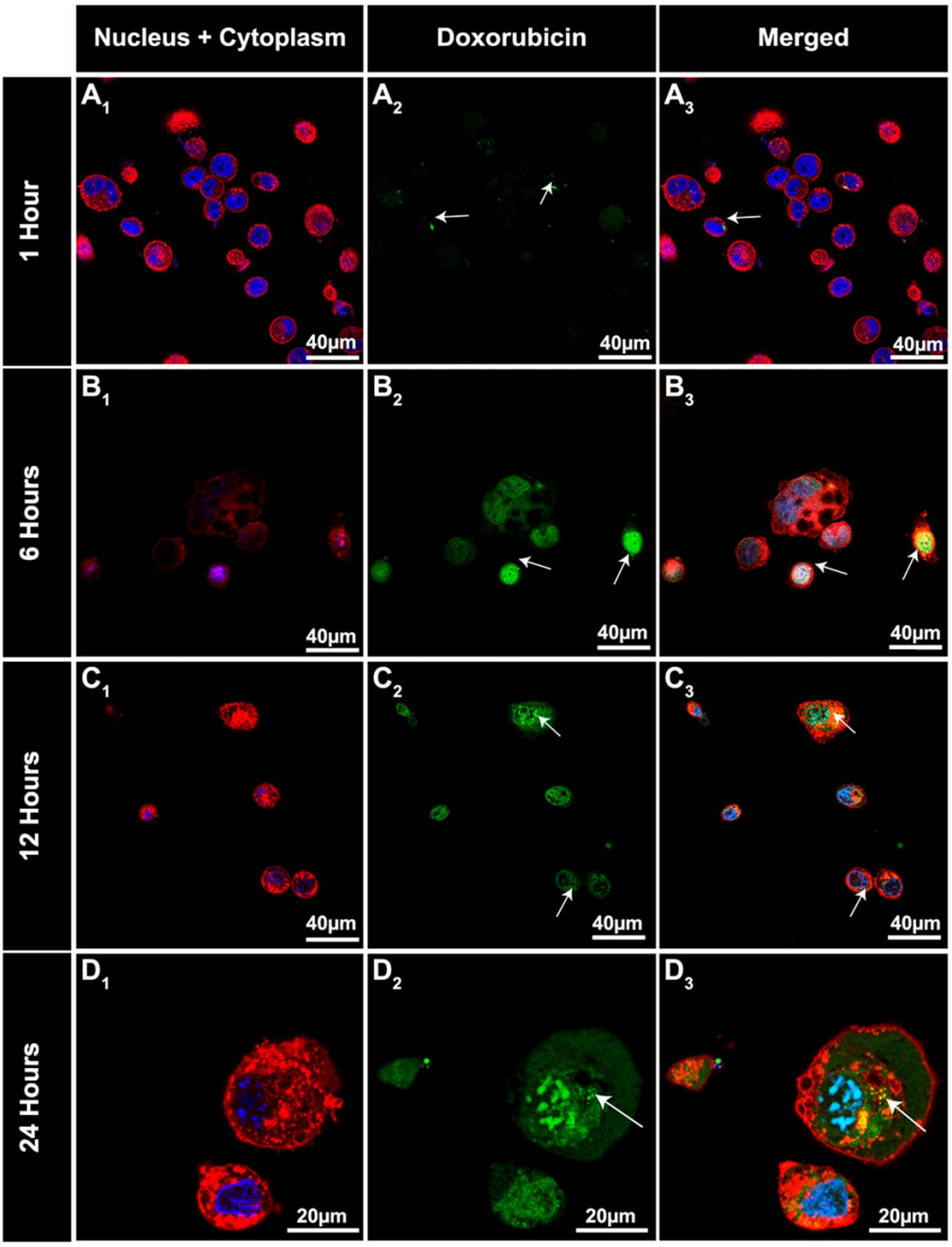

Figure 25 - Time course uptake analysis of Dox-Ibu-MSNs-$CaCO_3$. (A) 1 h, (B) 6 h, (C) 12 h and (D) 24 h. PC-3 cells were incubated with Dox-Ibu-MSNs-$CaCO_3$ particles and their cell internalization and Doxorubicin accumulation in nucleus was observed by confocal microscopy at different time points. The white arrows are pointing to internalized nanoparticles. Blue channel: Hoechst 33342® stained nucleus; Red channel: Alexa Fluor® 594 Conjugate for cell cytoplasm staining; Green channel: Doxorubicin fluorescence.

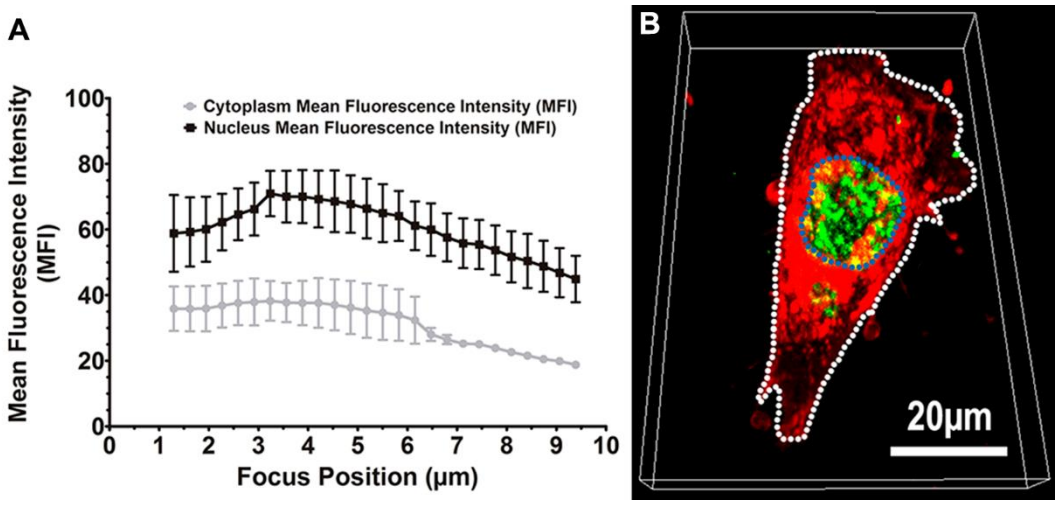

Figure 26 - (A) comparison between Doxorubicin mean fluorescence intensity (MFI) in the nucleus and in the cytoplasm, at 6 h. Calculated from each stack (0.285 µm thickness) mean fluorescence intensity of z-stack images of time course analysis at 6 h utilizing Zeiss Zen 2010 software Data is presented as mean ± s.d., n=3. (B) Representative 3D reconstruction of a PC-3 cell transfected with Dox-Ibu-MSNs-$CaCO_3$ nanoparticles. Cell nucleus (dashed blue lines) and cytoplasm (white dashed lines). Red channel: WGA-Alexa 594; Green channel: Doxorubicin.

3.11. IC50 determination

After characterizing MSNs biocompatibility and cellular uptake, the real cytotoxic activity of free Ibuprofen and Doxorubicin was determined in the PC-3 cell line. The IC50 determination indicates the minimum drug concentration that is able to kill half of the cell population.

In order to determine the IC 50 of Ibuprofen and Doxorubicin, PC-3 cancer cells were incubated with different concentrations of free drug. The IC50 calculated for Doxorubicin (70.317±4.361 µM) is about 35-fold higher than that reported in the literature ~2 µM (Eckman *et al.*, 2012). This fact can be explained by the acquisition of a Doxorubicin resistant phenotype by the PC-3 cells while in culture for long periods. Relatively to the Ibuprofen calculated IC50 value (2.134±0.053 mM), it was similar to that reported in the literature (2 mM) (Palayoor *et al.*, 1998). It is worth to notice that Doxorubicin had a significantly lower inhibitory concentration than Ibuprofen, which can be explained by its more direct mechanism of action.

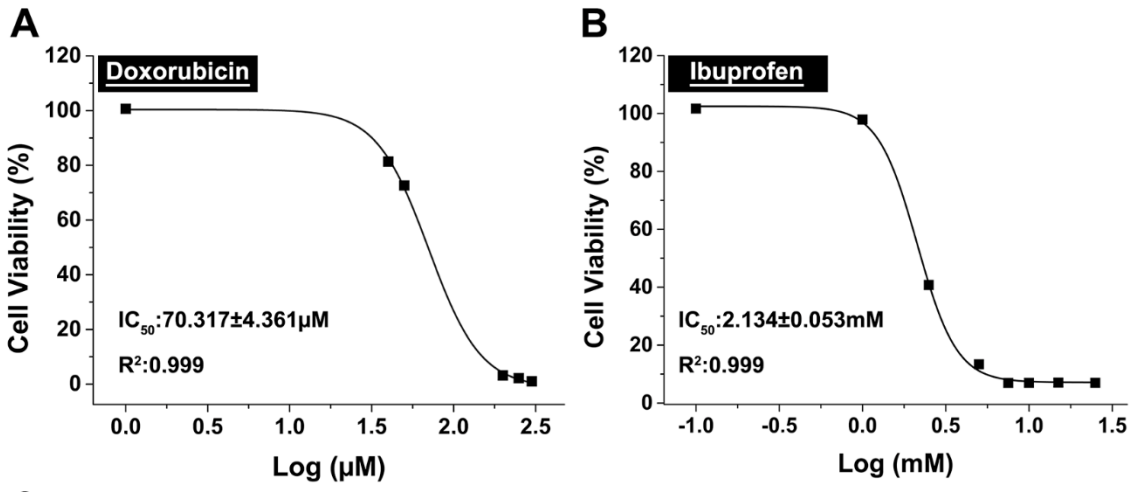

Figure 27 - Doxorubicin and Ibuprofen IC_{50} determination. PC-3 cells were exposed to different concentrations of Doxorubicin or Ibuprofen and the cell viability was measured at 48 h by MTS assay.

3.12. *In vitro* cytotoxic activity of drug loaded mesoporous silica nanoparticles

After determining the activity of free drugs in PC-3 cells the effect of their delivery by pH responsive MSNs was evaluated. Moreover, a comparison of the cytotoxic effect of carbonate coated and uncoated silica nanoparticles was also performed. In addition to the nanoparticle effects, the combinational effect of co-delivering Doxorubicin (16 μM) and Ibuprofen (4 mM) simultaneously was investigated, which is the same concentration resulting from the application of 100 μg of loaded MSNs in 1 mL.

For this purpose PC-3 cells were incubated with various particle formulations. As shown in Figure 28 A and B, the different MSNs formulations promoted a decrease in cell viability. These findings were also observed through optic microscopy images with cell density reduction and the higher presence of cells with spherical morphologies, indicative of cell death (Figure 28 C). Furthermore, the delivery of $CaCO_3$ coated MSNs resulted in an increased cytotoxic activity, especially with at a nanoparticle concentration of 100 μg/mL, at 72 h (Figure 28 B). Which showed to be a safe concentration in previous data. Moreover, at this time point MSNs-$CaCO_3$ mediated delivery promotes a significantly higher anti-tumoral effect when compared to that of the free drugs and by using 80 % less Ibuprofen and Doxorubicin concentration than the free drug combination (Figure 28 B). It is also important to notice that the $CaCO_3$ coated MSNs also presented a higher anti-proliferative effect when compared to their non-coated counterparts (Figure 28 B). A fact that is likely caused by the $CaCO_3$ end-capping, which entrap the drug loaded molecules when MSNs are in suspension in the medium before being internalized. Afterwards, when the particles are internalized and are exposed to the acidic lysosomal environment the $CaCO_3$ disassembles and the MSNs cargo is released, creating a bolus delivery (high concentration in a short period of time) inside the cell. On the other side the non-coated

particles begin to release their cargo when they are in suspension in the medium, so when the particles enter the cell the amount of drug released inside the cell cytoplasm will be smaller.

This data thus supports the applicability of MSNs-$CaCO_3$ nanocarriers for therapeutic applications and the influence $CaCO_3$ pH responsive coating in the therapeutic outcome.

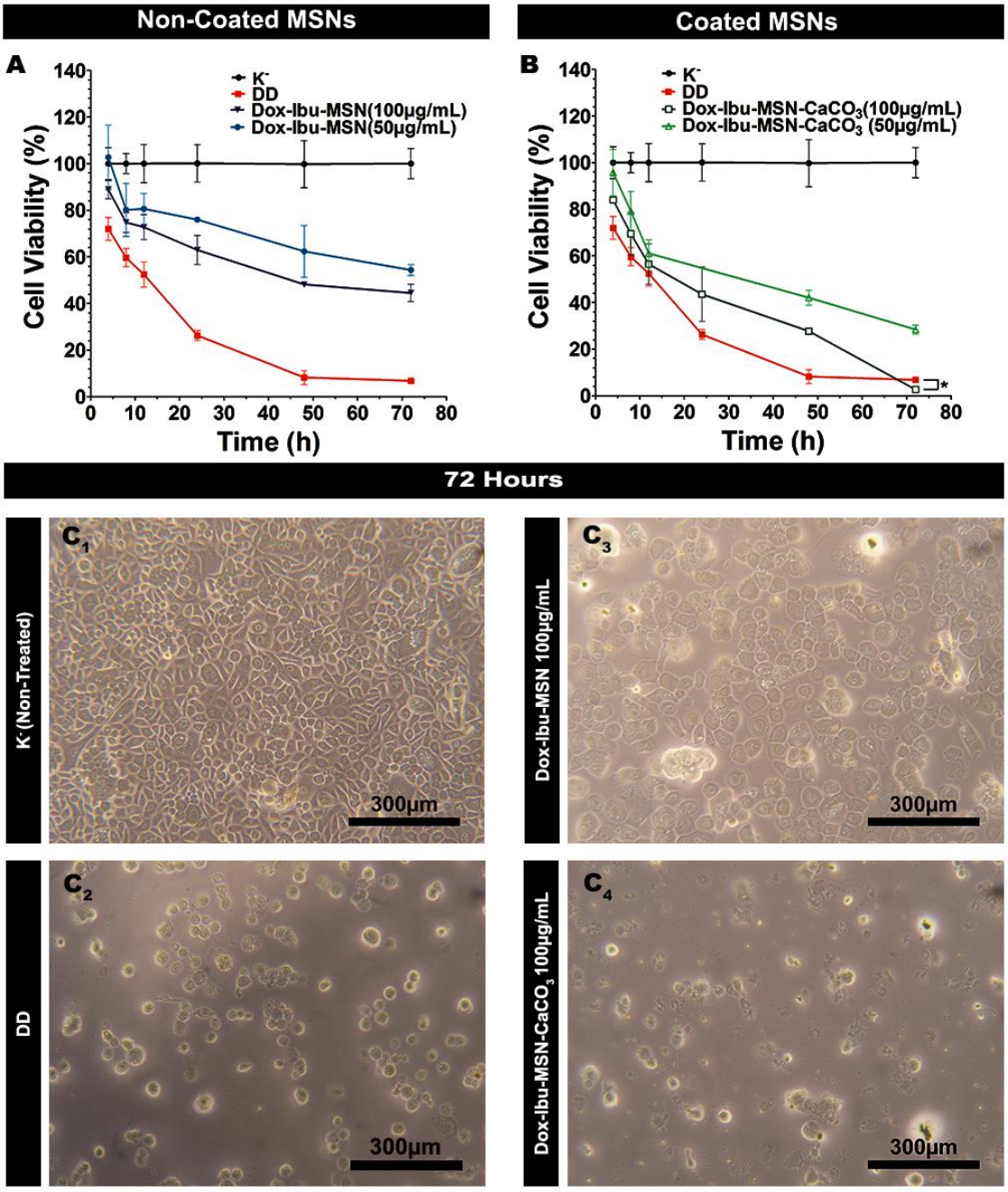

Figure 28 - Evaluation of MSNs anti-tumoral activity in PC-3 prostate cancer cells. Cell death study at different time points testing two different concentrations of (A) Non-coated MSNs, (B) Coated MSNs. DD represents the free delivery combination of Ibuprofen (4mM) and Doxorubicin (16µM). (C) Representative optical microscopy images from PC-3 cells at 72 h, (C_1) negative control, (C_2) free delivery combination of Ibuprofen and Doxorubicin, (C_3) and (C_4) incubation with Dox-Ibu-MSNs and Dox-Ibu-MSNs-$CaCO_3$, respectively, at 100 µg/mL. Data presents mean ± s.d., n=6; *p<0.05.

Chapter 4

Conclusions and Future Perspectives

4. Conclusions and Future Perspectives

The application of Nanotechnology in healthcare, and in particular in cancer therapy arises as one of the most compelling solutions to the problems faced by biotechnological and pharmaceutical industries in the development of novel therapeutics. Nevertheless, despite all the efforts made in the development of new strategies to cancer cells, no "magic bullet" as yet been developed. The search for drug carriers, which can be delivered to kill cancer cells with precision promoting far less or no cytotoxicity to healthy tissues has proven to be very difficult to achieve.

The research work described in this thesis reports the development of a novel, simple and economically viable $CaCO_3$ end-cap coating for MSNs. The MSM-41 type MSNs are a well described nanocarrier with specific characteristics that make it well suitable for drug delivery to cancer cells. Particularly, these nanoparticles possess a unique, uniform and tunable porous structure that allows drug loading in high amounts. Furthermore, the produced MSNs presented size and zeta potential suitable to be applied as DDSs, and also showed to be biocompatible in concentrations lower than 120 µg/mL, which is superior to the particle concentrations needed in most therapeutic treatments.

To control the drug release from MSNs it was proposed a new end-capping with $CaCO_3$ crystals. The coating was capable to imprint a pH-responsive effect on the nanoparticles and influenced the drug release profile of two chemotherapeutic drugs inside cancer cells. Since exposing MSNs to acidic medium prompted a fast drug release and at physiological pH a much slower kinetics was observed, this coating can be used for on-demand delivery in cancer cells or the tumor microenvironment with low pH. Furthermore, the mild capping conditions maintained the loaded drugs inside the pores of MSNs.

The *in vitro* uptake studies in PC-3 cells showed an effective internalization of MSNs. These findings assume great importance since it was observed that the drugs are capable to reach their local of action and exert their function. This capacity to deliver the drugs inside cells to enhance their efficacy is even more evident in cytotoxic studies, were the Dox-Ibu-MSNs-$CaCO_3$ exhibited a synergistic effect when compared to the simultaneous delivery of free Doxorubicin and Ibuprofen. It is also important to notice that the $CaCO_3$ coated MSNs obtained a cytotoxic effect when compared to their non-coated counterparts. Furthermore, the loaded $CaCO_3$ coated particles presented similar results to free drug administration with a drug concentration 80% inferior.

In summary, the findings presented in this thesis suggest that MSNs-$CaCO_3$ are promising candidates as drug carriers for cancer therapy. Furthermore, since the coating is promoted in

mild conditions, and MSNs can encapsulate both hydrophobic/hydrophilic bioactive molecules, this strategy can be employed for other therapeutic applications. Besides, due to their versatile nature, these nanocarriers can be combined with other moieties that can provide additional functions like diagnostic and imaging.

References

ABU LILA, A. S., ELDIN, N. E., ICHIHARA, M., ISHIDA, T. & KIWADA, H. 2012. Multiple administration of PEG-coated liposomal oxaliplatin enhances its therapeutic efficacy: a possible mechanism and the potential for clinical application. Int. J. Pharm., 438, 176-83.

AKBARZADEH, A., REZAEI-SADABADY, R., DAVARAN, S., JOO, S. W., ZARGHAMI, N., HANIFEHPOUR, Y., SAMIEI, M., KOUHI, M. & NEJATI-KOSHKI, K. 2013. Liposome: classification, preparation, and applications. Nanoscale Res Lett, 8, 102.

AKHTER, S., AHMAD, I., AHMAD, M. Z., RAMAZANI, F., SINGH, A., RAHMAN, Z., AHMAD, F. J., STORM, G. & KOK, R. J. 2013. Nanomedicines as cancer therapeutics: current status. Curr Cancer Drug Targets, 13, 362-78.

AL-JAMAL, W. T. & KOSTARELOS, K. 2011. Liposomes: from a clinically established drug delivery system to a nanoparticle platform for theranostic nanomedicine. Acc Chem Res, 44, 1094-104.

ALLEN, T. M. & CULLIS, P. R. 2004. Drug delivery systems: entering the mainstream. Science, 303, 1818-22.

ALLEN, T. M. & CULLIS, P. R. 2013. Liposomal drug delivery systems: from concept to clinical applications. Adv. Drug Delivery Rev., 65, 36-48.

ALMEIDA, A. J. & SOUTO, E. 2007. Solid lipid nanoparticles as a drug delivery system for peptides and proteins. Adv. Drug Delivery Rev., 59, 478-90.

ALONSO, M. J. 2004. Nanomedicines for overcoming biological barriers. Biomed Pharmacother, 58, 168-72.

ANDREWS, J., DJAKIEW, D., KRYGIER, S. & ANDREWS, P. 2002. Superior effectiveness of ibuprofen compared with other NSAIDs for reducing the survival of human prostate cancer cells. Cancer Chemother Pharmacol, 50, 277-84.

ARAUJO, J. C., MATHEW, P., ARMSTRONG, A. J., BRAUD, E. L., POSADAS, E., LONBERG, M., GALLICK, G. E., TRUDEL, G. C., PALIWAL, P., AGRAWAL, S. & LOGOTHETIS, C. J. 2012. Dasatinib combined with docetaxel for castration-resistant prostate cancer: results from a phase 1-2 study. Cancer, 118, 63-71.

ARCANGELI, S., PINZI, V. & ARCANGELI, G. 2012. Epidemiology of prostate cancer and treatment remarks. World J Radiol, 4, 241-6.

BAEK, S. J., WILSON, L. C., LEE, C. H. & ELING, T. E. 2002. Dual function of nonsteroidal anti-inflammatory drugs (NSAIDs): inhibition of cyclooxygenase and induction of NSAID-activated gene. J Pharmacol Exp Ther, 301, 1126-31.

BYRNE, J. D., BETANCOURT, T. & BRANNON-PEPPAS, L. 2008. Active targeting schemes for nanoparticle systems in cancer therapeutics. Adv. Drug Delivery Rev., 60, 1615-26.

CANEL, M., SERRELS, A., FRAME, M. C. & BRUNTON, V. G. 2013. E-cadherin-integrin crosstalk in cancer invasion and metastasis. J Cell Sci, 126, 393-401.

CENTER, M. M., JEMAL, A., LORTET-TIEULENT, J., WARD, E., FERLAY, J., BRAWLEY, O. & BRAY, F. 2012. International variation in prostate cancer incidence and mortality rates. Eur Urol, 61, 1079-92.

CHAFFER, C. L. & WEINBERG, R. A. 2011. A perspective on cancer cell metastasis. Science, 331, 1559-64.

CHARNAY, C., BEGU, S., TOURNE-PETEILH, C., NICOLE, L., LERNER, D. A. & DEVOISSELLE, J. M. 2004. Inclusion of ibuprofen in mesoporous templated silica: drug loading and release property. Eur J Pharm Biopharm, 57, 533-40.

CHEN, X., CHENG, X., SOERIYADI, A. H., SAGNELLA, S. M., LU, X., SCOTT, J. A., LOWE, S. B., KAVALLARIS, M. & GOODING, J. J. 2014. Stimuli-responsive functionalized mesoporous silica nanoparticles for drug release in response to various biological stimuli. Biomater. Sci., 2, 121-130.

CHENG, N., CHYTIL, A., SHYR, Y., JOLY, A. & MOSES, H. L. 2008a. Transforming growth factor-beta signaling-deficient fibroblasts enhance hepatocyte growth factor signaling in mammary carcinoma cells to promote scattering and invasion. Mol Cancer Res., 6, 1521-33.

CHENG, Y., XU, Z., MA, M. & XU, T. 2008b. Dendrimers as drug carriers: Applications in different routes of drug administration. J. Pharm. Sci., 97, 123-143.

CHITHRANI, B. D. & CHAN, W. C. 2007. Elucidating the mechanism of cellular uptake and removal of protein-coated gold nanoparticles of different sizes and shapes. Nano Lett., 7, 1542-50.

CHO, K., WANG, X., NIE, S., CHEN, Z. G. & SHIN, D. M. 2008. Therapeutic nanoparticles for drug delivery in cancer. Clin. Cancer Res., 14, 1310-6.

CHOI, K.-M. & KURODA, K. 2012. Polymorph Control of Calcium Carbonate on the Surface of Mesoporous Silica. Cryst. Growth Des., 12, 887-893.

CHUNG, A. S., LEE, J. & FERRARA, N. 2010. Targeting the tumour vasculature: insights from physiological angiogenesis. Nat. Rev. Cancer, 10, 505-14.

COSTA, C., SANTOS, M., MARTINEZ-FERNANDEZ, M., DUENAS, M., LORZ, C., GARCIA-ESCUDERO, R. & PARAMIO, J. M. 2013. E2F1 loss induces spontaneous tumour development in Rb-deficient epidermis. Oncogene, 32, 2937-51.

COTI, K. K., BELOWICH, M. E., LIONG, M., AMBROGIO, M. W., LAU, Y. A., KHATIB, H. A., ZINK, J. I., KHASHAB, N. M. & STODDART, J. F. 2009. Mechanised nanoparticles for drug delivery. Nanoscale, 1, 16-39.

DANHIER, F., FERON, O. & PREAT, V. 2010. To exploit the tumor microenvironment: Passive and active tumor targeting of nanocarriers for anti-cancer drug delivery. J. Controlled Release, 148, 135-46.

DANNENBERG, A. J., ALTORKI, N. K., BOYLE, J. O., DANG, C., HOWE, L. R., WEKSLER, B. B. & SUBBARAMAIAH, K. 2001. Cyclo-oxygenase 2: a pharmacological target for the prevention of cancer. Lancet Oncol., 2, 544-51.

DAROQUI, M. C., VAZQUEZ, P., BAL DE KIER JOFFE, E., BAKIN, A. V. & PURICELLI, L. I. 2012. TGF-beta autocrine pathway and MAPK signaling promote cell invasiveness and in vivo mammary adenocarcinoma tumor progression. Oncol Rep, 28, 567-75.

DAVIS, M. E., CHEN, Z. G. & SHIN, D. M. 2008. Nanoparticle therapeutics: an emerging treatment modality for cancer. Nat Rev Drug Discov, 7, 771-82.

DE MARZO, A. M., PLATZ, E. A., SUTCLIFFE, S., XU, J., GRONBERG, H., DRAKE, C. G., NAKAI, Y., ISAACS, W. B. & NELSON, W. G. 2007. Inflammation in prostate carcinogenesis. Nat. Rev. Cancer, 7, 256-69.

DI FIORE, R., D'ANNEO, A., TESORIERE, G. & VENTO, R. 2013. RB1 in cancer: different mechanisms of RB1 inactivation and alterations of pRb pathway in tumorigenesis. J Cell Physiol, 228, 1676-87.

DREHER, M. R., LIU, W., MICHELICH, C. R., DEWHIRST, M. W., YUAN, F. & CHILKOTI, A. 2006. Tumor vascular permeability, accumulation, and penetration of macromolecular drug carriers. J Natl Cancer Inst, 98, 335-44.

DU, J. Z., MAO, C. Q., YUAN, Y. Y., YANG, X. Z. & WANG, J. 2013. Tumor extracellular acidity-activated nanoparticles as drug delivery systems for enhanced cancer therapy. Biotechnol Adv.

ECKMAN, A. M., TSAKALOZOU, E., KANG, N. Y., PONTA, A. & BAE, Y. 2012. Drug release patterns and cytotoxicity of PEG-poly(aspartate) block copolymer micelles in cancer cells. Pharm. Res., 29, 1755-67.

EL-SHEIKH, S. M., EL-SHERBINY, S., BARHOUM, A. & DENG, Y. 2013. Effects of cationic surfactant during the precipitation of calcium carbonate nano-particles on their size, morphology, and other characteristics. Colloids Surf., A, 422, 44-49.

ELSABAHY, M. & WOOLEY, K. L. 2012. Design of polymeric nanoparticles for biomedical delivery applications. Chem. Soc. Rev., 41, 2545-61.

ERNSTING, M. J., MURAKAMI, M., ROY, A. & LI, S. D. 2013. Factors controlling the pharmacokinetics, biodistribution and intratumoral penetration of nanoparticles. J. Controlled Release, 172, 782-94.

EVAN, G. I. & VOUSDEN, K. H. 2001. Proliferation, cell cycle and apoptosis in cancer. Nature, 411, 342-8.

EVANS, W. E. & MCLEOD, H. L. 2003. Pharmacogenomics--drug disposition, drug targets, and side effects. N. Engl. J. Med., 348, 538-49.

FARAJI, A. H. & WIPF, P. 2009. Nanoparticles in cellular drug delivery. Bioorg Med Chem, 17, 2950-62.

FELDMAN, B. J. & FELDMAN, D. 2001. The development of androgen-independent prostate cancer. Nat. Rev. Cancer, 1, 34-45.

FERLAY, J., STELIAROVA-FOUCHER, E., LORTET-TIEULENT, J., ROSSO, S., COEBERGH, J. W., COMBER, H., FORMAN, D. & BRAY, F. 2013. Cancer incidence and mortality patterns in Europe: estimates for 40 countries in 2012. Eur. J. Cancer, 49, 1374-403.

FERLINI, C., SCAMBIA, G., DISTEFANO, M., FILIPPINI, P., ISOLA, G., RIVA, A., BOMBARDELLI, E., FATTOROSSI, A., BENEDETTI PANICI, P. & MANCUSO, S. 1997. Synergistic antiproliferative activity of tamoxifen and docetaxel on three oestrogen receptor-negative cancer cell lines is mediated by the induction of apoptosis. Br. J. Cancer, 75, 884-91.

FERRARI, M. 2010. Frontiers in cancer nanomedicine: directing mass transport through biological barriers. Trends Biotechnol., 28, 181-188.

FLEIGE, E., QUADIR, M. A. & HAAG, R. 2012. Stimuli-responsive polymeric nanocarriers for the controlled transport of active compounds: concepts and applications. Adv. Drug Delivery Rev., 64, 866-84.

FLOOR, S. L., DUMONT, J. E., MAENHAUT, C. & RASPE, E. 2012. Hallmarks of cancer: of all cancer cells, all the time? Trends Mol. Med., 18, 509-15.

FOX, E. J. 2004. Mechanism of action of mitoxantrone. Neurology, 63, S15-8.

FRECHET, J. M. 1994. Functional polymers and dendrimers: reactivity, molecular architecture, and interfacial energy. Science, 263, 1710-5.

FUKUMURA, D. & JAIN, R. K. 2008. Imaging angiogenesis and the microenvironment. APMIS, 116, 695-715.

GANTA, S., DEVALAPALLY, H., SHAHIWALA, A. & AMIJI, M. 2008. A review of stimuli-responsive nanocarriers for drug and gene delivery. J. Controlled Release, 126, 187-204.

GASPAR, V. M., CORREIA, I. J., SOUSA, A., SILVA, F., PAQUETE, C. M., QUEIROZ, J. A. & SOUSA, F. 2011. Nanoparticle mediated delivery of pure P53 supercoiled plasmid DNA for gene therapy. J. Controlled Release, 156, 212-22.

GASPAR, V. M., MARQUES, J. G., SOUSA, F., LOURO, R. O., QUEIROZ, J. A. & CORREIA, I. J. 2013. Biofunctionalized nanoparticles with pH-responsive and cell penetrating blocks for gene delivery. Nanotechnology, 24, 275101.

GESSNER, A., WAICZ, R., LIESKE, A., PAULKE, B., MADER, K. & MULLER, R. H. 2000. Nanoparticles with decreasing surface hydrophobicities: influence on plasma protein adsorption. Int. J. Pharm., 196, 245-9.

GOLDSTEIN, A. S., HUANG, J., GUO, C., GARRAWAY, I. P. & WITTE, O. N. 2010. Identification of a cell of origin for human prostate cancer. Science, 329, 568-71.

GRECO, F. & VICENT, M. J. 2009. Combination therapy: opportunities and challenges for polymer-drug conjugates as anticancer nanomedicines. Adv. Drug Delivery Rev., 61, 1203-13.

GREENWALD, R. B., CHOE, Y. H., MCGUIRE, J. & CONOVER, C. D. 2003. Effective drug delivery by PEGylated drug conjugates. Adv. Drug Delivery Rev., 55, 217-50.

GRÖNBERG, H. 2003. Prostate cancer epidemiology. Lancet, 361, 859-864.

GUO, J., EVANS, J. C. & O'DRISCOLL, C. M. 2013. Delivering RNAi therapeutics with non-viral technology: a promising strategy for prostate cancer? Trends Mol. Med., 19, 250-61.

HANAHAN, D. & COUSSENS, L. M. 2012. Accessories to the crime: functions of cells recruited to the tumor microenvironment. Cancer Cell, 21, 309-22.

HANAHAN, D. & WEINBERG, R. A. 2000. The hallmarks of cancer. Cell, 100, 57-70.

HANAHAN, D. & WEINBERG, R. A. 2011. Hallmarks of cancer: the next generation. Cell, 144, 646-74.

HARRIS, M. T., BRUNSON, R. R. & BYERS, C. H. 1990. The base-catalyzed hydrolysis and condensation reactions of dilute and concentrated TEOS solutions. J. Non-Cryst. Solids, 121, 397-403.

HARRIS, R. E., BEEBE, J. & ALSHAFIE, G. 2012. Reduction in cancer risk by selective and nonselective cyclooxygenase-2 (COX-2) inhibitors. J. Exp. Pharmacol., 6, 491-496.

HE, C., HU, Y., YIN, L., TANG, C. & YIN, C. 2010a. Effects of particle size and surface charge on cellular uptake and biodistribution of polymeric nanoparticles. Biomaterials, 31, 3657-66.

HE, Q., SHI, J., CHEN, F., ZHU, M. & ZHANG, L. 2010b. An anticancer drug delivery system based on surfactant-templated mesoporous silica nanoparticles. Biomaterials, 31, 3335-3346.

HE, Q., ZHANG, J., SHI, J., ZHU, Z., ZHANG, L., BU, W., GUO, L. & CHEN, Y. 2010c. The effect of PEGylation of mesoporous silica nanoparticles on nonspecific binding of serum proteins and cellular responses. Biomaterials, 31, 1085-92.

HERD, H., DAUM, N., JONES, A. T., HUWER, H., GHANDEHARI, H. & LEHR, C. M. 2013. Nanoparticle geometry and surface orientation influence mode of cellular uptake. ACS Nano, 7, 1961-73.

HUANG, X., TENG, X., CHEN, D., TANG, F. & HE, J. 2010. The effect of the shape of mesoporous silica nanoparticles on cellular uptake and cell function. Biomaterials, 31, 438-48.

HUDSON, S. P., PADERA, R. F., LANGER, R. & KOHANE, D. S. 2008. The biocompatibility of mesoporous silicates. Biomaterials, 29, 4045-55.

JAYAKUMAR, R., NAIR, A., REJINOLD, N. S., MAYA, S. & NAIR, S. V. 2012. Doxorubicin-loaded pH-responsive chitin nanogels for drug delivery to cancer cells. Carbohydr. Polym., 87, 2352-2356.

JENSTER, G. 1999. The role of the androgen receptor in the development and progression of prostate cancer. Semin. Oncol., 26, 407-21.

JI, W., LI, N., CHEN, D., QI, X., SHA, W., JIAO, Y., XU, Q. & LU, J. 2013. Coumarin-containing photo-responsive nanocomposites for NIR light-triggered controlled drug release via a two-photon process. J. Mater. Chem. B, 1, 5942-5949.

JIA, F., LIU, X., LI, L., MALLAPRAGADA, S., NARASIMHAN, B. & WANG, Q. 2013. Multifunctional nanoparticles for targeted delivery of immune activating and cancer therapeutic agents. J. Controlled Release, 172, 1020-34.

JUNTTILA, M. R. & DE SAUVAGE, F. J. 2013. Influence of tumour micro-environment heterogeneity on therapeutic response. Nature, 501, 346-54.

KAUR, I. P., BHANDARI, R., BHANDARI, S. & KAKKAR, V. 2008. Potential of solid lipid nanoparticles in brain targeting. J. Controlled Release, 127, 97-109.

KE, C. J., CHIANG, W. L., LIAO, Z. X., CHEN, H. L., LAI, P. S., SUN, J. S. & SUNG, H. W. 2013. Real-time visualization of pH-responsive PLGA hollow particles containing a gas-generating agent targeted for acidic organelles for overcoming multi-drug resistance. Biomaterials, 34, 1-10.

KEIZER, H. G., PINEDO, H. M., SCHUURHUIS, G. J. & JOENJE, H. 1990. Doxorubicin (adriamycin): a critical review of free radical-dependent mechanisms of cytotoxicity. Pharmacol. Ther., 47, 219-31.

KELLY, P. N. & STRASSER, A. 2011. The role of Bcl-2 and its pro-survival relatives in tumourigenesis and cancer therapy. Cell Death Differ., 18, 1414-24.

KESHARWANI, P., JAIN, K. & JAIN, N. K. 2014. Dendrimer as nanocarrier for drug delivery. Prog. Polym. Sci., 39, 268-307.

LADJ, R., BITAR, A., EISSA, M., MUGNIER, Y., LE DANTEC, R., FESSI, H. & ELAISSARI, A. 2013. Individual inorganic nanoparticles: preparation, functionalization and in vitro biomedical diagnostic applications. J. Mater. Chem. B, 1, 1381-1396.

LAVELLE, F., BISSERY, M. C., COMBEAU, C., RIOU, J. F., VRIGNAUD, P. & ANDRE, S. 1995. Preclinical evaluation of docetaxel (Taxotere). Semin. Oncol., 22, 3-16.

LEE, C. C., MACKAY, J. A., FRECHET, J. M. & SZOKA, F. C. 2005. Designing dendrimers for biological applications. Nat Biotechnol, 23, 1517-26.

LEE, C. H., AKIN-OLUGBADE, O. & KIRSCHENBAUM, A. 2011a. Overview of prostate anatomy, histology, and pathology. Endocrinol Metab Clin North Am, 40, 565-75, viii-ix.

LEE, S., YUN, H.-S. & KIM, S.-H. 2011b. The comparative effects of mesoporous silica nanoparticles and colloidal silica on inflammation and apoptosis. Biomaterials, 32, 9434-9443.

LEHNER, R., WANG, X., WOLF, M. & HUNZIKER, P. 2012. Designing switchable nanosystems for medical application. J. Controlled Release, 161, 307-16.

LI, Z., BARNES, J. C., BOSOY, A., STODDART, J. F. & ZINK, J. I. 2012. Mesoporous silica nanoparticles in biomedical applications. Chem. Soc. Rev., 41, 2590-605.

LIONG, M., LU, J., KOVOCHICH, M., XIA, T., RUEHM, S. G., NEL, A. E., TAMANOI, F. & ZINK, J. I. 2008. Multifunctional inorganic nanoparticles for imaging, targeting, and drug delivery. ACS Nano, 2, 889-96.

LIOTTA, L. A. & KOHN, E. C. 2001. The microenvironment of the tumour-host interface. Nature, 411, 375-9.

LIU, R., LIAO, P., LIU, J. & FENG, P. 2011. Responsive Polymer-Coated Mesoporous Silica as a pH-Sensitive Nanocarrier for Controlled Release. Langmuir, 27, 3095-3099.

LOEB, S. & SCHAEFFER, E. M. 2009. Risk factors, prevention and early detection of prostate cancer. Prim Care, 36, 603-21.

LOZANO, R., NAGHAVI, M., FOREMAN, K., LIM, S., SHIBUYA, K., ABOYANS, V., ABRAHAM, J., ADAIR, T., AGGARWAL, R., AHN, S. Y., ALMAZROA, M. A., ALVARADO, M., ANDERSON, H. R., ANDERSON, L. M., ANDREWS, K. G., ATKINSON, C., BADDOUR, L. M., BARKER-COLLO, S., BARTELS, D. H., BELL, M. L., BENJAMIN, E. J., BENNETT, D., BHALLA, K., BIKBOV, B., ABDULHAK, A. B., BIRBECK, G., BLYTH, F., BOLLIGER, I., BOUFOUS, S., BUCELLO, C., BURCH, M., BURNEY, P., CARAPETIS, J., CHEN, H., CHOU, D., CHUGH, S. S., COFFENG, L. E., COLAN, S. D., COLQUHOUN, S., COLSON, K. E., CONDON, J., CONNOR, M. D., COOPER, L. T., CORRIERE, M., CORTINOVIS, M., DE VACCARO, K. C., COUSER, W., COWIE, B. C., CRIQUI, M. H., CROSS, M., DABHADKAR, K. C., DAHODWALA, N., DE LEO, D., DEGENHARDT, L., DELOSSANTOS, A., DENENBERG, J., DES JARLAIS, D. C., DHARMARATNE, S. D., DORSEY, E. R., DRISCOLL, T., DUBER, H., EBEL, B., ERWIN, P. J., ESPINDOLA, P., EZZATI, M., FEIGIN, V., FLAXMAN, A. D., FOROUZANFAR, M. H., FOWKES, F. G. R., FRANKLIN, R., FRANSEN, M., FREEMAN, M. K., GABRIEL, S. E., GAKIDOU, E., GASPARI, F., GILLUM, R. F., GONZALEZ-MEDINA, D., HALASA, Y. A., HARING, D., HARRISON, J. E., HAVMOELLER, R., HAY, R. J., HOEN, B., HOTEZ, P. J., HOY, D., JACOBSEN, K. H., JAMES, S. L., JASRASARIA, R., JAYARAMAN, S., JOHNS, N., KARTHIKEYAN, G., KASSEBAUM, N., KEREN, A., KHOO, J.-P., KNOWLTON, L. M., KOBUSINGYE, O., KORANTENG, A., KRISHNAMURTHI, R., LIPNICK, M., LIPSHULTZ, S. E., et al. 2012. Global and regional mortality from 235 causes of death for 20 age groups in 1990 and 2010: a systematic analysis for the Global Burden of Disease Study 2010. Lancet, 380, 2095-2128.

MACEWAN, S. R., CALLAHAN, D. J. & CHILKOTI, A. 2010. Stimulus-responsive macromolecules and nanoparticles for cancer drug delivery. Nanomedicine, 5, 793-806.

MAHON, E., SALVATI, A., BALDELLI BOMBELLI, F., LYNCH, I. & DAWSON, K. A. 2012. Designing the nanoparticle-biomolecule interface for "targeting and therapeutic delivery". J. Controlled Release, 161, 164-74.

MARQUES, J. G., GASPAR, V. M., COSTA, E., PAQUETE, C. M. & CORREIA, I. J. 2014. Synthesis and characterization of micelles as carriers of non-steroidal anti-inflammatory drugs (NSAID) for application in breast cancer therapy. Colloids Surf., B, 113, 375-83.

MATSUMURA, Y. & MAEDA, H. 1986. A new concept for macromolecular therapeutics in cancer chemotherapy: mechanism of tumoritropic accumulation of proteins and the antitumor agent smancs. Cancer Res., 46, 6387-92.

MCNEAL, J. E. 1981. Normal and pathologic anatomy of prostate. Urology, 17, 11-6.

MEHNERT, W. & MADER, K. 2001. Solid lipid nanoparticles: production, characterization and applications. Adv. Drug Delivery Rev., 47, 165-96.

MILLER, T., BREYER, S., VAN COLEN, G., MIER, W., HABERKORN, U., GEISSLER, S., VOSS, S., WEIGANDT, M. & GOEPFERICH, A. 2013. Premature drug release of polymeric micelles and its effects on tumor targeting. Int. J. Pharm., 445, 117-24.

MIN, K. H., LEE, H. J., KIM, K., KWON, I. C., JEONG, S. Y. & LEE, S. C. 2012. The tumor accumulation and therapeutic efficacy of doxorubicin carried in calcium phosphate-reinforced polymer nanoparticles. Biomaterials, 33, 5788-5797.

MOCELLIN, S., POOLEY, K. A. & NITTI, D. 2013. Telomerase and the search for the end of cancer. Trends Mol. Med., 19, 125-33.

MONSUEZ, J. J., CHARNIOT, J. C., VIGNAT, N. & ARTIGOU, J. Y. 2010. Cardiac side-effects of cancer chemotherapy. Int. J. Cardiol., 144, 3-15.

MORNET, S., LAMBERT, O., DUGUET, E. & BRISSON, A. 2005. The formation of supported lipid bilayers on silica nanoparticles revealed by cryoelectron microscopy. Nano Lett., 5, 281-5.

MULLER, P. A. & VOUSDEN, K. H. 2013. p53 mutations in cancer. Nat. Cell Biol., 15, 2-8.

NABHOLTZ, J. M. & RIVA, A. 2001. The choice of adjuvant combination therapies with taxanes: rationale and issues addressed in ongoing studies. Clin. Breast Cancer, 2 Suppl 1, S7-14.

NAPIERSKA, D., THOMASSEN, L. C., RABOLLI, V., LISON, D., GONZALEZ, L., KIRSCH-VOLDERS, M., MARTENS, J. A. & HOET, P. H. 2009. Size-dependent cytotoxicity of monodisperse silica nanoparticles in human endothelial cells. Small, 5, 846-53.

NIE, D., CHE, M., GRIGNON, D., TANG, K. & HONN, K. V. 2001. Role of eicosanoids in prostate cancer progression. Cancer Metastasis Rev., 20, 195-206.

NIE, S., XING, Y., KIM, G. J. & SIMONS, J. W. 2007. Nanotechnology applications in cancer. Annu. Rev. Biomed. Eng., 9, 257-88.

NITISS, J. L. 2009. Targeting DNA topoisomerase II in cancer chemotherapy. Nat. Rev. Cancer, 9, 338-50.

O'BRIEN, J., WILSON, I., ORTON, T. & POGNAN, F. 2000. Investigation of the Alamar Blue (resazurin) fluorescent dye for the assessment of mammalian cell cytotoxicity. Eur. J. Biochem., 267, 5421-6.

OWENS, D. E., 3RD & PEPPAS, N. A. 2006. Opsonization, biodistribution, and pharmacokinetics of polymeric nanoparticles. Int. J. Pharm., 307, 93-102.

PALAYOOR, S. T., BUMP, E. A., CALDERWOOD, S. K., BARTOL, S. & COLEMAN, C. N. 1998. Combined antitumor effect of radiation and ibuprofen in human prostate carcinoma cells. Clin. Cancer Res., 4, 763-71.

PARAKHONSKIY, B. V., HAASE, A. & ANTOLINI, R. 2012. Sub-Micrometer Vaterite Containers: Synthesis, Substance Loading, and Release. Angew. Chem., 51, 1195-1197.

PARALA, H., WINKLER, H., KOLBE, M., WOHLFART, A., FISCHER, R. A., SCHMECHEL, R. & VON SEGGERN, H. 2000. Confinement of CdSe Nanoparticles Inside MCM-41. Adv. Funct. Mater., 12, 1050-1055.

PARVEEN, S., MISRA, R. & SAHOO, S. K. 2012. Nanoparticles: a boon to drug delivery, therapeutics, diagnostics and imaging. Nanomedicine, 8, 147-66.

PICARD, J. C., GOLSHAYAN, A. R., MARSHALL, D. T., OPFERMANN, K. J. & KEANE, T. E. 2012. The multi-disciplinary management of high-risk prostate cancer. Urol. Oncol.: Semin. Orig. Invest., 30, 3-15.

PIETRAS, K. & OSTMAN, A. 2010. Hallmarks of cancer: interactions with the tumor stroma. Exp Cell Res., 316, 1324-31.

POPAT, A., LIU, J., LU, G. Q. & QIAO, S. Z. 2012. A pH-responsive drug delivery system based on chitosan coated mesoporous silica nanoparticles. J. Mater. Chem., 22, 11173-11178.

PORCHE, D. 2011. Prostate cancer: overview of screening, diagnosis and treatment. Adv NPs PAs, 2, 18-21.

QUAIL, D. F. & JOYCE, J. A. 2013. Microenvironmental regulation of tumor progression and metastasis. Nat. Med., 19, 1423-37.

QUINN, D. I., TANGEN, C. M., HUSSAIN, M., LARA, P. N., JR., GOLDKORN, A., MOINPOUR, C. M., GARZOTTO, M. G., MACK, P. C., CARDUCCI, M. A., MONK, J. P., TWARDOWSKI, P. W., VAN VELDHUIZEN, P. J., AGARWAL, N., HIGANO, C. S., VOGELZANG, N. J. & THOMPSON, I. M., JR. 2013. Docetaxel and atrasentan versus docetaxel and placebo for men with advanced castration-resistant prostate cancer (SWOG S0421): a randomised phase 3 trial. Lancet Oncol., 14, 893-900.

RABANEL, J. M., AOUN, V., ELKIN, I., MOKHTAR, M. & HILDGEN, P. 2012. Drug-loaded nanocarriers: passive targeting and crossing of biological barriers. Curr. Med. Chem., 19, 3070-102.

RADU, D. R., LAI, C. Y., HUANG, J., SHU, X. & LIN, V. S. 2005. Fine-tuning the degree of organic functionalization of mesoporous silica nanosphere materials via an interfacially designed co-condensation method. Chem. Commun.,10, 1264-6.

ROMERO OTERO, J., GARCIA GOMEZ, B., CAMPOS JUANATEY, F. & TOUIJER, K. A. 2014. Prostate cancer biomarkers: An update. Urol. Oncol.: Semin. Orig. Invest., 32, 252-260.

ROSENHOLM, J. M., SAHLGREN, C. & LINDEN, M. 2010. Towards multifunctional, targeted drug delivery systems using mesoporous silica nanoparticles--opportunities & challenges. Nanoscale, 2, 1870-83.

RUENRAROENGSAK, P., COOK, J. M. & FLORENCE, A. T. 2010. Nanosystem drug targeting: Facing up to complex realities. J. Controlled Release, 141, 265-276.

SAAD, F. & HOTTE, S. J. 2010. Guidelines for the management of castrate-resistant prostate cancer. Can Urol Assoc J, 4, 380-4.

SAAD, F. & MILLER, K. 2014. Treatment options in castration-resistant prostate cancer: current therapies and emerging docetaxel-based regimens. Urol. Oncol.: Semin. Orig. Invest., 32, 70-9.

SAHAI, E. 2005. Mechanisms of cancer cell invasion. Curr. Opin. Genet. Dev., 15, 87-96.

SAHARINEN, P., EKLUND, L., PULKKI, K., BONO, P. & ALITALO, K. 2011. VEGF and angiopoietin signaling in tumor angiogenesis and metastasis. Trends Mol. Med., 17, 347-62.

SERRES, S., O'BRIEN, E. R. & SIBSON, N. R. 2014. Imaging angiogenesis, inflammation, and metastasis in the tumor microenvironment with magnetic resonance imaging. Adv. Exp. Med. Biol., 772, 263-83.

SHAHBAZI, M. A., HAMIDI, M., MAKILA, E. M., ZHANG, H., ALMEIDA, P. V., KAASALAINEN, M., SALONEN, J. J., HIRVONEN, J. T. & SANTOS, H. A. 2013. The mechanisms of surface chemistry effects of mesoporous silicon nanoparticles on immunotoxicity and biocompatibility. Biomaterials, 34, 7776-89.

SHAY, J. W. & WRIGHT, W. E. 2011. Role of telomeres and telomerase in cancer. Semin. Cancer Biol., 21, 349-53.

SHEN, M. M. & ABATE-SHEN, C. 2003. Roles of the Nkx3.1 homeobox gene in prostate organogenesis and carcinogenesis. Dev. Dyn., 228, 767-78.

SIEGEL, R., MA, J., ZOU, Z. & JEMAL, A. 2014. Cancer statistics, 2014. CA Cancer J Clin, 64, 9-29.

SLOWING, II, VIVERO-ESCOTO, J. L., WU, C. W. & LIN, V. S. 2008. Mesoporous silica nanoparticles as controlled release drug delivery and gene transfection carriers. Adv. Drug Delivery Rev., 60, 1278-88.

SO, A. I., HURTADO-COLL, A. & GLEAVE, M. E. 2003. Androgens and prostate cancer. World J. Urol., 21, 325-37.

SOMANI, S., BLATCHFORD, D. R., MILLINGTON, O., STEVENSON, M. L. & DUFES, C. 2014. Transferrin-bearing polypropylenimine dendrimer for targeted gene delivery to the brain. J. Controlled Release, in press.

STEICHEN, S. D., CALDORERA-MOORE, M. & PEPPAS, N. A. 2012. A review of current nanoparticle and targeting moieties for the delivery of cancer therapeutics. Eur. J. Pharm. Sci., 48, 416-427.

STÖBER, W., FINK, A. & BOHN, E. 1968. Controlled growth of monodisperse silica spheres in the micron size range. J. Colloid Interface Sci., 26, 62-69.

SVENSON, S. & TOMALIA, D. A. 2005. Dendrimers in biomedical applications--reflections on the field. Adv. Drug Delivery Rev., 57, 2106-29.

SWIFT, L. P., REPHAELI, A., NUDELMAN, A., PHILLIPS, D. R. & CUTTS, S. M. 2006. Doxorubicin-DNA adducts induce a non-topoisomerase II-mediated form of cell death. Cancer Res., 66, 4863-71.

TANG, F., LI, L. & CHEN, D. 2012. Mesoporous silica nanoparticles: synthesis, biocompatibility and drug delivery. Adv. Mater., 24, 1504-34.

TANNOCK, I. F., DE WIT, R., BERRY, W. R., HORTI, J., PLUZANSKA, A., CHI, K. N., OUDARD, S., THEODORE, C., JAMES, N. D., TURESSON, I., ROSENTHAL, M. A., EISENBERGER, M. A. & INVESTIGATORS, T. A. X. 2004. Docetaxel plus prednisone or mitoxantrone plus prednisone for advanced prostate cancer. N. Engl. J. Med., 351, 1502-12.

TAPLIN, M. E. 2007. Drug insight: role of the androgen receptor in the development and progression of prostate cancer. Nat. Clin. Pract. Oncol., 4, 236-44.

THORN, C. F., OSHIRO, C., MARSH, S., HERNANDEZ-BOUSSARD, T., MCLEOD, H., KLEIN, T. E. & ALTMAN, R. B. 2011. Doxorubicin pathways: pharmacodynamics and adverse effects. Pharmacogenet. Genomics, 21, 440-6.

TIAN, L. & BAE, Y. H. 2012. Cancer nanomedicines targeting tumor extracellular pH. Colloids Surf., B, 99, 116-26.

TREWYN, B. G., NIEWEG, J. A., ZHAO, Y. & LIN, V. S. Y. 2008. Biocompatible mesoporous silica nanoparticles with different morphologies for animal cell membrane penetration. Chem. Eng. J. , 137, 23-29.

VANDER HEIDEN, M. G., CANTLEY, L. C. & THOMPSON, C. B. 2009. Understanding the Warburg effect: the metabolic requirements of cell proliferation. Science, 324, 1029-33.

VERONESE, F. M. & PASUT, G. 2005. PEGylation, successful approach to drug delivery. Drug Discovery Today, 10, 1451-8.

VIVERO-ESCOTO, J. L., SLOWING, II, TREWYN, B. G. & LIN, V. S. 2010. Mesoporous silica nanoparticles for intracellular controlled drug delivery. Small, 6, 1952-67.

WADAJKAR, A. S., MENON, J. U., TSAI, Y. S., GORE, C., DOBIN, T., GANDEE, L., KANGASNIEMI, K., TAKAHASHI, M., MANANDHAR, B., AHN, J. M., HSIEH, J. T. & NGUYEN, K. T. 2013. Prostate cancer-specific thermo-responsive polymer-coated iron oxide nanoparticles. Biomaterials, 34, 3618-25.

WADE, M., LI, Y. C. & WAHL, G. M. 2013. MDM2, MDMX and p53 in oncogenesis and cancer therapy. Nat. Rev. Cancer, 13, 83-96.

WANG, E. C. & WANG, A. Z. 2014. Nanoparticles and their applications in cell and molecular biology. Integr. Biol., 6, 9-26.

WANG, M. & THANOU, M. 2010. Targeting nanoparticles to cancer. Pharmacol. Res., 62, 90-9.

WANG, X., CAI, X., HU, J., SHAO, N., WANG, F., ZHANG, Q., XIAO, J. & CHENG, Y. 2013. Glutathione-triggered "off-on" release of anticancer drugs from dendrimer-encapsulated gold nanoparticles. J. Am. Chem. Soc., 135, 9805-10.

WANG, Y., SHIM, M. S., LEVINSON, N. S., SUNG, H. W. & XIA, Y. 2014. Stimuli-Responsive Materials for Controlled Release of Theranostic Agents. Adv. Funct. Mater., in press.

WEIS, S. M. & CHERESH, D. A. 2011. Tumor angiogenesis: molecular pathways and therapeutic targets. Nat. Med., 17, 1359-70.

WIJAGKANALAN, W., KAWAKAMI, S. & HASHIDA, M. 2011. Designing dendrimers for drug delivery and imaging: pharmacokinetic considerations. Pharm. Res., 28, 1500-19.

WISSING, S. A., KAYSER, O. & MULLER, R. H. 2004. Solid lipid nanoparticles for parenteral drug delivery. Adv. Drug Delivery Rev., 56, 1257-72.

WU, S. H., MOU, C. Y. & LIN, H. P. 2013. Synthesis of mesoporous silica nanoparticles. Chem. Soc. Rev., 42, 3862-75.

WU, X., WU, M. & ZHAO, J. X. 2014. Recent development of silica nanoparticles as delivery vectors for cancer imaging and therapy. Nanomedicine, 10, 297-312.

XING, X., HE, X., PENG, J., WANG, K. & TAN, W. 2005. Uptake of silica-coated nanoparticles by HeLa cells. J. Nanosci. Nanotechnol., 5, 1688-93.

YANG, F., JIN, C., JIANG, Y., LI, J., DI, Y., NI, Q. & FU, D. 2011. Liposome based delivery systems in pancreatic cancer treatment: from bench to bedside. Cancer Treat. Rev., 37, 633-42.

YANG, F., TEVES, S. S., KEMP, C. J. & HENIKOFF, S. 2014. Doxorubicin, DNA torsion, and chromatin dynamics. Biochim. Biophys. Acta, 1845, 84-9.

YIH, T. C. & AL-FANDI, M. 2006. Engineered nanoparticles as precise drug delivery systems. J J. Cell. Biochem., 97, 1184-90.

YILMAZ, M. & CHRISTOFORI, G. 2009. EMT, the cytoskeleton, and cancer cell invasion. Cancer Metastasis Rev., 28, 15-33.

YUAN, L., TANG, Q., YANG, D., ZHANG, J. Z., ZHANG, F. & HU, J. 2011. Preparation of pH-Responsive Mesoporous Silica Nanoparticles and Their Application in Controlled Drug Delivery. J. Phys. Chem. C, 115, 9926-9932.

ZHANG, H., WANG, G. & YANG, H. 2011. Drug delivery systems for differential release in combination therapy. Expert Opin. Drug Delivery, 8, 171-90.

ZHANG, L., FENG, Y., TIAN, H., ZHAO, M., KHAN, M. & GUO, J. 2013. Amphiphilic depsipeptide-based block copolymers as nanocarriers for controlled release of ibuprofen with doxorubicin. J. Polym. Sci., Part A: Polym. Chem., 51, 3213-3226.